

School of Civil and Mechanical Engineering

**Characterisation and Performance of Pindan Soils Modified with
Polymer Stabilisers**

Hyun Kyu Park

**This thesis is presented for the Degree of
Master of Philosophy (Civil Engineering)
of
Curtin University**

November 2018

Declaration

To the best of my knowledge and belief this thesis contains no material previously published by any other person except where due acknowledgment has been made.

This thesis contains no material which has been accepted for the award of any other degree or diploma in any university.

Signature: ... 

Date: ...04/07/2018...

Abstract

Moisture susceptibility of materials or substances are important aspects when pavements are designed, as moisture can weaken the bonds between aggregates, or between aggregates and binders. Traditional stabilisation using cement or lime have significant uncertainty factors, such as mix design, curing process and condition, and a proper amount of water while mixing and compacting. Therefore, non-traditional stabilisation has been used popularly and has become increasingly available for engineering purposes due to its low cost and easy application. Studies of the polymer-Pindan soil stabilisation have been focused on engineering performances, but literature shows no information on Pindan particles on micro- and nanoscale. Pindan is a type of red soil, known as a soft and moisture sensitive soil. Little is known about the fundamental interaction and stabilisation mechanism of pindan soil with polymers, which govern mechanical properties. This project focuses on the fundamental information of Pindan soil and the stabilisation to improve its performance using polymer stabilisers and determines the chemical and physical bonding mechanisms associated with polymer stabilisers. Plastic index, specific gravity and particle size distribution were tested to obtain the basic properties. Compaction, collapsibility, unconfined compressive strength and California bearing ratio tests were performed to determine the mechanical properties. The waterproof effect of the polymers on the stabilised Pindan soil was investigated from capillary rise tests. Furthermore, chemical and microstructural properties were examined using X-ray diffraction (XRD) and scanning electron microscope (SEM), and linked with the mechanical properties. The mechanical behaviour and properties of soil grains were investigated using nanoindentation tests. Hardness, elastic modulus, and packing density were determined as 10.6 ± 0.9 GPa, 68.1 ± 12.7 GPa and 0.863 ± 0.032 , respectively. Based on microporomechanics, stiffness and cohesion of Pindan soil are 92.7 GPa and 4.1 GPa, respectively. The fracture toughness of Pindan soil based on the energy transferred and the measurement of radial and later cracks indentation points are 3.1 ± 0.8 MPa m^{1/2} and 3.7 ± 0.5 MPa m^{1/2}, respectively. Based on the results, the mechanical properties and microstructure changes show a close relationship. Basically, it is evident that the failure behaviour, strain and strength as well as the basic properties are affected and changed by the microstructure change.

Acknowledgements

Firstly, my deep gratitude and appreciation go to my supervisor, **Dr. Vanissorn Vimonsatit** for her continuous encouragement and support during my Master's degree at Curtin University. I also would like to express my appreciation to my co-supervisor, **Dr Peerapong Jitsangiam** for providing continuous guidance for completing this research. I am really thankful to them.

My special thanks of gratitude also go to **Dr Hyuk Lee** and **Dr Korakod Nusit** for their support and advice with this research. This thesis would not be completed without their help.

I am also greatly thankful to Mr, Mark Whittaker and Mirzet Sehic for their help with laboratory work at the Department of Civil Engineering. And, I would like to acknowledge the assistance and help with their technical advice by Paul Bright and Siva Thillainath.

Lastly, I would like to express my special thanks to my family for their continuous support and love to complete this Thesis.

Thanks again to all who helped me in completing my degree.

Contents

1	Introduction	1
1.1	Background.....	1
1.2	Location of Pindan Sample	3
1.2.1	Current Condition.....	4
1.3	Research Aim and Objective	4
1.4	Significance	5
1.5	Research Method	6
1.6	Thesis Organisation	7
2	Literature Review	8
2.1	Introduction	8
2.2	Soil Formation	8
2.3	Pindan Soil.....	9
2.3.1	Location of Pindan	9
2.3.2	Characteristics of Pindan soil.....	10
2.3.3	Problems of Pindan soil	14
2.3.4	Stabilisation of Pindan soil.....	15
2.4	Unsealed Pavement	18
2.5	Problematic soil.....	21
2.5.1	Identification of Collapse potential	22
2.5.2	Bonding and Collapsing Mechanism	27
2.6	Soil Stabilisation.....	29
2.6.1	Non-traditional soil stabiliser	29
2.6.2	Polymer Stabiliser	32
2.6.3	Polymer stabilised soil for pavement	34
2.7	Summary.....	36

3	Preliminary Test.....	38
3.1	Introduction	38
3.2	Pindan Properties and classification.....	39
3.2.1	Index Properties and Classification Test.....	39
3.2.2	Mechanical Properties	42
3.2.2.1	Compaction Test.....	43
3.2.2.2	California Bearing Ratio (CBR) Test	45
3.2.3	A Representative of Broome-Pindan Soil.....	47
3.2.4	Collapsible Potential and Texture	48
3.3	Summary.....	51
4	Nanoindentation	52
4.1	Introduction	52
4.2	Evaluating Indentation Properties of Pindan Soil	53
4.3	Experimental Result and Discussion.....	55
4.4	Summary.....	61
5	Stabilisation of Broom-Pindan.....	62
5.1	Introduction	62
5.2	Material Preparation	63
5.3	Modified Compaction Test.....	67
5.4	Capillary Rise	71
5.5	Unconfined Compressive Strength Test.....	75
5.6	California Bearing Ratio (CBR).....	80
5.7	Chemical and Physical Bonding Mechanism	83
5.7.1	Chemical and Microstructural Properties.....	84
5.7.2	Interaction of Microstructural Properties and Mechanical properties.....	92
5.8	Chapter Summary.....	94
6	Conclusion and Future Research.....	96

6.1	Conclusion.....	96
6.2	Recommendation for future research	97
	Appendices	99
	Appendix A	99
	Appendix B	102
	Appendix C	106
	Appendix D	111
	References	113

List of Figures

Figure 2.1: Distribution map of Red Deep Sand in Western Australia (Schoknecht & Pathan, 2013).....	10
Figure 2.2: Strength change of Lateritic Gravel Base on Great Eastern Highway in Western Australia with Time (adopted after (Main Roads, 2003))	16
Figure 2.3: Variation of dry density with moisture content of a range of North West soils containing 10 percent Portland cement (Western Australia. Department of Regional Development and the North West, 1984)	16
Figure 2.4: Unsealed road pavement layers (adopted after (Austroads, 2009)).....	19
Figure 2.5: Suggested Particle Size Distribution Range for Unsealed wearing course (Austroads, 2009).....	20
Figure 2.6: Design Chart for granular pavement (80% confidence) (Austroads, 2009)	21
Figure 2.7: Classification of collapsible soils (Rogers, 1995)	23
Figure 2.8: Criterion to identify soil collapsibility (adopted after (Holtz, 1961))	24
Figure 2.9: Typical Consolidation Test Result (ASTM International, 2011b)	25
Figure 2.10: Typical Single oedometer collapse potential test result (Pells et al., 1975)	25
Figure 2.11: Typical Double oedometer collapse potential test result (Lutenegger & Saber, 1988)	26
Figure 2.12: Collapse pressure definition (Popescu, 1986)	27
Figure 2.13: Typical Bonding structure of collapsible soils (Clemence & Finbarr, 1981)	28
Figure 2.14: Microstructure of collapsible soils and Clay Bridges from SEM (adopted after (Haeri et al., 2013), (Jackson et al., 2006). (a) Loose and Open structure. (b) Cementation of clay matrices form. (c) Clay bridge bonds.	28
Figure 2.15: Classification of Polymer-based admixtures (Ohama, 1998).....	33
Figure 3.1: Chapter3 Overall Flow Chart	39
Figure 3.2: Particle Size Distribution of Broome-Pindan Soil.....	41
Figure 3.3: Compaction Test of Broome-Pindan Soil with Air-voids (Av) curve....	44
Figure 3.4: Load-Penetration Curves of Broome-Pindan Soil	45

Figure 3.5: Particle Size Distribution Interval for A Representative Broome-Pindan Soil	47
Figure 3.6: Void Ratio vs Applied Stress Test on Unsaturated and Saturated Sample	49
Figure 3.7: Collapse Index vs Stress	49
Figure 3.8: Sample of Pindan Soil Located in Broome. (A) Pindan Sand. (B) Pindan Sand in Water for Specific gravity testing.	50
Figure 3.9: Wet and Dry Broome-Pindan Sand. (A) Optimum Moisture Condition. (B) Wet Sand. (C) Dry-back after full-saturated. (D) Cracks on sand in dry condition.	50
Figure 4.1 Principles of Indentation Testing (Constantinides et al., 2006).....	53
Figure 4.2: Typical load – displacement curve for indentation.	55
Figure 4.3: Statistical Indentation Analysis; Top - cumulative distribution functions (CDF), Bottom – probability density function of elastic modulus (left) and hardness (right).....	56
Figure 4.4: Statistical Indentation Analysis; Top - cumulative distribution functions (CDF), Bottom – probability density function of packing density.	57
Figure 4.5: Geometrical relationship between the extended radial cracks and the indentation impression with Berkovich tip	58
Figure 4.6: Inverted 3D image (left) and residual impression (right)	59
Figure 4.7: Fracture energy graph of linear material (Bazant & Pfeiffer, 1987)	60
Figure 5.1: Microscope Images of Polymers. (A) Polymer A, (B) Polymer C, (C) and (D) Polymer B.	64
Figure 5.2: Polymer C Active Range Zone. (a) Maximum dry density versus Polymer content, (b) Degree of Activation for Polymer C.....	66
Figure 5.3: Comparison of the untreated sample and the treated samples.....	68
Figure 5.4: Compaction Test using the Modified Proctor Compaction Method. (a) Pindan soil, (b) Mixture A, (c) Mixture B, and (d) Mixture C.	70
Figure 5.5: Capillary Rise of Compacted Samples	74
Figure 5.6: Typical Unconfined Compressive Strength Curves of the compacted samples. (a) 1hour cured samples, (b) 16day cured samples.	76
Figure 5.7: UCS Results for 1 Hour curing.....	79
Figure 5.8: UCS Results for 16 Day curing	79
Figure 5.9: UCS Samples. (a) Untreated Pindan Sample, (b) Mixture A	80
Figure 5.10: Typical UCS. (a) Unsoaked Condition, (b) Soaked Condition.	82

Figure 5.11: Polymer C for QXRD became a thin film of plastic after dried.....	84
Figure 5.12: G.P and C.L Sand Grain. (A) G.P Sub-rounded Grain, (B) C.L Sub-rounded Grain, (C) G.P Microstructure, (D) C.L Microstructure, (E) Magnification of (C) showing the clear form, (F) Magnification of (D) showing the clear form.	85
Figure 5.13: SEM Images of Mixture A after 16day curing. (A) Bonding of Mixture A, (B) Magnification of (A) showing the bonding structure.	86
Figure 5.14: XRD phase analysis of Pindan sand and Mixture A	87
Figure 5.15: EDS Spectra of the mixture A. (A) EDS on bonding, (B) EDS on Sand Particle.....	87
Figure 5.16: SEM Images of Mixture B and C after 16day curing. (A) Bonding of Mixture B, (B) Bonding of Mixture C, (C) Magnification of (A) showing the bonding structure, (D) Magnification of (B) showing the bonding structure, (E) Magnification of (C) showing microstructures, (F) Magnification of (C) showing microstructures.	89
Figure 5.17: EDS Spectra of the mixture B. (A) EDS on bonding, (B) EDS on Sand Particle.....	90
Figure 5.18: EDS Spectra of the mixture C. (A) EDS on bonding, (B) EDS on Sand Particle.....	91
Figure 5.19: XRD phase analysis of Pindan sand, Mixture B and C.....	91
Figure 5.20: XRD Phase analysis of Polymers	92
Figure 5.21: CBR Test for the Mixtures with 0.5% and 0.7% of Polymer C	93

List of Tables

Table 2.1: Properties of Broome Pindan (adopted after (Emery et al., 2003))	12
Table 2.2: Guide to Collapse Potential Values (adopted after (Pells, Robertson, Jennings, & Knight, 1975)).....	12
Table 2.3: General Definition of Site Classifications (adopted after (Standards Australia, 2011))	13
Table 2.4: Unconfined Compression Strength for cement Stabilised Pindan Soils..	17
Table 2.5: Suggested CBR and Permeability Values for pavement material for unsealed roads (adopted after (Austroads, 2009)).....	20
Table 2.6: Location of Problem soils in Western Australia (adopted after (Davenport, 2007))	22
Table 2.7: Proposed stabilisation mechanisms for Non-traditional stabilisation (adopted after (Tingle et al., 2007))	32
Table 3.1: Seven Broome-Pindan samples for Index and Classification Test	40
Table 3.2: Specific gravity and Plasticity index of Broome-Pindan.....	41
Table 3.3: Percentage of Gravel, Sand and Silt of Broome-Pindan Soil	42
Table 3.4: Classification of Broome-Pindan soil	42
Table 3.5: Six Broome-Pindan Samples for Compaction Test	43
Table 3.6: Optimum Moisture Contents (OMC) and Maximum Dry Density (MDD) of Broome-Pindan Soils	44
Table 3.7: California Bearing Ratio (CBR) Test Results for Broome-Pindan soil...	46
Table 4.1: Properties of Pindan soil grain used in Nanoindentation.....	54
Table 5.1: Polymer Information	64
Table 5.2: Optimum Moisture Contents (OMC) and Maximum Dry Density (MDD) of Broome-Pindan Soil and Mixtures	71
Table 5.3: Averages of UCS Results for the 1 hour cured samples	77
Table 5.4: Averages of UCS Results for the 16 day cured samples	77
Table 5.5: Averages of the CBR values for saturated and unsaturated samples.....	81
Table 5.6: Quantitative XRD Analysis for Pindan Sand.....	84

List of Symbols

Symbol	Description
CL	Cape Levique
GP	Gantheaume Point Rd
CR	Capillary Rise
CBR	California Bearing Ratio
EDS	Energy Dispersive X-ray Spectroscopy
SEM	Scanning Electron Microscope
UCS	Unconfined Compression Strength
XRD	X-ray Diffraction
QXRD	Quantitative X-ray Diffraction
RVE	Representative Volume Element
SC	Clayey Sand
SM	Silty Sand
G_s	Specific Gravity
LL	Liquid Limit
PL	Plastic Limit
PI	Plasticity Index
NP	Non-Plastic
R_w	Moisture Ratio
OMC	Optimum Moisture Content
MDD	Maximum Dry Density
LDR	Laboratory Density Ratio
A_v	Air-Voids
C_r	Recompression Index
C_c	Compression Index
σ_p	Pre-Consolidation Stress
P_{cs}	Limiting pressure in Saturated Condition
P_{cn}	Limiting pressure in Natural Condition
P_o	Overburden Vertical Pressure
C_p	Collapse Potential

e	Void Ratio
Δe	Difference or Change in Void ratio
e°	Initial Void ratio of specimens
I_c	Collapse Index
H	Hardness
E	Elastic modulus
E_r	Reduced Modulus
E'	Elastic modulus of indenter tip,
A_c	Contact Area
h_c	Contact depth
P_{max}	Maximum Indentation Load
S	Slope of the upper portion of the unloading curve
ν'	Poisson's ratio of indenter tip
ν_s	Poisson's ratio of sample
ζ	Total porosity of material
η	Packing density of material
ε	Empirical calibration constant
c	Radial crack length
W_p	Plastic energy
W_e	Elastic energy
W_t	Total energy
W_{other}	Another energy
$U_{fracture}$	Fracture dissipated energy
K_c	Fracture toughness
G_c	Critical energy
G_f	Fracture Energy
U_f	Deformation
H	Initial Height of Sample
$H(t)$	Capillary Rise with time
h	Height of Capillary Rise
S	Swelling
γ_{LV}	Surface tension of the liquid
R	Pore radius

η	Shear viscosity of the liquid.
Q	Quartz
S	Corundum
K	Kaolinite
C	Calcite
d_i	Characteristic length scale in RVE
h_i	Indentation depth
a_i	Indentation radius
D_i	Characteristic microstructural length scale,
L_i	RVE of Homogeneous mechanical characteristic size

Chapter 1

1 Introduction

1.1 Background

Soils are very complex granular materials with different characteristics and behaviour. Each soil type has different colour, texture, structure and chemical composition. There are many factors that have a strong influence on soil properties such as climate, time, organisms, parent material, topographic and other factors (Jenny, 1994). Soil properties are important for predicting potential behaviour and understanding its characteristics. About 60% of the Australian road network is unsealed road and maintenance costs of the roads are approximately one billion dollars per kilometre per year in the nation. Unsealed roads generally use natural materials and use on-site soils. This has a significant impact on cost, environmental and social factors. However, unsealed roads have high accident risks and operating costs associated with dust, slippery surface, loose surface and surface maintenance (Sharp & Andrews, 2009).

Pindan Sand-clay is a red soil, known as a soft and moisture sensitive soil and is mainly found in the Kimberley region of Western Australia. Pindan comes from a local term used in the Kimberley region to describe the soil of the Kimberley area (Kenneally, Edinger, & Willing, 1996). Pindan material has a red colour, which is due to high iron in the soil (Main Roads, 2003). Emery et al. (2003) suggested that the particle bridges also form from Fe-kaolinite which contains both aluminium oxides and iron. They described Pindan as a red sand which can be classified as clayey sand (SC) or silty sand (SM). Pindan is a potentially collapsible soil due to high void ratio, low density and low water content. Since Pindan is a collapsible soil, it can be easily changed in volume on relatively high moisture contents and is very destructive to the pavement structure. However, Pindan has self-cementation capabilities in a dry condition, which can be used as a material for pavement structures (Emery et al., 2003). Pindan soils gain substantial strength upon drying and lose strength when wet. This causes pavement structures on Pindan soil uneven. A Pindan report (Western Australia. Department of Regional Development and the North West, 1984)

investigated over 30 selected Pindan soils in Western Australia. The pindan soil presents high variability in optimum moisture content, dry density and strength. Further, according to an engineering report by Sinclair Knight Merz (2009), Broom-Pindan soils that were classified as a silty clayey sand did not show any collapsibility.

The Kimberley region has a wet season (or called tropical summer season) from November to April and a dry winter season from April to November. The region receives over 75% of its rainfall during the wet season and the high concentration of rain over short periods can damage the pavement structure on moisture sensitive soils (Sinclair Knight Merz, 2009).

Strength is one of the important components of materials that resist deformation from imposed stresses (Sharp & Andrews, 2009). In order to increase the capacity of road pavement, it may be necessary to strengthen the pavement materials. The process of strengthening the pavement materials by means of additives is known as stabilisation, of which there are many types. Soil stabilisation methods are typically chemically and mechanically based. Mechanical stabilisation improves the performance of soils through the application of compaction or loads to improve the strength. Chemical stabilisation improves strength by adding chemical stabilisers such as cement, fly ash, lime and polymer (Welling, 2012).

Cement and lime are well documented for a stabilisation of low plasticity soils and have been used in various projects that have moisture sensitive soils (Smith & Sullivan, 2014). Both stabilising agents can improve soil performance. However, chemically stabilised materials using cement or lime have significant uncertainty factors, such as proper mix design, curing process and condition, and a proper amount of water while mixing and compacting. These factors could result in poor performance of the final product of chemically treated materials. For the fundamental characteristics of Pindan soils which can provide good strength when subjected to relatively dry conditions (i.e., moisture contents lower than its optimum moisture content), this could lead to a viable option of how to fundamentally improve Pindan soils. If Pindan soils can maintain their dry condition by not allowing them to be wetted, it can provide sufficient strength to use for construction purposes. With advancement in soil stabilising technology nowadays, a preferred drying condition of soils can be maintained by using some polymers as a stabilising agent that can

generate, so-called, hydrophobic (water-repellence) properties. The Pindan soils problem could be fundamentally solved using polymer stabilising binders as internal waterproofing. So, the dry strength can be retained through any wet condition (Lacey, 2004).

Based on recent studies, a polymer for soil stabilisation has a high resistance to water and good physical properties. Strength improvement and physical bonding depend on the ability of the polymer because the aggregate is coated with a film of the polymer and it provides bonding (Welling, 2012). With the advancement of polymer technology in which waterproofing properties can be created, such problems with Pindan soil could be fundamentally resolved by using polymer stabilising binders as an internal waterproofing (Lacey, 2004). Most of the polymer-Pindan soil stabilisation studies have been focused on engineering performances of the stabilised soil. Therefore, there is limited information on Pindan properties for road pavement, but it has been used as road material in Western Australia. Information about Pindan particles is also not available on micro- and nanoscale, and little is known about the fundamental interaction and stabilisation mechanism with polymers, which govern mechanical properties.

1.2 Location of Pindan Sample

Seven samples of Pindan soil collected locally from two sites in Broom, Kimberly region, Western Australia, were used in this research. The samples were collected from the wearing course of unsealed roads, and raw materials were taken from the bush next roads.

Seven Samples from two locations are:

A) Gantheaume Point Rd

- Raw material
- shoulder and surface material

B) Cape Levique

- Raw Material
- surface material (site1)
- shoulder and surface material (site2)

1.2.1 Current Condition

Two unsealed roads that carry reasonable amounts of traffic give the Shire of Broome problems – Gantheaume Point Road and Cape Leveque Road. Both roads are closed to all traffic when there is any sign of imminent rain. Currently, both roads look like drains as the only solution to reinstating the road after heavy rain is to cut the wet material off the surface to expose the dry material below to form a new surface.

Broome has very little rocky material close to town. It has been accessed to a fine crushed rock that is brought to town from a remote quarry. It is used primarily as the top 100 mm of base-course for heavy traffic roads and Main Roads use this material for the main roads into Broome, but it is very expensive to construct roads using these materials.

It is significant to find a treatment that allows the material that has been cut off the surface to be recombined with the sandy residue material to form a base course. If this material remains unsealed, there should be a requirement that any damage could be repaired by reworking and re-compaction.

1.3 Research Aim and Objective

This study examines the properties of Pindan soils to determine nanostructure, microstructure, chemical and mechanical properties and evaluates polymer stabilised Pindan soils to determine the performance of polymer-based products, and the chemical and microstructural reactions between Pindan and Polymer. This project also aims to explore an opportunity in stabilising Pindan soils with potential polymers in order to fundamentally prevent a wetting condition by creating a hydrophobic property through Pindan soils-polymer mixtures.

The main objectives of this study are;

- To obtain the physical-mechanical, chemical, nanostructural and microstructural properties of Broome-Pindan soils
- To evaluate the potential of stabilising Pindan soils using polymers based on the pavement and geotechnical engineering's perspectives.
- To obtain the chemical and physical bonding mechanisms between Pindan particles associated with polymer stabilisers.

The specific objective of this project is to investigate on:

- ✓ Characterisation of Broome-Pindan soils.
- ✓ Production of Pindan soils mixed with polymers.
- ✓ Bonding mechanisms of polymer-Pindan soil
- ✓ Effects of polymer-Pindan soil mixtures on the performance of Pindan soil
- ✓ Effect of different curing times on the compressive and bearing properties of Polymer modified Pindan soil.

This project mainly focuses on the fundamental information of Pindan soil and the stabilisation to improve the performance of the Pindan soil using polymer stabilisers and provides the chemical and physical bonding mechanisms associated with polymer stabilisers.

The laboratory works are performed to investigate properties of Pindan soils and effects of polymer types with different polymer contents on the polymer-modified Pindan soil properties and performance. This project provides all properties of Pindan soils and a guideline of using polymer in improving Pindan soils to be useable materials for construction purposes, based on testing undertaken using particular Pindan soils in Western Australia with altering polymer contents.

1.4 Significance

Pindan sand-clay deposits are common throughout the Kimberley region of WA. Emery et al. (2003) and Kenneally et al. (1996) described the Pindan soils as a red moisture sensitive soil and have shown problems when using as compacted fills for roads and embankments with causes of wetting induced losing bonding strength. The pavement constructed on problematic soils which bring deformation can cause a significant failure to structures. Therefore, of key significance in the project is the generation of a new guideline for use of Pindan soils-polymer stabilised materials for Australian pavements, based on extensive laboratory and a full consideration of realistic pavement conditions, and mainly advance the information of Pindan soils.

The main points of significance are as follows:

- Contribute to the evaluation of the fundamental properties of Pindan soils.
- Enhance the polymeric stabilising additive on Strength of Pindan soils.

- Understanding the bonding mechanism between soil and various polymers
- Finding the relationship between bonding mechanism and mechanical properties.

1.5 Research Method

As this project aims to provide useful information in facilitating the establishment of a reliable design procedure for Pindan soils modified with polymers from a series of tests which are undertaken. The following outlines the research methodology of this project. The laboratory experiment consists of producing a number of Pindan soils-polymer mixture batches with varying polymer contents.

The method for this assessment will be to:

- Prepare test specimens of Pindan soils, using materials commonly found in Broome, the Kimberley region of Western Australia,
- Investigate the basic properties such as index and classification, and collapsibility of Broome-Pindan soils,
- Investigate the nanostructures, chemical and microstructural properties of Pindan soils by Nanoindentation, XRD and SEM respectively,
- Vary polymer contents in Pindan soils and polymer mixtures, to obtain a clear range of comparative data,
- Determine the suitability of Polymers for the stabilisation of Pindan soil; Maximum dry density, plasticity index (PI) and moisture content,
- Assess the waterproof effect of the polymers on the stabilised Pindan soil through the capillary rise test of compacted materials,
- Obtain the compressive and bearing strength of Pindan soils and polymer modified Pindan soils with respect to polymer contents and curing times through unconfined compression strength tests (UCS), and California bearing tests (CBR).

In the experimental work, maximum dry density, plasticity index and optimum moisture content were undertaken to check the suitability of the polymers for the stabilisation of Pindan soils. Capillary rise of compacted materials was also performed for sampling and testing the stabilised Pindan soils to assess the waterproofing effect

of the polymers in accordance with testing guideline specified in Australian standard AS1141.53 (1996a). Double oedometer test was performed to identify the potential collapsibility of Broome-Pindan. A series of performance tests; unconfined compression strength tests (UCS), and California bearing tests (CBR) were performed to evaluate and compare material properties and characteristics with respect to polymer contents and curing times. Test samples for UCS and CBR tests were compacted in accordance with sample preparation guidelines specified in AS 5101.4 (2008) and AS 1289.6.1.1 (2014), respectively. Chemical, Microstructure, nanostructure properties of Pindan soils were also obtained by, XRD, SEM and Nanoindentation respectively.

1.6 Thesis Organisation

The thesis content is presented in the following chapters;

Chapter 2. Literature Review

Chapter 3 Representative of Broom-Pindan soil

Chapter 4 Nanoindentation of Broom-Pindan

Chapter 5 Chemical and Microstructural properties of Broom-Pindan and Composite

Chapter 6 Stabilisation of Broom-Pindan

Chapter 7 Conclusion and Recommendation

Chapter 2 reviews the literature on the background of Pindan soil, unsealed pavement, problematic soil and identification of moisture sensitivity for engineering. Chapter 3 provides physical properties of Pindan soils, collapsibility and creating a sample to represent Broome-Pindan soils for the experiments. Chapters 4 and 5, present an application of nanotechnology and micro-technology to Broome-Pindan soil, respectively, for determining Nano-structure, microstructure and chemical structure of Broome-Pindan soil. Chapter 6 provides polymer information and a series of performance test results through stabilisation. This chapter also provides links to stabilisation and curing time, and also provides guidelines to design using Pindan soil. Conclusion and recommendation are provided in Chapter 7.

Chapter 2

2 Literature Review

2.1 Introduction

This chapter provides a review of literature related to Pindan soil and soil stabilisation with polymers in detail. General topics including unsealed pavement, soil formation, polymer structures and polymer stabilisation for pavement are also discussed as a fundamental knowledge of this research. A considerable amount of review on the various studies has been undertaken on the soil and polymer stabilisation and properties.

2.2 Soil Formation

There are many different types of soils in the world with different colour, texture, structure, and chemical composition, each with different characteristics and behaviours. According to Jenny (1994), the soil classification system has two main principles: soil characteristics such as colour and texture, and soil formation factors such as parent material, climate, terrain, time, and organisms.

In the late 1800s, five factors of soil formation were introduced by Dokuchaev as parent material, climate, topographic, time, and organisms, and the first soil classification was invented and developed based on these five factors. Soil formations can also be determined and explained by the five factors (Graham & Indorante, 2017), (Jenny, 1994). Jenny (1994) referred to these five factors as “p, cl, r, t, o”, respectively, to show a quantitative correlation between soil properties and soil formation factors in a mathematical language using mathematical equations in 1941. These mathematical expressions explained the relationship between soil properties and soil formation factors and also provided a mathematical relationship between soil parameters.

The composition of the parent material has the most important effect in the early stage of soil formation. The geochemical foundation of the soil depends on the chemical composition and physical properties of parent materials, but over time, the influence

is diminishing. The climate over a long time has a strong influence on soil formation. The effects of weather conditions such as water and temperature have a strong influence on soil properties. The effect of topography on soil formation also has a strong influence as it is related to the movements of water. The water velocity and movement across the surface depend on the land slope that affects erosion, deposition, accumulation and leaching. The microclimate is also affected by the slope as the difference of sun angle in relation to the heating of the sun against the soils. Organisms, vegetation, animals and microbes also play an important role in soil formation. For example, these organisms can react chemically or directly affect soil physical properties because dead vegetation produces soil acids and plant roots impact on soil aggregation. Soil formation requires time to be processed and affected by these factors. All of these factors occur and behave over time, and more development happens over a longer period of time. For example, the influence of time changes soil formation as the climate changes over time. The soil is produced, altered or leached over time, and the soil formation is determined by the period (Graham & Indorante, 2017), (Singh & Huat, 2004).

2.3 Pindan Soil

Pindan is a name from a local term used in Kimberley region to describe a particular type of soil in Kimberley. The Aboriginal term of “Pindan” refers to a red soil in the Pilbara region in Western Australia. This term is also used to describe vegetation of the Kimberley region and the characteristic red colour of the soil. The local name of the large pindan soil area is also called “Pindan” or “Pindan country” (Kenneally et al., 1996), (Smolinski, Galloway, & Laycock, 2016).

2.3.1 Location of Pindan

The Kimberley region has two distinct seasons; wet and dry seasons. The typical wet season has high rainfall, high humidity and high temperature while the typical dry season has low rainfall and warm temperature (Smolinski et al., 2016). Papadakis (1975) and Lowe (2003) described the climate of the Kimberley region as semi-arid tropical with hot and wet summers and dry winters. The high concentration of rainfall occurs in a short period during the rainy season and high evaporation rate occurs in November. The region receives more than 75% of its rainfall during the wet season, but mostly from Jan to Feb. During this period, heavy rainfall and tropical cyclones

from the Indian Ocean can produce extensive flooding (J. N. Jennings, 1975) (Sinclair Knight Merz, 2009). The land is also affected by the wind of the cyclones. The power of the cyclone's wind can cause major damage to the land (Kenneally et al., 1996).

Smolinski et al. (2016) and Kenneally et al. (1996) explained the development of sand dunes of the Kimberley region. The Kimberley surface is partly covered by the sand dunes of the Upper Pleistocene developed during periods of low sea level and dry climates (Smolinski et al., 2016). Kenneally et al. (1996) suggested that Pindan was developed from a desert dune sandstone during Quaternary period, immature soil developed in the Pleistocene dunes. The distribution of red deep sand in Western Australia is shown in Figure 2.1.

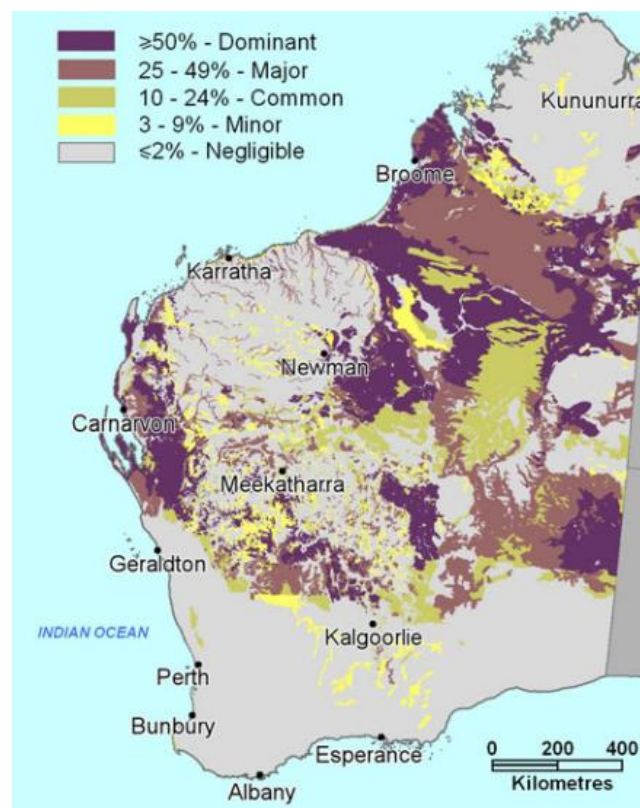


Figure 2.1: Distribution map of Red Deep Sand in Western Australia (Schoknecht & Pathan, 2013)

2.3.2 Characteristics of Pindan soil

Correctly identifying material properties, problems and their causes are significantly important for road design. The colour of the soil is one of the important soil properties

that can be used to identify the soil to determine its characteristics (Rossel, Minasny, Roudier, & McBratney, 2006). Soil colour is produced during the weathering process and is related to temperature and precipitation. Mostly the composition of the soil and the influence of temperature and precipitation decide the colour of the soil (Balsam, Ji, & Chen, 2004).

In 1883, Edward Townley Hardman first mentioned “Pindan” in print and describe the soil as “Pindan ironstone” with a poor hematite but in large quantity (Smolinski et al., 2016). The colour of soil is influenced by even a small amount of Haematite (Emery et al., 2003). A geologist, Woodward (1891) stated that “Pindan sands and gravels are often cemented by oxide of iron” in the geological formation of Pliocene. Pindan is known as a red sand which is due to the quartz sand particles are coated with high iron and aluminium hydroxide (Main Roads, 2003), and Smith and Sullivan (Smith & Sullivan, 2014) proposed that the bridges between soil particles also form from Fe-kaolinite which contains both iron (Haematite:Fe₂O₃) and aluminium oxides (Al(OH)₃). When leaching happens during weathering in tropical regions, it results in the soil highly enriched in iron and aluminium oxides, which makes the soil a deep red colour (Huat, Gue, & Ali, 2007).

Kenneally et al. (1996) mentioned that Pindan becomes soft and greasy when the moisture content increases. Airey et al. (2012) explained the process of the chemical weathering in tropical climates. Due to weathering in tropical, silica is leached from the soil and leaving only its most of the iron content, which makes the soil highly concentrated in iron and aluminium oxides. This laterisation process creates the formation of iron nodules and cemented aggregates and it can lead to soft and high porous soils. Heelas (2001) also explained this process in the tropical area as using a term “Ferrallitisation”. Clay particles in soil are broken down into silica and sesquioxides and the silica is moved downwards under the hot weather while the sesquioxides remain in the soil, which makes the form of iron oxides and the soil becomes soft.

Emery et al. (2003) described the properties of Pindan as a high void ratio and low density in an undisturbed condition, which could easily collapse. They classified pindan as either clayey sand (SC) or silty sand (SM) according to Standard Australia AS 1726 -1993. The physical and chemical properties of Pindan from Broome were

tested in two distinct types of pindan material; Silty Sand (SM) and Clayey sand (SC) with an amorphous clay content of 9% and 18% respectively. The general information on the classification testing results of Broome-Pindan is summarised in Table 2.1. Double oedometer test of Pindan-Clayey sand (SC) for loading condition from 0 kPa to 100 kPa showed 9% of the collapse potential, which indicated a “trouble” collapse potential according to Guide to Collapse Potential Values as shown in Table 2.2. The Pindan-Silty sand (SM) was not able to be performed due to the characteristic of very friable in an undisturbed condition. The shear strength increased with increasing in suction, which means the strength gain of Pindan is also influenced by not only the bridges between soils, but also by changes in the voids geometry. It has been proven that the suction of SC-Pindan is higher than SM-Pindan due to its higher clay content (Emery et al., 2003).

Table 2.1: Properties of Broome Pindan (adopted after (Emery et al., 2003))

Property	SM Silty sand	SC Clayey sand
Liquid Limit (Cup)	NP	18-23
Plasticity Index	NP	4-11
Insitu Density (t/m ³)	1.39-1.46	1.57-1.59
Maximum dry density (MDD; modified t/m ³)	1.88-2.04	2.08-2.10
Optimum Moisture Content (OMC)	8.0-8.5	8.0-9.5

Table 2.2: Guide to Collapse Potential Values (adopted after (Pells, Robertson, Jennings, & Knight, 1975))

Collapse Potential (%)	Severity of Collapse Problem
0 – 1	No problem
1 – 5	Moderate trouble
5 – 10	Trouble
10 – 20	Severe trouble
>20	Very severe trouble

According to an engineering report by Sinclair Knight Merz (2009), they investigated typical Pindan soil at Broome and classified it as a silty clayey sand with low plasticity and has a fine content between 16% to 26% by mass. The sites at Broome were classified as Class “S” in Australia Standard AS2870 (1996b). This Class “S” is defined in accordance with Australia standard AS2870 (2011) as, “the soil includes silts and some clays and expects only slight ground movements from moisture changes”. It is also said that “sites classified class S may be treated as non-reactive sites”. The classification regarding the potential amount of the movement is shown in Table 2.3, which indicates that soil reacts to the increasing moisture content. From the experiments in this report, the properties of Pindan varied from 4.5 to 13.9 and from 4 to 30, respectively, for plastic index and CBR values. Class P is for problematic soils, such as soft clay or silt or loose sands, landslip, mine subsidence, collapsing soils and soils subject to erosion, reactive sites subject to abnormal moisture conditions.

Table 2.3: General Definition of Site Classifications (adopted after (Standards Australia, 2011))

Site Classification	Reaction class	Characteristic of Movement from Moisture Change
Class A	stable (non-reactive)	No movement (0 mm)
Class S	slightly reactive	May experience only slight movement (0 – 20 mm)
Class M	moderately reactive	May experience Moderate movement (20 – 40 mm)
Class H1	highly reactive	High ground movement (40 – 60 mm)
Class H2	highly reactive	High ground movement (60 – 75 mm)
Class E	extremely reactive	Extreme ground movement (>75mm)
Class P	problematic soil	Problem Site

The Pindan has been successfully used as a pavement material in Western Australia, although limited information exists with pindan properties for road pavement. Collapsible soils have been stabilised by compacting the soil with high energy. When Pindan gets wet, it behaves like wet loose sand and has a low strength. However, the strength increases with high cohesion when the pindan is “dried back” after compaction. Pindan has self-cementation ability due to the bridging effect of clay under dry moisture conditions, which can be used as the material of the pavement layers, but it is a challenge to select the suitable Pindan for a pavement material due to its variability and difficulties in quality control. It is difficult to detect the suitability from visual inspection and simple laboratory tests to use Pindan for a pavement material (Emery et al., 2003).

2.3.3 Problems of Pindan soil

Tropical cyclones with heavy rainfall over short periods during wet seasons can damage the pavement structure and even the sealed roads are often flooded in the Kimberley region (Sinclair Knight Merz, 2009). It is widely recognised that the impact of water damage on pavement needs to be considered when designing roads to minimise moisture damage to pavement structures. It affects service life and contributes to durability problems. However, It is almost impossible to prevent water coming into the pavement structure as water can enter from many different sources, such as groundwater, snow and rain. Up to 40% of the rainfall gets into the pavement structure (ARA Inc, 2004). The effect on the pavement may show in various ways such as collapsing or expanding which can damage the pavement structure due to shrink-swell behaviour. Failure issues due to volume changes under pavement can be identified using material properties. Moisture also affects the bonding mechanism between the soil particles and between the pavement layers and makes the binding soft and weak (Gaaver, 2012). Kenneally et al. (1996) described the problem of Pindan as they become soft and greasy after water immersion and erode rapidly. Emery et al. (2003) also described Pindan as a red collapsible soil that can be densified under high enough load at a high moisture condition due to its high void ratio and low density, while unsaturated soils can be used in the pavement layer without a significant change in volume.

Thousands of problematic soils are across the world, which can be collapsing soils, expansive soils, loose sands, soft soils or soils subject to erosion. Pindan has two characteristics of softening and/or collapsibility under saturated conditions. Pindan is a moisture sensitive soil which earns its title by collapsing and losing strength when subjected to moisture ingress and it is very destructive to the pavement structure as collapsible soils can be easily changed in volume on moisture content, resulting in deformations that can cause uneven and even failure of the pavement structure on this soil (Emery et al., 2003), (Gaaver, 2012), (Kenneally et al., 1996).

The Kimberley region is a very large land and has a huge road network with a small population. Therefore, it is necessary to consider the cost savings by using local natural materials for roads. However, little research has been done on Pindan properties and problems of Pindan material. The Pindan material has been generally used for roads with low to medium traffic and it has also been successfully used on roads where many heavy vehicles travel in Western Australia (WA). However, the Pindan material used for the heavily trafficked roads must be constructed with correctly applied principles (Cocks et al., 2015).

2.3.4 Stabilisation of Pindan soil

Some of the gravels used as base-course materials in Western Australia are capable of self-stabilisation. As can be seen in Figure 2.2, the potential of increasing the strength of the lateritic gravel was proven in the 1989 data. Hamory and Ladner (1976) conducted Clegg impact tests to measure the potential strength gain over time using lateritic gravels on the Great Eastern Highway in Western Australia. Similarly, Kilvington and Hamory (1986) obtained the potential strength gain over time from calcrete and lateritic gravel base courses in the Kimberley region. The self-bonding over time was also presented in the red clayey sand (also known as Pindan) used as the base course on the Hamelin Denham Road in Western Australia (Main Roads, 2003).

A Pindan report (Western Australia. Department of Regional Development and the North West, 1984) provided information on Pindan soils proposed for use in making bricks by stabilising Pindan soil with cement. The strength tests were carried out on more than 30 selected Pindan soils of the North West Australia. They provided the properties of Pindan soils from Broome, Derby, Fitzroy Crossing, Pandanus Park,

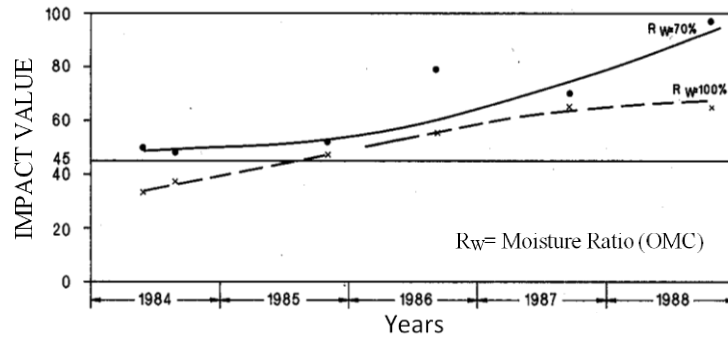


Figure 2.2: Strength change of Lateritic Gravel Base on Great Eastern Highway in Western Australia with Time (adopted after (Main Roads, 2003))

Wyndham, Carnarvon, Kununurra, Karratha and Port Hedland area. The samples from Broome, Derby, Fitzroy Crossing and Pandanus Park are basically similar in the mineralogical compositions from the basic properties of Pindan soils. The results of stabilised soils with a cement are as shown in Figure 2.3, the moisture-density graph showed very different results even in samples from the same area. Sample number 1 from the Derby area and the sample number 6 from the Fitzroy Crossing area show very different results in relation to moisture content and dry density of stabilised soil. The graph indicated that the dry density of Sample number 6 seems to be not affected by the moisture content while Sample number 1 had such a big effect on the moisture content. Even Samples 1 and 2 from the Derby area (but different locations in the Derby area) also show different relationships. The difference between the optimum moisture content and the maximum dry density between the Pindan samples is very large.

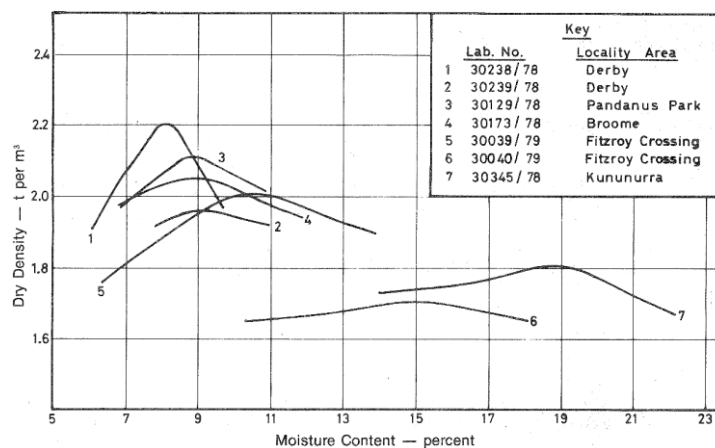


Figure 2.3: Variation of dry density with moisture content of a range of North West soils containing 10 percent Portland cement (Western Australia. Department of Regional Development and the North West, 1984)

Not only the relationship between the dry density and moisture content of stabilised Pindan soils was different and also the results of Unconfined Compression Strength (UCS) test show a big difference in strength even between samples from the same area as shown in Table 2.4. This table clearly illustrates the high variability of the Pindan soils in strength.

Table 2.4: Unconfined Compression Strength for cement Stabilised Pindan Soils (adopted after ((Western Australia. Department of Regional Development and the North West, 1984))

Soil Identification	Average Unconfined Compression Strength (MPa)				
	Dry Curing Period				
	No curing	14days	11weeks	24 weeks	50 weeks
Broome					
A	15.1	27.7	28.6	25.4	25.5
B	14.5	24.8	26.5	23.4	27.8
C	17.7	29.3	31.4	27.5	33.0
Derby					
A	28.8	34.6	40.6	33.9	40.4
B	11.0	18.5	20.2	15.8	21.8
C	12.1	23.1	22.8	18.3	2.2
D	18.1	29.0	29.	26.5	31.3
E	16.8	29.6	31.2	27.5	28.8
Fitzroy Crossing					
A	14.9	30.7	30.6	26.5	30.4
B	14.8	21.6	24.0	23.7	24.4
C	2.2	3.9	4.1	3.9	4.1
D	14.6	15.1	16.4	15.9	16.9
Wyndham					
A	7.0	9.3	9.6	7.2	5.7
B	4.9	5.0	4.1	3.1	3.3
C	5.2	10.2	9.5	7.3	9.3
Kununurra					
A	12.4	24.9	23.6	21.9	26.1
B	8.5	9.9	11.9	8.2	9.1
Pandanus Park					
A	18.4	32.0	30.6	27.2	32.8

Smith and Sullivan (2014) provided information on Pindan soils proposed for use on embankments structures in Pilbara, North Western Australia. Using highly erodible soils for the embankments structures, is a challenge and required to be controlled by appropriate embankment design and construction processes. They described Pindan soils as a material highly susceptible to erosion, therefore, they focused on erosion controls. Low-plasticity soils such as Pindan has been well studied and documented with stabilisation binders such as cement and lime. Emery *et al.* (2003) investigated on Pindan soils for the Broome Airport. In this study, cement, lime and bitumen emulsion stabilisers were compared. The cement and lime stabilised samples with low percentages of stabilisers provided satisfactory results but lost strength due to carbonation.

2.4 Unsealed Pavement

Approximately 60% of the Australian road network is unsealed roads. The role of the unsealed road network in Australia is very important for rural or local communities, mining and timber industries. It is also used as a transportation route for products and supplies. Therefore, improving the performance of unsealed road is an important issue in Australia. Stabilisation of unsealed road would result in safety, economic maintenance and ride quality (R. Andrews & Duffy, 2008). Unsealed roads typically carry light vehicles and about 10% are heavy vehicles, except for mine haul roads. Low volume rural roads are often built using locally available materials due to economic considerations, and the maintenance of roads can be done easily and quickly into service after damage (i.e. flooding) (Cocks et al., 2015), (Ferry, 1998). Therefore, locally available materials suitable for pavements are a valuable resource in Western Australia. A good understanding of fundamental pavement materials is important for the construction of unsealed pavement and they need to be tested and well managed to make good quality pavements in rural areas (Cocks et al., 2015).

There are four pavement layers in unsealed road structures as shown in Figure 2.4. Wearing course needs to be maintained when its thickness is reduced due to losing its fine materials as dust. Generally, in situ soils are used for the subgrade layer, and base layer protects against subgrade deformation (Austroads, 2009). Failures of the pavement can be due to the weakness in road pavement structures; surface, base, subbase or subgrade. Especially, unsealed pavements are susceptible to water and

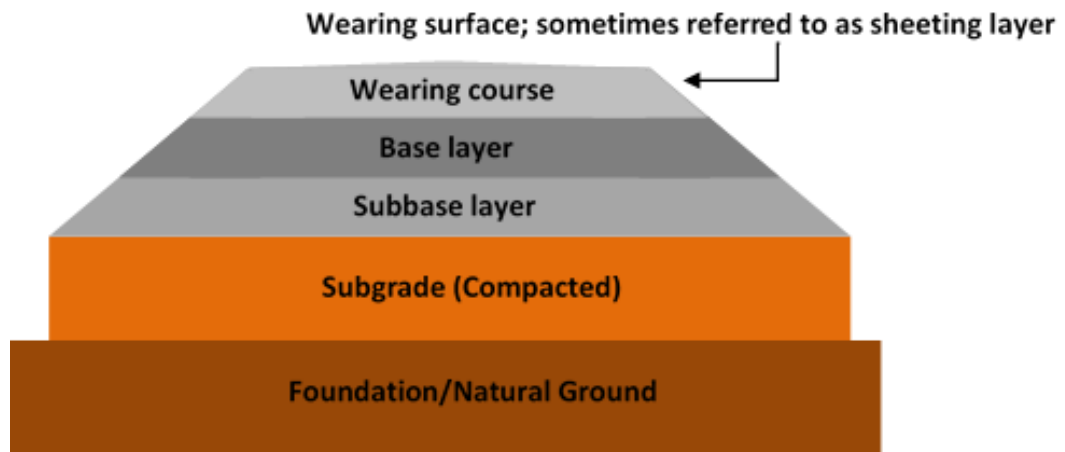


Figure 2.4: Unsealed road pavement layers (adopted after (Austroads, 2009))

erosion, so the materials for unsealed pavement are important and their properties must be examined to avoid potential problems (Cocks et al., 2015). Sediments produced from unsealed roads are caused by so many factors such as rainfall, wind, characteristics of surface materials, traffic volume and road slope. (Fu, Newham, & Ramos-Scharron, 2010). All materials on unsealed roads, which are susceptible to erosion must be protected through stabilisation. Soil erosion on pavement surfaces, resulting from water, is an issue in the unsealed pavement (Kemp, 2004). Half the wear loss from unsealed roads is due to climate-related without any traffic and up to 60% of sediments from unsealed roads is fine particles (e.g. clay and silt). Maintenance is, therefore, often required due to climatic erosion and vehicle attrition on unsealed pavements (Ferry, 1998), (Kemp, 2004). Some of the local materials for roads are required high serviceability even with low traffic. The principal factors such as stability, resistance to wear, impermeability and workability are considered as affecting the performance quality in relation to unsealed roads. These factors are also related to safety issues such as dust, poor resistance, tyre wear and vehicle damages with flying stones (Austroads, 2009).

Guide to Pavement Technology Part 6: Unsealed Pavements by Austroads (2009) provides a considerable volume of information on unsealed pavement with relevant technical information to guide the principles of unsealed road designs. As a guide, Table 2.5 suggests the minimum CBR values and the maximum permeability values

associated with the selected materials for unsealed roads. The recommended particle size distribution range for unsealed wearing course is shown in Figure 2.5 below. The design chart for granular pavements presented in Figure 2.6 represents a minimum structural thickness regarding the subgrade to protect from deformation during its life. The thickness of the subgrade is governed by CBR values and the minimum thickness of the base is 100mm. These information addresses unsealed pavement road materials and designs.

Table 2.5: Suggested CBR and Permeability Values for pavement material for unsealed roads (adopted after (Austroads, 2009))

Pavement layer	Minimum Typical CBR Value (Soaked)	Suggested Maximum Permeability (m/s)
Wearing Course	40%	1×10^{-4}
Base	50%	1×10^{-3}
Subbase	30%	

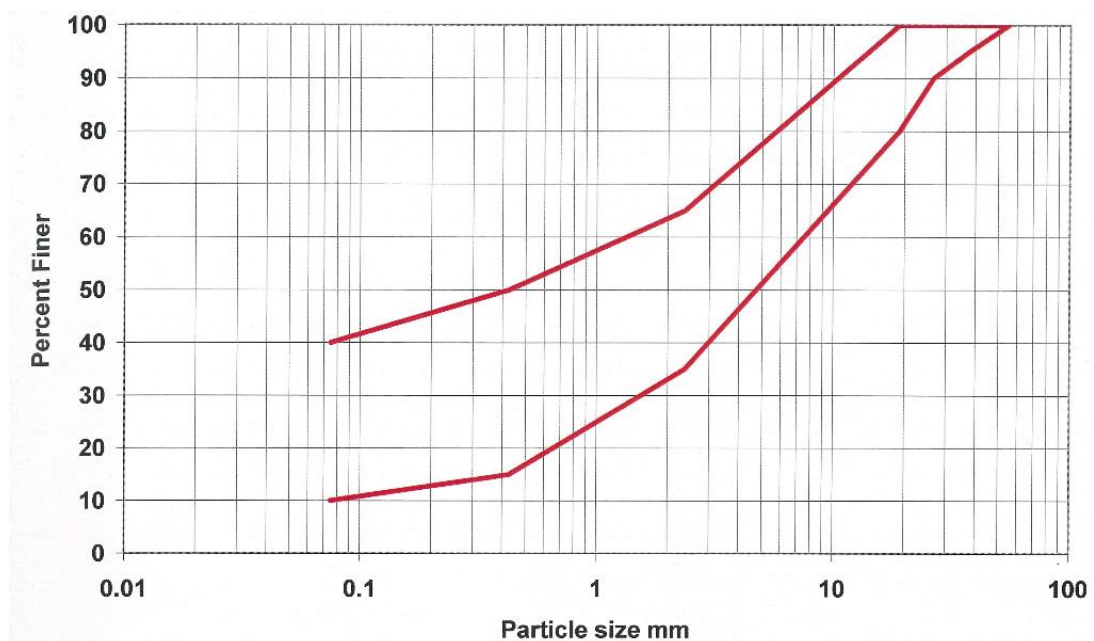


Figure 2.5: Suggested Particle Size Distribution Range for Unsealed wearing course (Austroads, 2009)

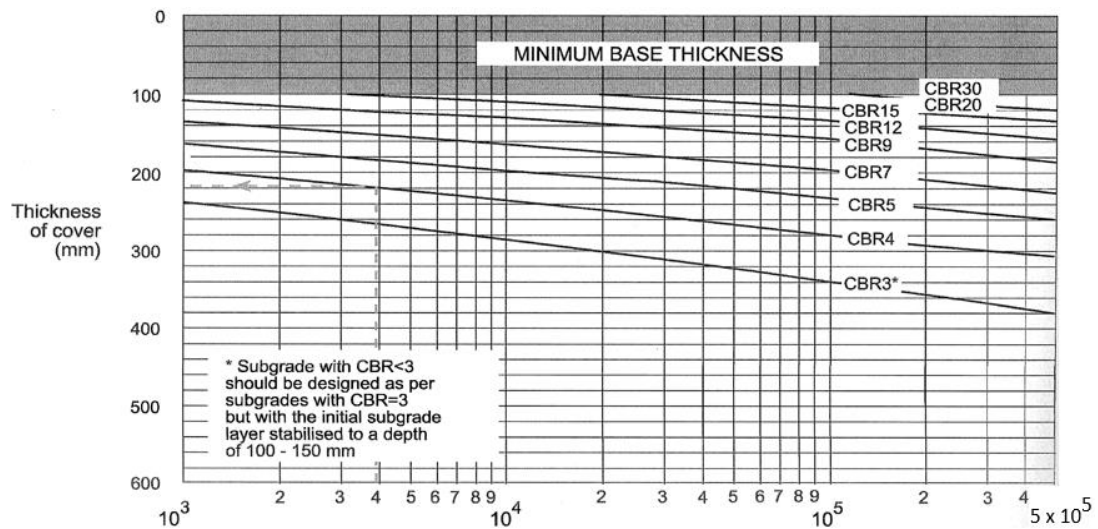


Figure 2.6: Design Chart for granular pavement (80% confidence) (Austrroads, 2009)

2.5 Problematic soil

In recent years, a lot of research has been done on problematic soils that are not suitable, but metastable to be used as the foundation of structures. Some researchers (Gaaver, 2012), (Lawton, Fragaszy, & Hetherington, 1992), (Khemissa & Mahamedi, 2014), (Kalantari, 2013), (Petry & Little, 2002), (Popescu, 1986), (Saride, Puppala, & Chikyala, 2013) have suggested various methods to identify these soils in order to stabilise the material and design the structures and the foundation of the structures in which the materials are used. Most of the problematic soils are sensitive to moisture, so volume can be changed as the moisture content increases. These types of soils are commonly collapsible or expansive or soft or weak soils, which decrease or increase in volume with or without applied stress when their moisture content changes. When water is applied to the problematic soils, their physical and chemical properties change (e.g. from dry and hard to wet and soft). These soils have different behaviours, movements and settlements, so they must be identified and designed to be used. They might be compacted easily due to low dry densities, low bearing capacity, low shear strength and very high compressibility behaviours. Billions of dollars have been spent on damages due to volumetric changes. These moisture sensitive soils are usually improved by stabilised with various types of binders such as Portland cement and lime, or by applying a preload with heavy compacted to increase the bearing capacity of soils. However, even when improved problematic soils are used, results in

volumetric change due to lack of information on the soils and sometimes the improvement of these soils are not properly achieved or disappears quickly over time.

Davenport (2007) investigated problematic soils throughout Western Australia (WA) in 2007 and identified the locations of the soils as shown in Table 2.6. It was also noted that the expansive clay soils commonly contain clay minerals of the smectite group and the collapsing soils have a structure of partly saturated open-voided soils. Both soil types have high moisture sensitivity to volume. When partly saturated with an open structure, significant changes in volume occur with or without external forces (Vázquez, Justo, & Durand, 2013).

Table 2.6: Location of Problem soils in Western Australia (adopted after (Davenport, 2007))

Expansive Soils Location in WA	Collapsible Soil Location in WA
Armadale, Boulder, Bunbury, Collie, Coolgardie, Dalwallinu, Geraldton, Gooseberry Hill, Jerramungup, Kalgoorlie, Katanning, Kununurra, Lake King, Mundijong, Moora, Newman, Ongerup, Perth metropolitan area (Kalamunda, Midland, Guilford, Swanview, Maylands, Kenwick, Maddington, Viveash), Ravensthorpe.	Balladonia, Broome, Cranbrook, Derby, Geraldton, Karratha, Newman, Perth coastal area, Port Hedland.

2.5.1 Identification of Collapse potential

Collapsible soils are one of the problematic soils and are defined as unsaturated soils that are stable and able to withstand relatively high pressures, but quickly become dense due to moisture intrusion. Collapsible soils are soils that when water is added they collapse at constant stress, which causes volume reduction. Identifying collapsible soils and predicting the potential collapsing behaviour are significantly important. Some laboratory tests have been proposed to detect collapsing behaviour (Gaaver, 2012).

Roger (1995) presented a general category of collapsible soils, which is either from compacted soils or natural soils as shown in Figure 2.7. Natural soils are formed during weathering process of parent rocks. Loess is an Aeolian deposit that normally

exhibits collapsing behaviour. Some alluvial soils that normally formed by water flow (e.g. flash flood) have the high collapsible potential. Also, Compacted soils may show collapsing behaviour (El Howayek, Huang, Bisnett, & Santagata, 2011). The potential for collapsing behaviour is also present in other soils when saturated, the soils that are “derived from volcanic tuff, gypsum, loose sands cemented by soluble salts, dispersive clays, and sodium-rich montmorillonite clays” (Clemence & Finbarr, 1981).

Predicting the collapsing potential through natural dry density and liquid limit (LL) was proposed in some papers (H. J. Gibbs & Holland, 1960), (Holtz, 1961), (H. J. Gibbs, 1961), (H. Gibbs & Bara, 1962) and was confirmed by Basma and Kallas (2004) and Gaaver (2012). They suggested that the density and liquid limit of collapsible soils can be used to measure the collapse potential which can be estimated from Figure 2.8. It can be used for all types of soil to evaluate collapsibility through simple tests. This method is based on the void ratio which can keep the moisture content at full saturation since the void ratio is sufficient for collapsing. When the specific gravity of the soil is above the line, the soil may be susceptible to collapse when saturated as collapsibility increases with respect to dry density decreases. It has also represented that the area under the curve signifies the soil with no collapsibility.

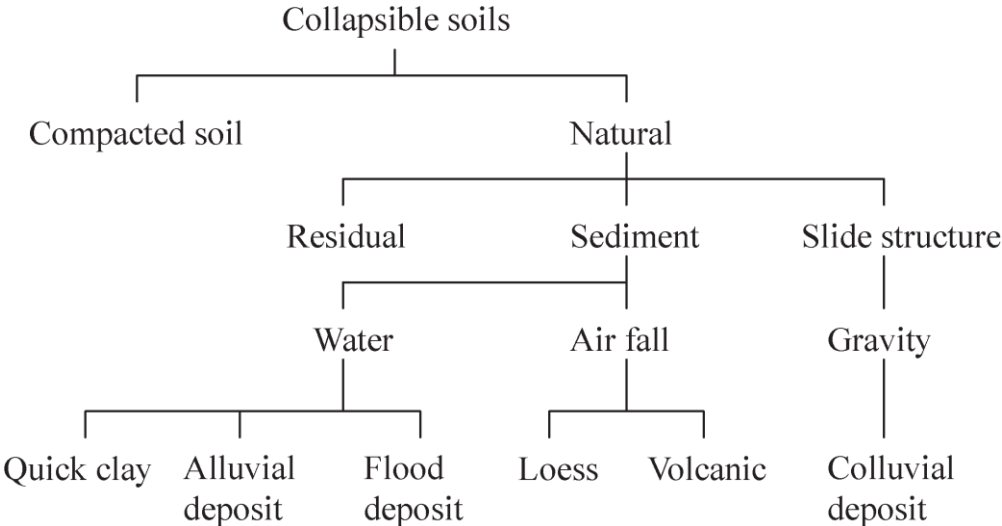


Figure 2.7: Classification of collapsible soils (Rogers, 1995)

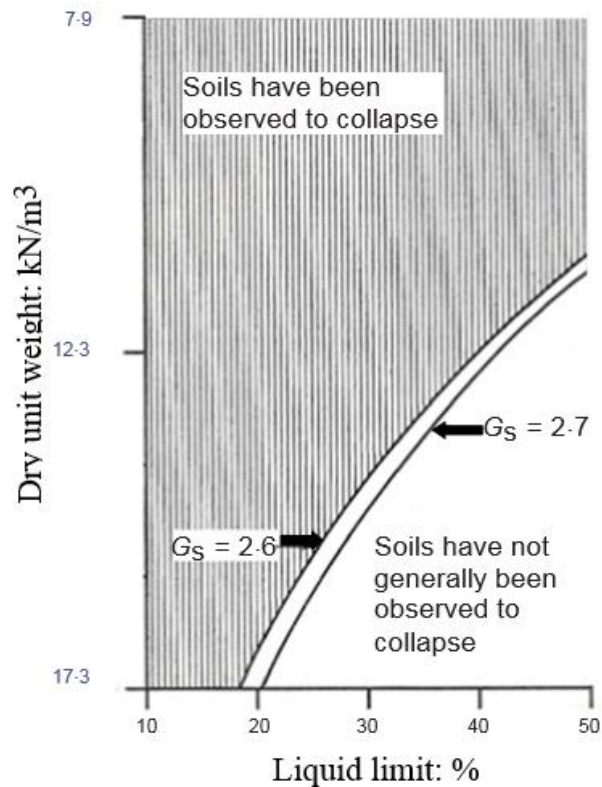


Figure 2.8: Criterion to identify soil collapsibility (adopted after (Holtz, 1961))

The standard oedometer test is performed on an undistributed sample of saturated soil as shown in Figure 2.9 in relation to vertical static load and void ratio. The first curve begins to flat and the point at which this flat curve ends is the preconsolidation pressure and as the preconsolidation pressure passes, the slope of the curve steeply declines. Compression index can be obtained from this steep curve section. Apart of evaluating the collapse potential through the single oedometer test, another procedure of a single oedometer method was suggested in 1975. By observing the single oedometer test, the collapse potential can be obtained as presented in Figure 2.10. Gradually increase the load on the sample up to a specific stress (about 200kPa) and allow the sample to remain in the water for 24hrs and continue to load the sample until the maximum load (Kalantari, 2013). Jennings and Knight (1957) proposed the double oedometer test as an alternative method. Two oedometer tests were conducted for each specimen in pre-saturated condition and natural moisture content condition. The distance between the two curves of the oedometer test results presented in Figure 2.11 can predict the collapse potential.

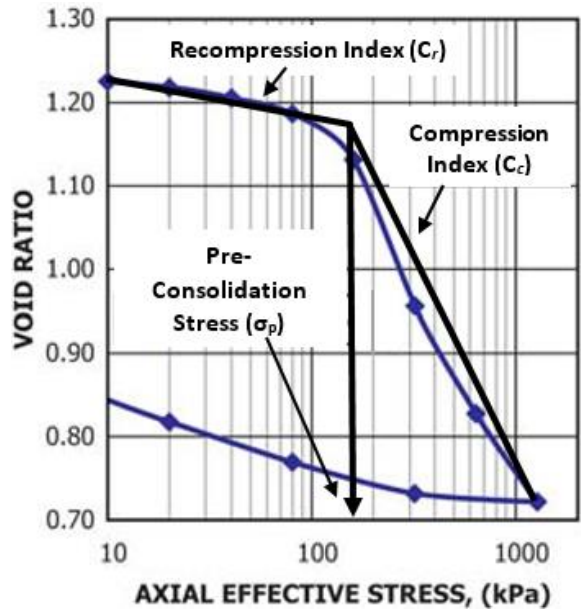


Figure 2.9: Typical Consolidation Test Result (ASTM International, 2011b)

Table 2.2, which provides a relative indication, can be used to indicate the degree of severity for collapsible soils from the results of the double oedometer test. Figure 2.10 and Figure 2.11 display typical single and double oedometer test results for collapsible soils in relation to void ratio and effective stress to predict collapse potential. Both methods are based on the void ratio and assuming that the void ratio is the same when the soil is wet, regardless of whether it is before or after the effective stress (Popescu, 1986).

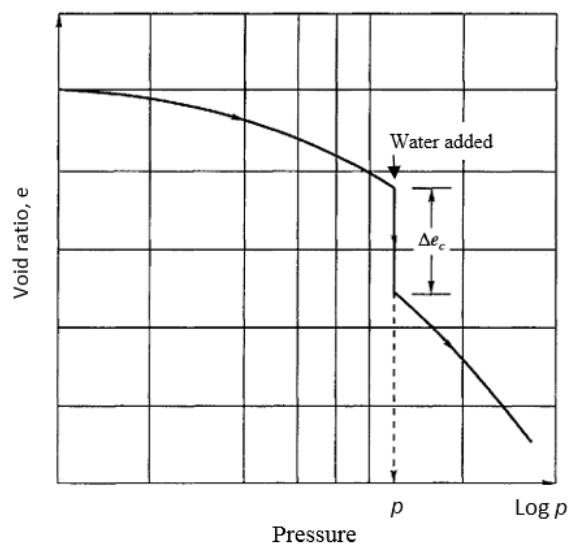


Figure 2.10: Typical Single oedometer collapse potential test result (Pells et al., 1975)

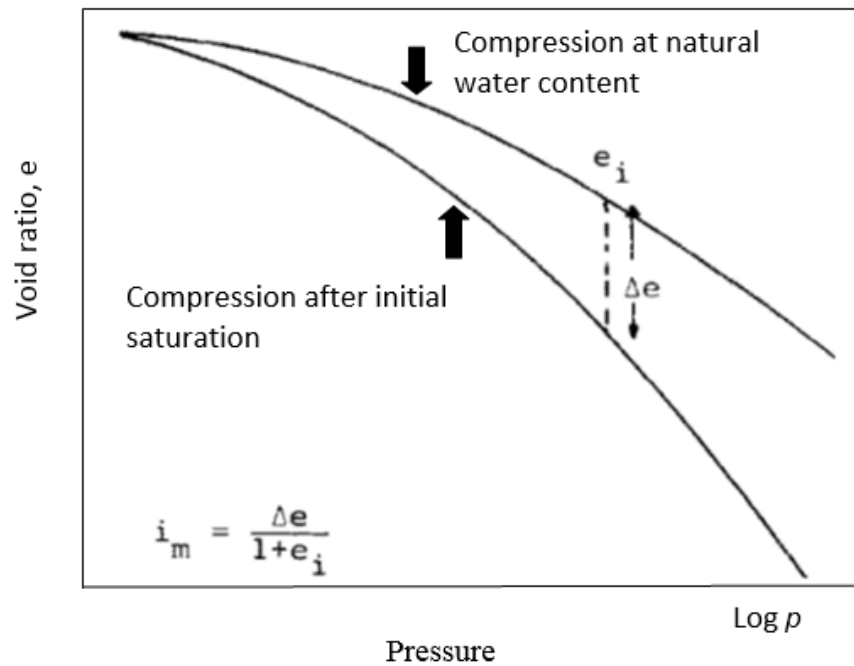


Figure 2.11: Typical Double oedometer collapse potential test result (Lutenegger & Saber, 1988)

Popescu (1986) defined the collapse potential using the double oedometer test, where P_{cs} and P_{cn} are the limiting pressure at which collapsing increases considerably for the samples performed respectively at saturated and natural conditions as presented in Figure 2.12. When the stress at P_{cn} is higher than the stress at P_{cs} , the soil refers to the collapsible soil. Truly collapsible soils and conditionally collapsible soils are distinguished using pressures P_{cs} and P_o , where P_o is the overburden vertical pressure. If the pressure P_o is higher than the pressure P_{cs} , it signifies that the soil has a certain degree of collapsibility defined as “truly collapsible”. And when the pressure P_o is lower than the pressure P_{cs} , it signifies the soil defined as “conditionally collapsible” that possess a certain degree of collapsibility but supports a certain level of stress upon wetting. If the pressure P_{cs} is higher than the pressure P_o , the soils are able to withstand the pressure without collapsing upon saturation until the pressure P_o is higher than the pressure P_{cs} .

The collapse deformation begins from a small stress value, called the collapse pressure. After the collapse pressure point, the deformation due to water is significantly increased and then a fairly constant value is obtained.

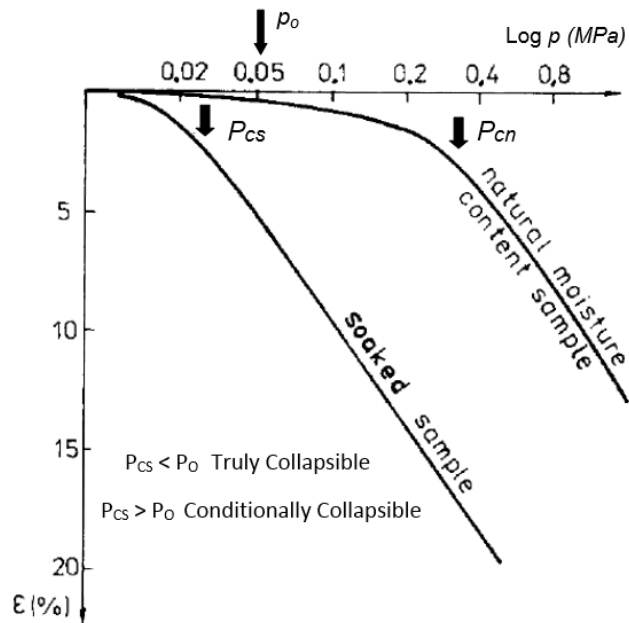


Figure 2.12: Collapse pressure definition (Popescu, 1986)

2.5.2 Bonding and Collapsing Mechanism

According to Barden et al., Dudley and Mitchell, the collapse occurred in four factors (Elkady, 2002). The soil would be an open structure and partially unstable, and a high enough applied load that develops to be metastable. And a bonding or cementing agent to stabilise the soil, which leads to collapse upon wetting, and water that reduces the strength of bonding or cementing agents. There are a number of bonding forms due to self-cementation or physical or chemical attraction. They can be simple capillary forces with a fine silt binder or clay bridges or soluble salts or chemical cementing binders such as calcium carbonate and iron oxide. The physical bonding is weakened by moisture, and the capillary suction loses its strength as soon as water is added. Figure 2.13 illustrates the typical bonding structures of collapsible soils, and the structure of undisturbed collapsible soils and clay bridges from Scanning Electron Microscope (SEM) pictures are provided in Figure 2.14. It provides a representative structure and clay bonding of unsaturated collapsible soils. Figure 2.14(A) indicates the open structure with a loose arrangement and Figure 2.14(B) and (C) indicate the inner particles bonded by clay bridges. The sand grains are not fully coated with clays but the particles are still connected with clay bonding (Haeri, Garakani, Khosravi, & Meehan, 2013), (El Howayek et al., 2011).

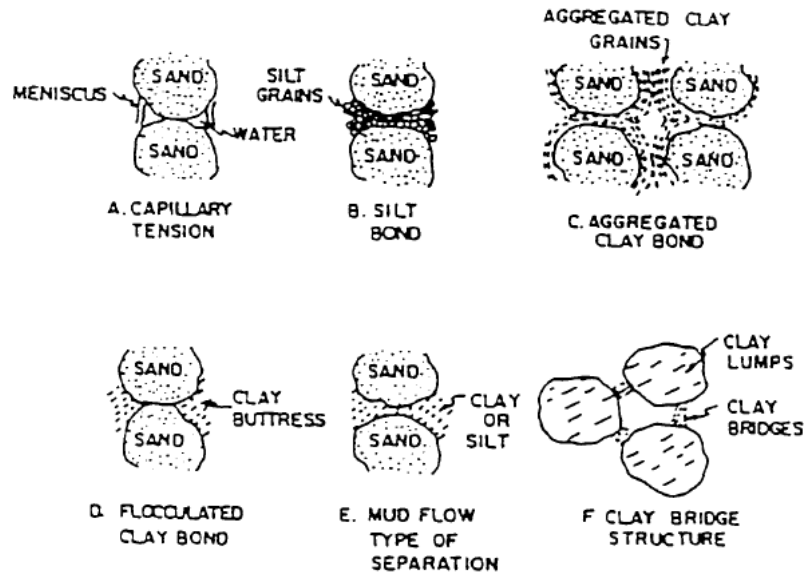


Figure 2.13: Typical Bonding structure of collapsible soils (Clemence & Finbarr, 1981)

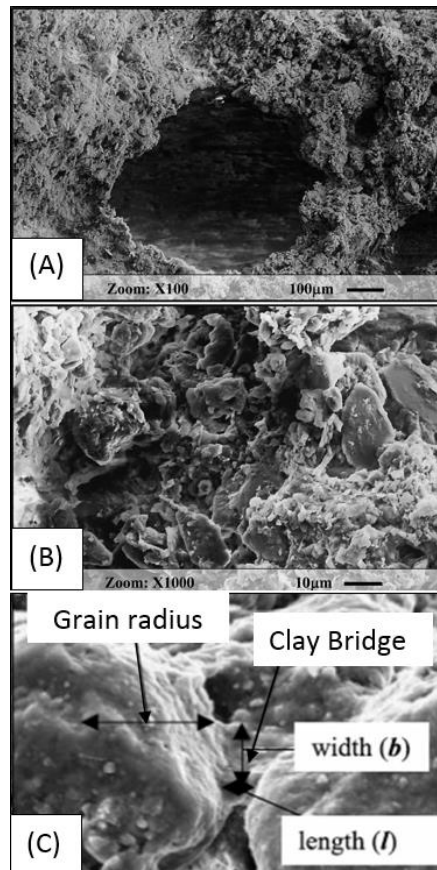


Figure 2.14: Microstructure of collapsible soils and Clay Bridges from SEM (adopted after (Haeri et al., 2013), (Jackson et al., 2006). (a) Loose and Open structure. (b) Cementation of clay matrices form. (c) Clay bridge bonds.

2.6 Soil Stabilisation

Numerous soil types demonstrate problems due to their characteristics and behaviours such as swelling, dispersion, softness, collapse and weak strength. There are a number of problematic soils that need to be stabilised to be used. Soil stabilisation has been discussed and researched for solving soil problems. Soil stabilisers are used to increase strength and durability, and to reduce sediment (erosion), dust, and maintenance requirements to meet the requirements of engineering projects. Many stabilisers have been used to improve soil performance with mechanical or chemical stabilisation. Soil treatment using products such as sulphur cement, lime, polymers, cement, electrolytes, enzymes, chlorides, clay, resin, fly ash and some combination of these have been commonly used in the past. The stability and strength of soils are always considered in design and construction. There are a number of methods for soil stabilisation can be selected depending on the soil properties and conditions of the construction site. There are three stabilisations; mechanical, chemical and geosynthetic soil stabilisation. Mechanical stabilisation generally has two different methods of replacing or mixing the problematic soils with suitable soils, and another method is compacting on the soil to improve strength, compression, water absorption, permeability and stress-strain characteristics. And, chemical soil stabilisation produces new properties by mixing some chemical compounds in the problematic soils. Geo-synthetic soil stabilisation includes geogrids, geowebbs and geotextiles and is used to upgrade highway sub-grade conditions (Mohamed & El Gamal, 2012), (Huat et al., 2007).

There are traditional stabilisations such as cement, lime, fly ash and asphalt, which require high cost, large amounts and long curing times. And non-tradition stabilisations such as polymers, electrolytes, tree resins, salts, mineral pitches, enzymes and petroleum emulsions, which need to be more researched due to lack of information while traditional stabilisation has been well researched and widely used. (Santoni, Tingle, & Nieves, 2005), (Mohamed & El Gamal, 2012), (Tingle, Newman, Larson, Weiss, & Rushing, 2007).

2.6.1 Non-traditional soil stabiliser

Engineers have tried to produce soil improvement using different methods over the years. Typically, lime, Portland cement and fly ash are widely used and are considered

as traditional stabilisers which are generally based on cation exchange or pozzolanic reactions (Little & Nair, 2009). However, the traditional stabilisers such as cement and lime have been proven in many studies to have major disadvantages such as carbonation, sulphate attack and various environment impacts (Jawad, Taha, Majeed, & Khan, 2014).

Non-traditional stabilisation is one of the most important methods used recently. Non-traditional stabilisers have been used and developed for soil stabilisation purposes due to low cost, short curing time and ease of application compared to traditional stabilisation. Non-traditional stabilisers, such as polymer and copolymer based products and calcium chloride, sodium chloride and fibre reinforcement, have been used. Non-traditional pavement stabilisation has been popularly used in recent years, but most of the non-traditional stabilisers are based on a variety of chemical agents and been modified based on market tendency and, therefore, there is not much information on recent products due to frequent modifications of chemical formulas (Santoni et al., 2005). And, unlike traditional stabilisers, little literature has been conducted on the mechanism of non-traditional stabilisers, since most of them focus on the performance evaluation on non-traditional stabilisation (Tingle et al., 2007).

Table 2.7 proposed by Tingle et al. (2007) presents a summary of stabilisation mechanism for seven non-traditional additives. Ionic stabilisers react slowly and are material-dependent, and salts stabilisers require humidity to be active. Polymer stabilisers are effective in sandy soils and organic stabilisers make the bonds between fine particles and larger aggregates to interlink. Biological stabilisers are one of the chemical binders that require a high content of clay. Clay additives also make bonds between soil particles (B. Andrews, 2006), (Tingle et al., 2007).

Santoni et al. (2005) stabilised a silty sand (SM) using nine non-traditional stabilisers, two traditional stabilisers and two accelerator products to enhance the strength of the soil. Two accelerator products; a Cement and a Polymer are designed to accelerate for helping the strength improvement quickly during the stabilisation process. They evaluated strength improvement related curing times and focused on increased early strength using non-traditional stabilisers with accelerate products to reduce cure times. A tree resin, a silicate, a lignosulfonate and six different polymers are used as non-traditional stabilisers, and an acrylic polymer and a Type I Portland cement product

are used as two accelerator products in this paper. An asphalt emulsion and a cement are used as traditional stabilisers for comparison with the non-traditional stabilisers. All samples were cured up to 7 days. All soils with nine non-stabilisers developed more than doubled in strength within 7 days when compared to the strength of 1 day cured samples. Traditional stabilisers provided high performance waterproofing with significantly high resistance to water. Soils mixed with cement increased strength in both wet and dry conditions, but soils mixed emulsified asphalt increased strength only in wet conditions. Emulsified asphalt actually reduced the soil strength in dry condition. Lignosulfonate showed high water resistance but did not affect the strength of the SM soil even used with accelerators together. Some of the polymers did greatly improve the strength of the soil. However, some other polymers produced a decrease in strength, and stabilisers, a polymer and a silicate without accelerators are weakened by moisture and are disintegrated by contact with water. Traditional and non-traditional stabilisers produced an increase or decrease or no effect in strength under at dry and wet conditions, but non-traditional stabilisers provided significantly strength improvements in 1 to 7days. It was proved that non-traditional stabilisation can rapidly develop soil strength within 7days for both dry and wet conditions.

And, several researchers investigated stabilised soils with non-traditional stabilisers. Natural and synthetic stabilisers have been used to stabilise various soils; clay soils mixed with Alginate and wool fibre (Galán-Marín, Rivera-Gómez, & Petric, 2010), soft clay soils mixed with fibres (fibrillated polypropylene, monofilament polypropylene, nylon and PVA fibres) (Rafalko, Brandon, Filz, & Mitchell, 2007), expansive clays mixed with two polymers (Formaldehyde and melamine formaldehyde) (Yazdandoust & Yasrobi, 2010), silty sands mixed with emulsion copolymer (poly methyl Mehta acrylate) (S. Naeini & Mahdavi, 2009) and epoxy resin polymer emulsion (mixtures of epoxy resin and polyamide hardener) (S. A. Naeini & Ghorbanalizadeh, 2010) were investigated and some other papers (Newman & Tingle, 2004), (Newman, Gill, & McCaffrey, 2007), (Al-Khanbashi & Abdalla, 2006) also studied on polymer stabilised soils. They focused on stabilisation of soils using non-traditional stabilisers or mixtures of traditional stabilisers and non-traditional stabilisers to improve and evaluate its engineering performance and some of them compared to traditional stabilisers. Some papers (Waseim R Azzam, 2014), (Liu et al., 2011), (Blanton, Majumdar, & Melpolder, 2000) revealed the bonding

structures between the soil particles and between the soil particles and stabilisers. However, most of the above-mentioned studies focused on engineering performances such as shear, flexural, compressive strength and swelling potential.

Table 2.7: Proposed stabilisation mechanisms for Non-traditional stabilisation (adopted after (Tingle et al., 2007))

Stabilisation Additive	Stabilisation Mechanism	Additional Information
Ionic	Cationic exchange and flocculation	Altering the electrolyte concentration of the pore fluid
Enzymes	Organic molecule encapsulation	Variations in the soil-specific reactions
Lignosulfonates	Physical bonding/cementation	Coating individual soil particles
Salts	Hygroscopy/cation exchange and flocculation/crystallisation and cementation	Keep the soils moist that from environment, which increases effective particle size by surface tension
Petroleum Resins	Physical bonding/cementation	Coating individual soil particles
Polymers	Physical bonding/cementation	Coating individual fine soil particles
Tree resins	Physical bonding/cementation	Coating individual soil particles

2.6.2 Polymer Stabiliser

Polymer is a material consisting of macromolecules that made up of repeating monomers bonded together by covalent bonds. The characteristics of the polymer depend on the mixture of monomers (molecules). There are various types of polymers that may be natural or synthetic. In general, polymers can be classified based on structures or molecular forces or made of polymerisation or origin of source. The structural characteristics of the polymers (i.e. polymer chains) can be linear or branched or cross-linked or networked, which is related to material properties (Kumar & Gupta, 2003). Yoshihiko Ohama (1998) provided a classification of polymer-based admixtures as shown in Figure 2.15. He studied about polymer modified mortars and

concrete. A polymer-based admixture is an admixture which contains a polymeric compound as a main element effective for improving the properties of concrete. Generally, most of the produced polymers are homopolymers. The polymer latexes are copolymers that composed of two or more different monomers.

Polymer stabilisation has been increased and researched to solve soil problems and to find technological applications. Numerous researches have been done on polymer modified soil stabilisation using various polymers in different types of soils. Shirsavkar and Koranne (2010) investigated on the soil modified with natural polymers such as molasses. The results showed that the natural polymers reduced the plasticity index and increased the maximum dry density and California Bearing Ratio of the soil. Natural polymers have a great potential to be used as road stabilisers. For example, there is an industrial waste such as molasses used in the above paper.

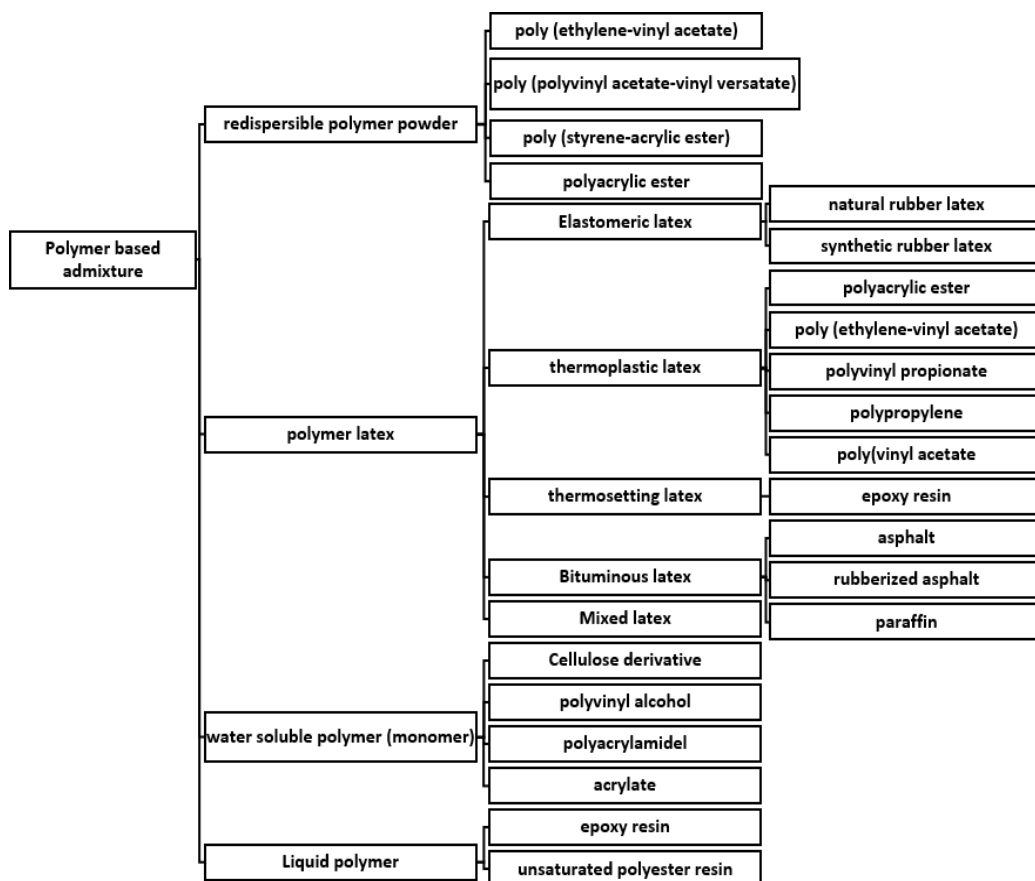


Figure 2.15: Classification of Polymer-based admixtures (Ohama, 1998)

Polymer soil stabilisation experiments has been performed using waterborne polymers (S. A. Naeini, Naderinia, & Izadi, 2012), polymeric materials (Moustafa,

Bazaraa, & Nour El Din, 1981), polymer grids (Miura, Sakai, Taesiri, Yamanouchi, & Yasuhara, 1990), synthetic polymers (Homauoni & Yasrobi, 2011), (Zandieh & Yasrobi, 2010) and polymer based mixtures (Ateş, 2013). The polymers were applied to various soils and examined using physical and mechanical tests. It was observed that the polymers are very varied in the applicability and performance and that the amount of polymer is significantly important when determining strength. The performance of polymers varied greatly depending on the type of soil. Some of the polymers worked well only in specific soil types, but most of the polymers showed successful results in the strength experiments.

Polymers have been widely used to stabilise the lack of suitable soils. The use of polymer stabilisers for soil improvement is growing rapidly. However, since little research has been documented on interaction or reaction between polymer and soil, the application of polymers is limited due to the lack of information on the relationship between polymer and soil (Ateş, 2013), (Waseim R Azzam, 2014), (Waseim Ragab Azzam, 2014).

2.6.3 Polymer stabilised soil for pavement

Polymers are used in a variety of ways for road stabilisation reasons and can be used for dust suppression or soil stabilisation or performance improvement. Some polymers have been provided excellent performance as stabilisers for pavement constructions. The use of polymers is not only good for cost but also for performance. Srinath et al. (2012) stabilised gravel-sand-silt-clay mixtures (GM-GC) containing less than 2% (by volume) of Palygorskite clay with three different water-soluble polymers. Untreated soils and treated soils were tested and polymer modified soils were compared with the Portland cement (Type 1) treated soils using mechanical and microstructural properties. The performance analysis results of polymer stabilised soils showed higher UCS, stiffness and toughness compared to Portland cement stabilised soils.

Polymer-modified asphalts have been successfully used on heavy-duty vehicle routes such as airports and vehicle weigh stations. Ramasamooj (2001) tested for jointed rigid airport pavements using polymer composites. The E-glass polyesters provided good flexibility and fatigue resistance with high tensile strength. Yildirim (2007) reviewed polymer modified asphalt binders such as rubber, styrene-butadiene-styrene

(SBR), styrene-butadiene-rubber (SBS) and Elvaloy® to research the rheological properties of polymers used as asphalt binders. The polymers modified pavements have been shown to be highly resistance to rutting and thermal cracking, and to reduce fatigue damage and stripping. Some other researchers (Lynde & Brooks, 2005), (Tayfur, Ozen, & Aksoy, 2007), (Al-Hadidy & Yi-qiu, 2009), (Lu, Soenen, Heyrman, & Redelius, 2013) used polymers as an additive in asphalt road construction. They focused on improving the service life (durability) of asphalt pavements and the impact of polymers on the stripping resistance of asphalt pavements in the field. The polymer provided a good aging resistance, and improved shear resistance and durability with higher resistance to rutting and cracking. Polymer modified binders tend to improve viscosity and elastic recovery. Compatibility between an asphalt and a modifier can cause poor performance. Improvement of elastic recovery, softening point, ductility and cohesive strength in the pavement design are the main objectives of the polymer modified binders. In fact, asphalts modified with different polymers can behave very differently, even when developed or altered for modified binders. They may come out very differently in a force ductility test and measurements of softening point and elastic recovery.

It has been proved that the polymers can improve soil mechanical properties such as strength. On unsealed roads, however, dust and soil loss are another matter because road dust and soil loss affect safety, dust control and soil loss prevention are issues that need to be considered with unsealed roads. Most of the soils lost from the road are fine aggregates that provide a bond between larger particles. Loosing fine aggregates cause the road roughness and the incidence of vehicle damage to increase. Polymer additives used for roads have been applied on unsealed roads to reduce dust levels and erosion and improve resistance to water. Dust control can be achieved by stabilising with synthetic polymer emulsions, for example, polymer dispersions, (Shirsavkar & Koranne, 2010). Waterproofing is one of the best ways to stabilise the soil. This is because the bond between the soil particles is weakened by water and the soil particles become softer when wetted. The polymer can provide “internal waterproofing” which reduces the general softening and lubrication of the incoming moisture in the granular pavement (Lacey, 2004).

2.7 Summary

Pindan is a local term used to describe the soil of the Kimberley, a type of red soil known as a moisture-sensitive soil in the Kimberley area. The characteristics of Pindan soil produce the greatest susceptibility to densification during wetting. Pindan presents high variability in strength and collapsibility even in similar properties. Some Pindan samples from other locations in the Kimberley region have similar properties, but they showed different strengths and collapsibility and also even occurred in samples from other locations in the same area. The Kimberley region has two distinct seasons; wet and dry season. Typical wet periods have high rainfall, high humidity and high temperature, and sometimes even tropical cyclones. These tropical cyclones cause damage to the road when accompanied by heavy rain for a short time.

Pavement structures may come in contact with water from rain or snow or groundwater. The moisture weakens the bonds between aggregates or between aggregates and binders. Moisture damages on pavement structures can cause unexpected collapse or expansive issues due to large volume changes under the pavement, which result uneven pavement surfaces. To prevent the moisture damages in pavements, it is important to consider the moisture susceptibility of materials or substances when pavements are designed and built. The failure issues due to volume changes under the pavement can be identified using material properties. In particular, unsealed pavements are susceptible to water and erosion, so the materials for the unsealed pavement are important and their properties must be examined to prevent potential problems. Improvements to unsealed road networks would solve the issues of lower safety, performance and high maintenance costs.

Soil classification systems can provide information about types of soils, which can predict their properties and behaviours on the fields. The shrink-swell capacity of soils, which can damage roads and structures, can be predicted by the expected behaviours of the soil using the classification systems. The determination of collapsible soil can be completed by analysing the information of the soil in terms of dry density, liquid limits, single and double oedometer methods can be used to identify the collapsibility of the soil.

Non-traditional stabilisation has been used popularly and has become increasingly available for engineering purposes as an alternative to traditional stabilisation due to

its low cost and easy application. Polymer modified soils are present in a number of conducted studies. Most polymers have been successful in improving soil strength, waterproofing and dust suppression. And, polymer modification roads in high-stress locations have been successfully used.

However, most of the researches are limited to physical and mechanical performance and there is no information about Pindan particles. A single particle of Pindan needs to be identified to found out the properties of Pindan particles. In order to improve the performance of unsealed pavement roads, it is necessary to identify the properties of problematic soils and Polymers, and research the pavement stabilisation. Research on Pindan soils and polymer stabilised Pindan soils need to be more conducted due to the lack of information to be used for pavement structures.

Chapter 3

3 Preliminary Test

3.1 Introduction

Pindan soils used in this study are located in Broome within the Kimberley region of Western Australia. This chapter contains preliminary tests to obtain a representative sample of Broome-Pindan soils and investigate the properties of collapsibility of the Pindan soil. The preliminary tests include particle size distribution, index, specific gravity, collapsibility, texture, standard compaction and California Bearing Ratio (CBR) tests. Particle size distribution and index testing are performed to identify the classification of the Pindan soil samples and to compare the samples collected from different locations. Standard compaction and CBR tests are performed to compare the mechanical properties of the samples, and double oedometer test is carried out to identify the potential collapsibility of the Broome-Pindan soil since the Pindan soils exhibit high variability in strength and collapsibility according to literature reviews (Emery et al., 2003), (Sinclair Knight Merz, 2009), (Western Australia. Department of Regional Development and the North West, 1984). This chapter proves and provides the representative sample of Broome-Pindan samples.

There were two validations in order to combine the Pindan samples for making a representative sample of Broome-Pindan soils. The basic properties and basic mechanical properties of the samples were used to combine the samples. The proposed methodology in this chapter is shown in Figure 3.1. All samples and mixtures were compared as well as comparison of two area samples; Gantheaume Point Rd (G.P) and Cape Leveque (C.L). All samples were compared and combined through classification tests, and the raw materials and mixtures were compared through compaction tests to combine them together. G.P samples and C.L samples were compared by CBR tests to obtain a representative sample. The samples were verified using two validation properties, physical and mechanical properties, through several experiments to determine whether they can be combined as a representative sample of Broome-Pindan soils.

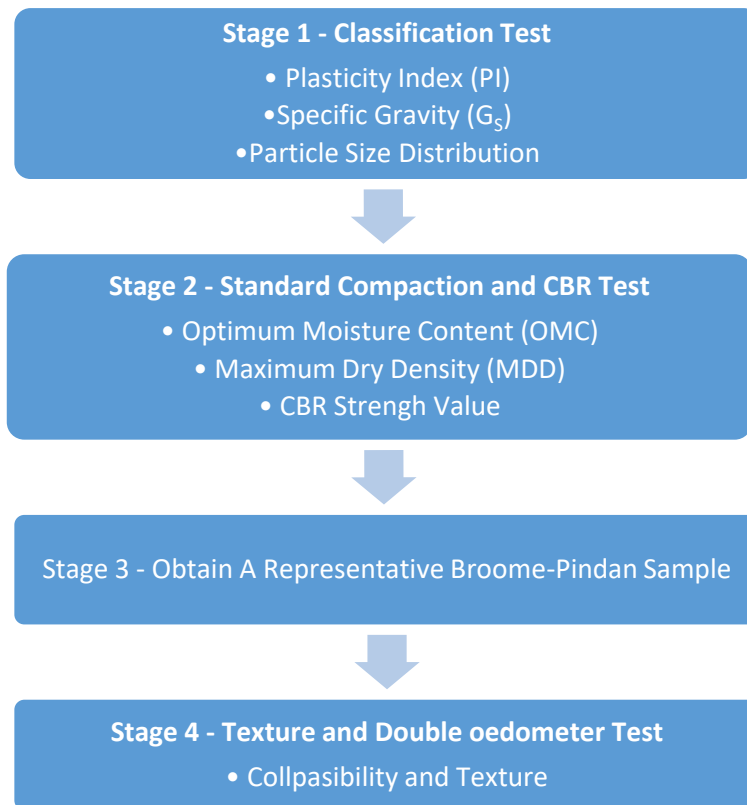


Figure 3.1: Chapter3 Overall Flow Chart

3.2 Pindan Properties and classification

Soils can be divided into classification categories based on basic physical characteristics such as index properties. Soil classification systems generally group soils together with similar properties into relatively broad categories because soils have a variety of characteristic and behaviours. The basic mechanical properties of the Broome Pindan samples can be obtained by performing the compaction and California Bearing Ratio (CBR) tests.

3.2.1 Index Properties and Classification Test

The results of index and classification tests are provided in this chapter. Specific gravity and Atterberg limit tests were carried out according to AS 1289.3.5.1 (2006) and ASTM D4318 (2010), respectively. Particle size distribution was performed in accordance with AS 1289.3.6.1 (2009) and classified according to the Unified soil classification system ASTM D2487 (2011a). The tests were determined from disturbed soil samples. Seven Pindan samples collected locally in two sites of Broome shown in Table 3.1 were used for the index and classification tests.

Table 3.1: Seven Broome-Pindan samples for Index and Classification Test

Collected location	
Gantheaume Point Rd (G.P)	Cape Levique (C.L)
Raw material	Raw material
Shoulder	Surface (site1)
Surface	Shoulder (site2)
	Surface (site2)

Specific gravity testing to determine the particle density of Pindan samples is calculated based on void ratio, degree of saturation and temperature. Specific gravity is required to calculate soil porosity. The plasticity index (PI) is calculated based on the difference between the liquid limit (LL) and the plastic limit (PL). The plasticity index (PI) is obtained by the following relationship provided by ASTM D4318 (2010):

$$PI = LL - PL \quad (3.2.1)$$

where PI is the plasticity index, LL is the liquid limit and PL is the plastic limit of the soil. The soil is considered as Non-Plastic (NP) if the plastic limit is zero or has a negative number or if the plastic limit or liquid limit cannot be determined. Shrinkage limit (SL), liquid limit (LL) and plastic limit (PL) of fine grained soils can be determined through the Atterberg limit test that based on the moisture content of the soil. The results of the specific gravity and plasticity index of the seven Broome-Pindan samples are shown in Table 3.2. Liquid limit of the samples could not be determined, therefore, the Broome-Pindan soils are considered as non-plastic. Pindan soils have a specific gravity ranging from 2.57 to 2.61, which means that Pindan soils contains a large amount of porous particles. Broome-Pindan soils are non-plastic soils based on the plasticity index, which means that it generally tends to have little silt or clay.

Quantitative determination by sieve analysis was used in this study. This system is used to determine soil gradations. The particle size distribution of the seven samples for Broome-Pindan soils is presented in Figure 3.2. Soils can be classified by their physical and chemical composition, but they are more influenced by their physical properties (e.g. size). Chemical analysis of soils is not essential for soil classification.

Table 3.2: Specific gravity and Plasticity index of Broome-Pindan

Pindan Soil	Specific Gravity (G_s)	Plasticity Index (PI)
G.P Raw	2.60	Non-Plastic
G.P Surface	2.60	
G.P Shoulder	2.57	
C.L Raw	2.61	
C.L Surface 1	2.59	
C.L Surface 2	2.59	
C.L Shoulder	2.58	

In this study, the samples were classified according to their particle size distribution and plasticity. Table 3.3 provides the percentage of gravel, sand and silt of the seven samples based on the Unified soil classification system ASTM D2487 (2011a). The classification of the Broome-Pindan soils was derived from the particle size distribution as shown in Table 3.4. The seven Broome-Pindan samples are classified as silty sand (SM) according to the Unified soil classification system ASTM D2487 (2011a). The Broome-Pindan samples are in the same classification category, therefore, the samples can be grouped into a single sample.

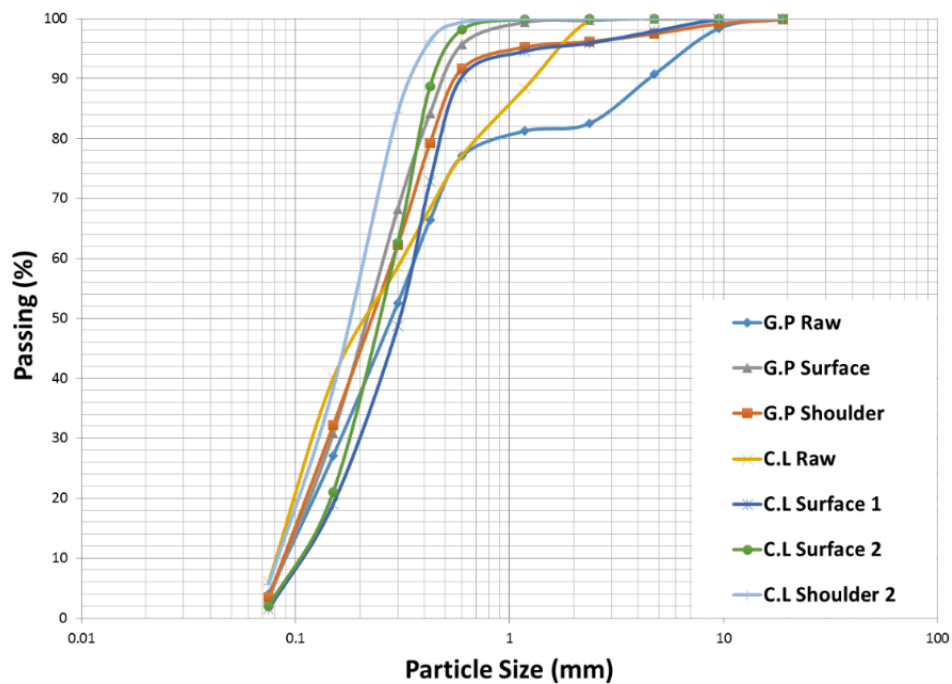


Figure 3.2: Particle Size Distribution of Broome-Pindan Soil

Table 3.3: Percentage of Gravel, Sand and Silt of Broome-Pindan Soil

Component	G.P	G.P	G.P	C.L	C.L	C.L	C.L
	Raw	Surface	Shoulder	Raw	Surface 1	Surface 2	Shoulder 2
Gravel %	9.31	2.55	0.01	0.16	2.11	0.02	0.01
Sand %	86.65	93.99	96.7	93.81	96.36	98.03	94.29
Silt %	4.04	3.46	3.29	6.03	1.53	1.95	5.70

Table 3.4: Classification of Broome-Pindan soil

Soil Classification	
G.P Raw	
G.P Surface	
G.P Shoulder	
C.L Raw	Silty Sand (SM)
C.L Surface 1	
C.L Surface 2	
C.L Shoulder	

3.2.2 Mechanical Properties

Since they belong to the same classification category, the Broome-Pindan samples can be grouped together, but even if they have similar basic properties, Pindan soils may show different strengths according to a report (Western Australia. Department of Regional Development and the North West, 1984). In this chapter, more tests such as compaction and strength tests are carried out to compare the basic mechanical properties of Broome-Pindan samples in order to obtain a representative Broome-Pindan sample.

The bearing capacity of soils has been used to design pavement structures. The California Bearing Ratio (CBR) test is developed by California state highway Department. It is a simple test for evaluating the mechanical strength of soils using its resistance against the pushed plunger. It is also used in a quick and inexpensive method instead of a Triaxial test to evaluate the resilient modulus of soils. The CBR test was performed according to AS 1289.6.1.1 (2014) using the standard proctor

compaction effort with the standard compaction rammer described in Australia standard AS 1289.5.1.1(2017b).

In addition, the compaction test was performed on Pindan samples in accordance with the standard proctor procedure, AS1289.5.1.1 (2017b). Compaction is the process of densification of soils to reduce subsequent settlement under working loads by reducing the void ratio. The compaction test was carried out to determine the moisture-density relationship of the soil. This test provides for understanding characteristics of the compacted soil with changes in moisture content. Moisture content has a significant impact on behavioural properties of soils and also compressive resistance and shear strength are related to soil density because higher density of soils can resistance to higher compression.

3.2.2.1 Compaction Test

There are six group of samples to investigate; raw materials, unsealed road materials and mixtures of these two group of samples as shown in Table 3.5 for compaction tests. This chapter provides the comparison of raw materials, materials from the unsealed roads and the mixtures of raw materials and materials from the unsealed roads using compaction tests.

The standard proctor test was used as detailed in AS1289.5.1.1 (2017b) to achieve the relationship between the dry density and moisture content of the soils as presented in Figure 3.3. The test was performed to obtain the respective optimum moisture content correspondence to its maximum dry density and to provide the air-voids contents. It can be generally seen that an increase of the soil density accompanies by a decrease of the air volume. The results did not show any moisture-sensitivity behaviour in the

Table 3.5: Six Broome-Pindan Samples for Compaction Test

Six Broome-Pindan samples for Compaction Test	
G.P Raw	C.L Raw
G.P Mixture 1 (Surface + Shoulder)	C.L Mixture 1 (Surface + Shoulder)
G.P Mixture 2 (Raw + Surface + Shoulder)	C.L Mixture 2 (Raw+ Surface + Shoulder)

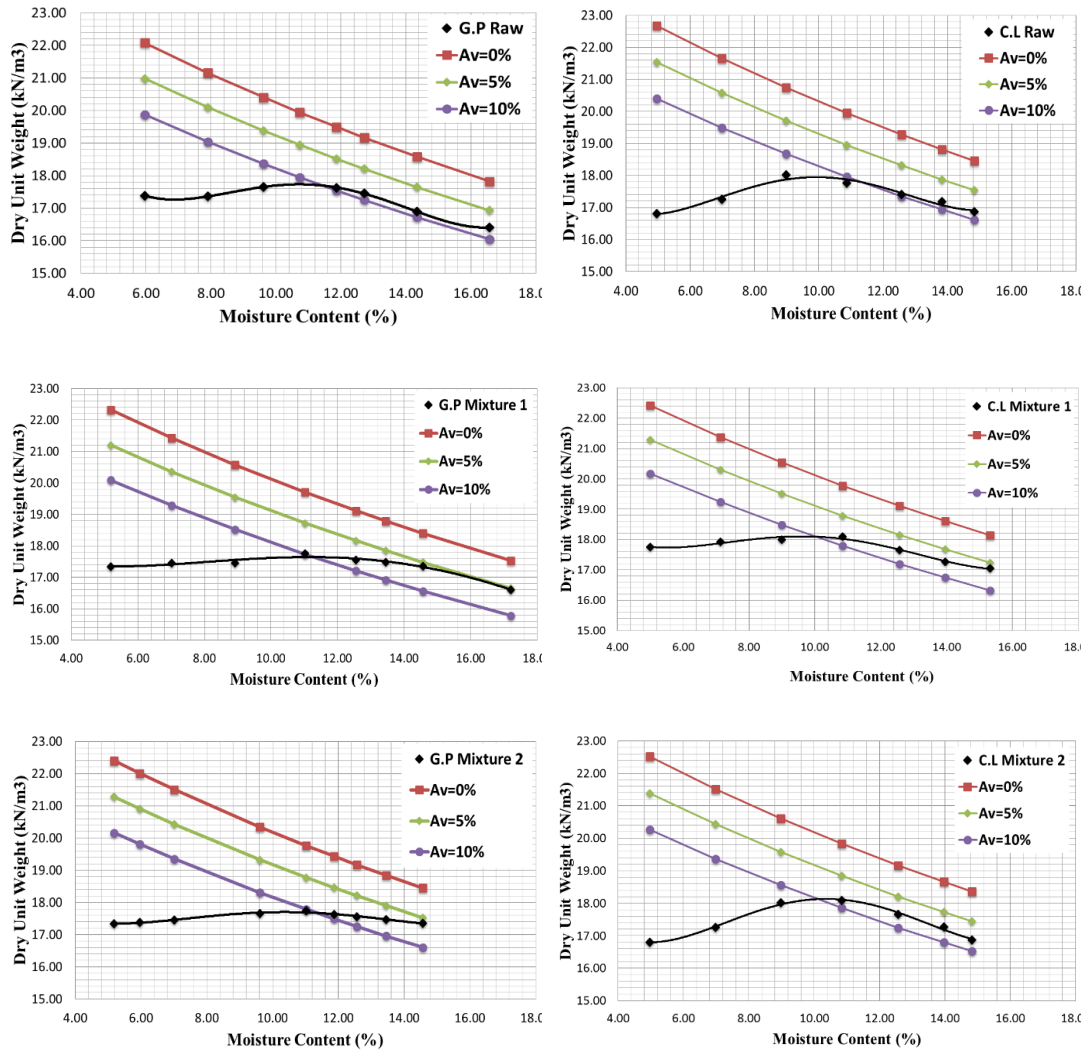


Figure 3.3: Compaction Test of Broome-Pindan Soil with Air-voids (Av) curve

Table 3.6: Optimum Moisture Contents (OMC) and Maximum Dry Density (MDD) of Broome-Pindan Soils

Standard Proctor Compaction Test		
Sample	OMC (%)	MDD (KN/m ³)
G.P Raw	10.8	17.7
G.P Mixture 1	11.2	17.6
G.P Mixture 2	10.8	17.7
C.L Raw	10.0	17.9
C.L Mixture 1	9.8	18.1
C.L Mixture 2	10.2	18.1

compaction tests as most of the moisture-density curves were nearly flat. Table 3.6 provides the values for the optimum moisture content (OMC) and maximum dry density (MDD) of the six Pindan samples that lies between 9.8 to 10.8 % and 17.6 to 18.1 KN/m³, respectively. They displayed similar OMC and MDD results and showed no signification change with increasing moisture content in the compaction test.

3.2.2.2 California Bearing Ratio (CBR) Test

The Broome-Pindan samples can be grouped together as they are in the same classification category with similar OMC and MDD values. In this chapter, two samples; Mixtures of Raw, Surface and Shoulder from Gantheaume Point Rd and Cape Levique were used and the strength of two Pindan samples were checked in order to mix them together. The comparison of materials from Gantheaume Point Rd (G.P) and Cape Levique (C.L) were carried out through CBR tests as shown in Figure 3.4. CBR test is used for evaluating the suitability of the subgrade, subbase and base for flexible pavement design. This test was conducted on remoulded samples.

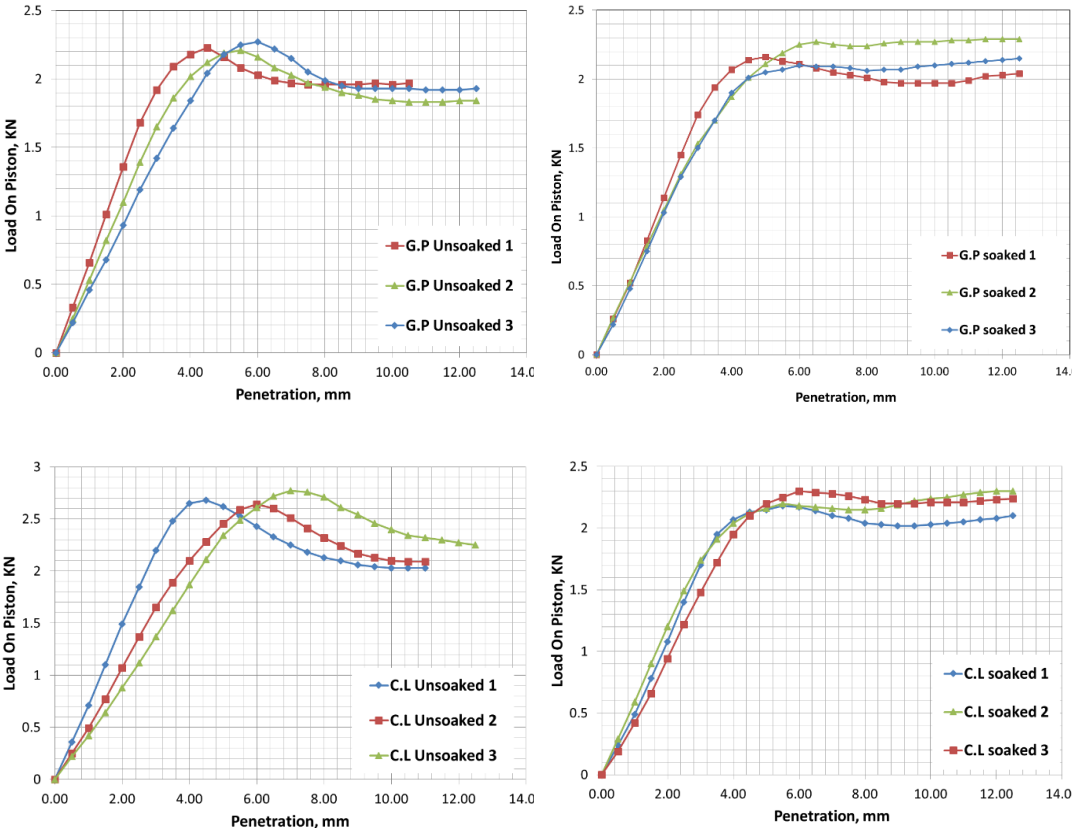


Figure 3.4: Load-Penetration Curves of Broome-Pindan Soil

The graphical representation in Figure 3.4 established the relationship between the penetration and the load on a piston for the Broome-Pindan samples. These tests were performed immediately after compaction for unsoaked samples. For soaked samples, the samples were soaked for 4 days in water after compaction, and then a penetration test was conducted. All samples were compacted to exceed 95% of the standard proctor maximum dry density (MDD). Table 3.7 provides CBR values for the unsoaked and soaked samples, and swelling percentage for the soaked samples. The laboratory density ratio (LDR) of the specimens is also provided in the table, which are the achieved dry density ratio in the laboratory. The relative compaction was to be 95% to 98% of MDD for all test. The CBR values were calculated for penetration of 2.5mm and 5mm. The CBR values in Table 3.7 were selected with a greater value of either the CBR value at 2.5mm or 5mm. The CBR tests on the unsoaked Broome-Pindan samples result in the range CBR 11.01 – 12.72% for G.P samples and CBR

Table 3.7: California Bearing Ratio (CBR) Test Results for Broome-Pindan soil

Sample No.	CBR (%)	Swell (%)	Dry Density before Soaking (g/cm ³)	LDR (%)
G.P - Unsoaked Condition				
1	12.72		1.75	96.8
2	11.06		1.77	97.9
3	11.01	N/A	1.75	97.0
Average	11.60			
G.P - Soaked Condition				
1	10.98	-0.08	1.76	97.3
2	10.66	-0.11	1.75	97.2
3	10.35	-0.06	1.75	96.8
Average	10.66			
C.L - Unsoaked Condition				
1	14.00		1.79	97.2
2	12.40		1.79	96.8
3	11.82	N/A	1.77	95.9
Average	12.74			
C.L - Soaked Condition				
1	10.86	0	1.78	96.7
2	11.29	-0.08	1.79	96.9
3	11.11	-0.15	1.77	95.9
Average	11.09			

11.82 – 14.00% for C.L samples and on soaked samples result in CBR 10.35 – 10.98% for G.P samples and CBR 10.86 – 11.29% for C.L samples. Based on CBR test results, the Broome-Pindan soils are able to use as a road material for pavement structures of subgrade, subbase and base at both dry and wet conditions.

3.2.3 A Representative of Broome-Pindan Soil

The specimen must be representative of the soils from which they were taken. Figure 3.5 represents the particle size distribution interval of the Broome-Pindan samples collected from different location in Broome, which represents the particle size distribution interval of representative samples. It has proven to be able to combine the Broome-Pindan samples as they have similar properties and behaviours. This chapter further provides information on the texture of Broome-Pindan soils and the collapse potential of a representative Broome-Pindan soil sample.

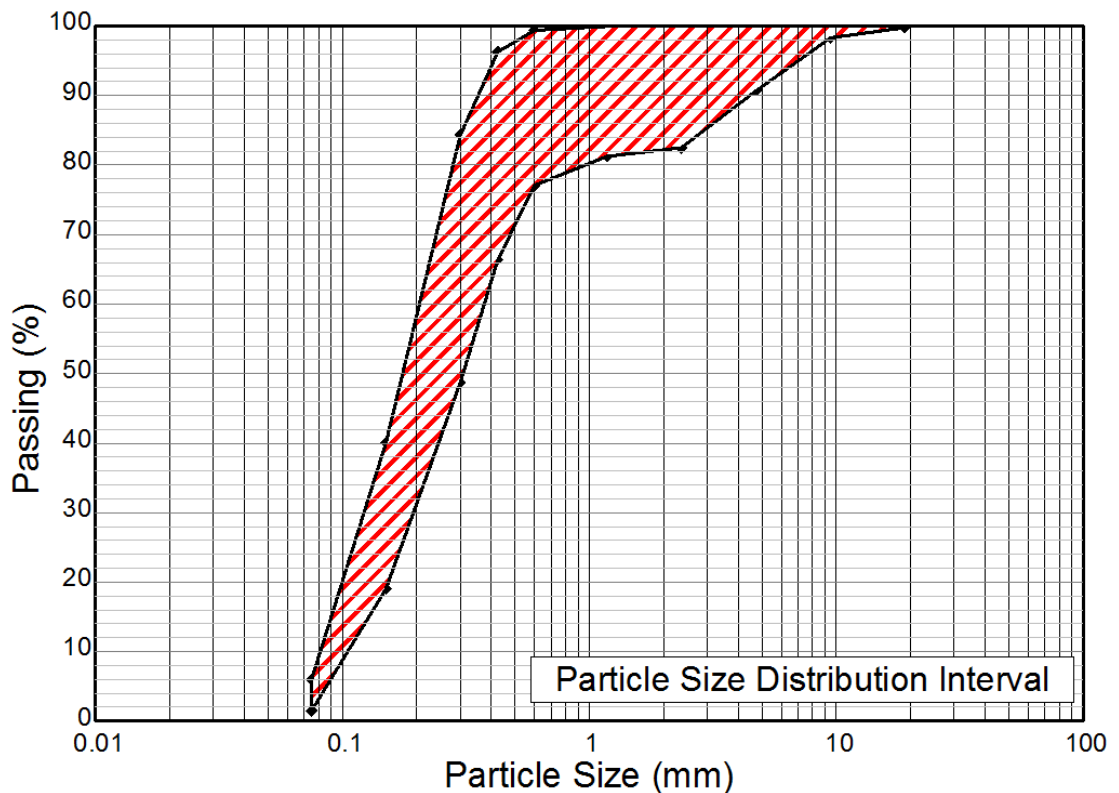


Figure 3.5: Particle Size Distribution Interval for A Representative Broome-Pindan Soil

3.2.4 Collapsible Potential and Texture

Pindan located in Broome has been studied by a few researchers. According to Kenneally et al. (1996), Pindan becomes soft and greasy when pindan is wet and Emery et al. (2003) described Pindan as a collapsible soil but an engineering report by Sinclair Knight Merz (2009) classified Pindan located in Broome as a slightly-reactive or non-reactive site in relation to increasing moisture content. This chapter investigates the texture information and collapsible potential of a representative Broome-Pindan sample used in this study.

The double odometer method was used for determining the Broome-Pindan soil collapse potential. Each sample was used in a dry and fully saturated conditions, respectively. The test was performed based on ASTM D2435/2435M (2011b) with particles less than 2.36mm in soil samples. The sample was saturated for 24hours to make the soaked condition while the other is kept at its natural moisture content. The consolidometer was placed in the loading machine applied with 6kPa seating pressure. The results were recorded for each increment at 6, 12.5, 25, 50, 100, 200, 400 and 800kPa. The samples were tested in remoulded condition as it is very difficult to keep the undisturbed condition in the laboratory. Emery et al. (2003) also mentioned the Pindan samples classified as silty sand (SM) could not be tested due to the characteristic of very friable in an undisturbed condition. The results of the double oedometer test are presented in Figure 3.6 for unsaturated and saturated samples. For the unsaturated and saturated samples, a large change in the void ratio was initiated in the double oedometer test at vertical stresses of 200kPa and 100kPa, respectively. The results were plotted using corrected data for ease of comparison. The results in Figure 3.6 clearly show that the soaked condition of the sample experienced higher void ratio than the unsoaked condition. The saturated specimen was weakened by water and more densified due to reducing the frictional and bonding strengths of soils. The result in Figure 3.7 shows the collapse index versus the applied stress calculated based on the graph in Figure 3.6 using the following Equation (3.2.2) (Pells et al., 1975):

$$C_p = \frac{\Delta e}{1+e^o} \times 100 \quad (3.2.2)$$

where C_p is collapse potential, Δe is difference or change in void ratio between dry and wet specimens and e^o is initial void ratio of specimens.

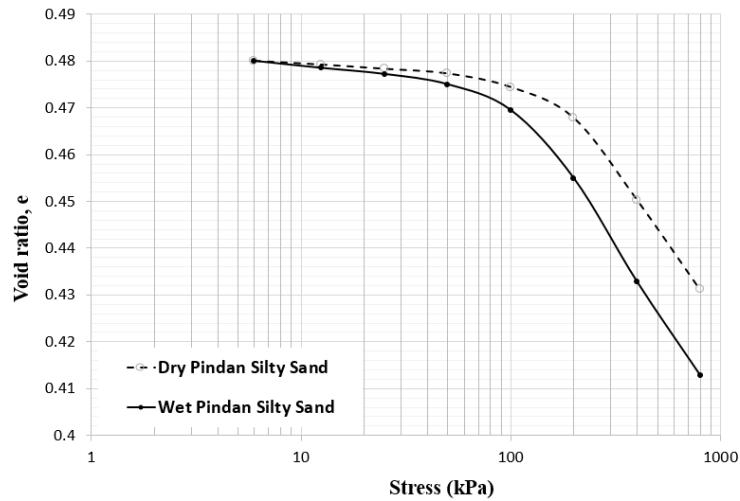


Figure 3.6: Void Ratio vs Applied Stress Test on Unsaturated and Saturated Sample

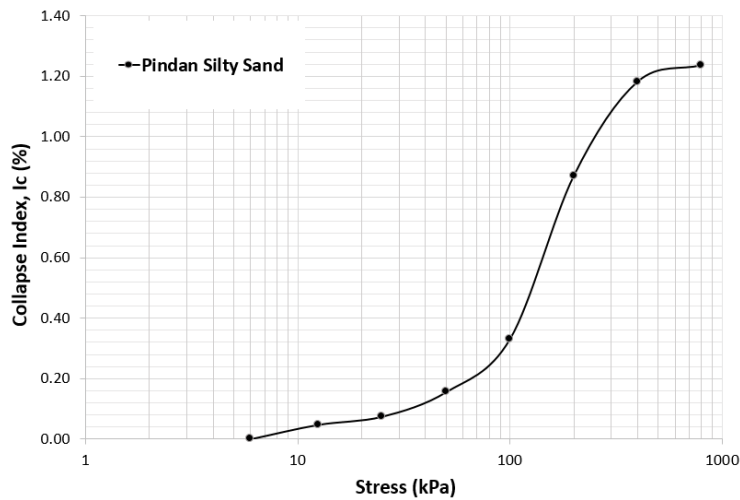


Figure 3.7: Collapse Index vs Stress

In the double oedometer test, the collapse index between the two samples was rapidly increased between 100KPa and 200KPa, and the largest collapse index of 1.24% between two samples was recorded at 800KPa. The collapse index of 1.24% corresponds to a moderate trouble soil (i.e. a slightly collapsible soil) according to Table 2.2 guide to collapse potential values. The results of the double oedometer test on Broome-Pindan specimens did not display any significant collapsibility (i.e. collapse potential). The specimens showed similar behaviour to Pindan soils located in Broome reported in the engineering report of Sinclair Knight Merz (2009) as they classified the soil as slightly-reactive or non-reactive with respect to water content.

The basic information of the texture was identified by a feel test. The Pindan samples have a red colour as shown in Figure 3.8. The Pindan samples are very loose and friable and have no soil adheres to fingers at dry condition, and as moisture increases, they were becoming very smooth, soft and sticky. The large particles fall apart easily between fingers with gently squeeze and are easily crumbled by fingers in dry condition. Figure 3.9(A) and (B) provide photos of the Broome-Pindan sand at OMC and wet condition, respectively. As shown in Figure 3.9(A) and (B), the sample becomes wet sand when the moisture content increased; becoming soft and sticky similar to a mud condition. The sample became highly compressible due to losing its strength, which may cause problems on unsealed road surfaces. And it became slippery materials that wheels might fall into a loose and wet sand. Figure 3.9(C) and (D) are a sample when dry-back. It may exhibit surface cracks in the field similarly as shown in Figure 3.9(D) that applied a small pressure on dry sand in Figure 3.9(C).

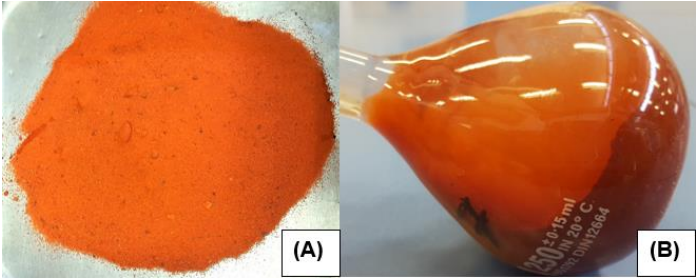


Figure 3.8: Sample of Pindan Soil Located in Broome. (A) Pindan Sand. (B) Pindan Sand in Water for Specific gravity testing.

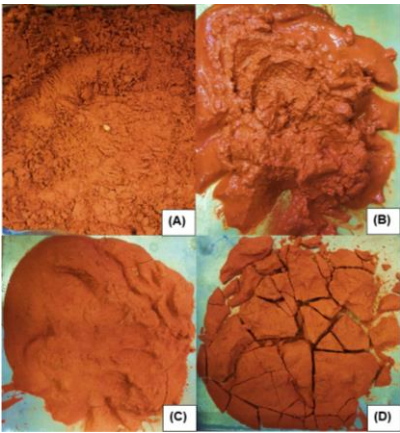


Figure 3.9: Wet and Dry Broome-Pindan Sand. (A) Optimum Moisture Condition. (B) Wet Sand. (C) Dry-back after full-saturated. (D) Cracks on sand in dry condition.

Double oedometer test results for Broome-Pindan specimens display the level of collapsible potential in a low degree so the materials are able to use as a pavement structure material, but the soil needs to be stabilised for use as a surface material of unsealed roads.

3.3 Summary

Index and classification tests to identify the basic properties of the Broome-Pindan soil and strength tests to determine engineering design parameters are carried out, and texture and collapsibility tests are also investigated in this chapter. The laboratory tests indicated that the Pindan samples are Silty Sand (SM) contains 0.1-9.31% gravel, 86.65-98.03% sand and 1.53-6.03% silty and clay contents with the plasticity index of non-plastic. The samples were verified and combined by index, classification, compaction and CBR tests to produce a representative soil of Broome-Pindan soils. All tests were used to compare the different samples and provided basic information of the samples. The samples were compacted to be greater than 95% of standard proctor maximum dry density for CBR and collapsibility tests. It is noted that moisture-sensitivity behaviour did not be presented in the compaction and CBR tests. Based on CBR test results, the Broome-Pindan soil can be used as a road material for base, subbase and subgrade pavement structures in both dry and wet conditions. The strength of Broome-Pindan samples is high enough for pavement design with a low collapse potential in the result of the double oedometer test. However, based on texture of the soil, it may cause a problem on the surface of the unsealed roads as it became soft and lost strength when water was added. The soil is highly compressible in a wet condition, and the soil was easily crumbed due to high friability at dry moisture condition. The compacted pindan soil showed satisfactory strength in confined conditions, but it may not have satisfactory strength without being stabilised in unconfined conditions.

Chapter 4

4 Nanoindentation

4.1 Introduction

The soil characteristics of the site are one of the most important factors for road construction. However, in order to know the properties of the soil properly, sometimes it is necessary to do some in situ field testings for the properties in natural state. Therefore, the standard soil investigation methods such as the standard penetration test (SPT) and pressuremeter are widely used, but they are not simple experiments. Nanoindentation can provide the properties of individual phases of materials in the in-situ condition. Many researchers (Constantinides, Chandran, Ulm, & Van Vliet, 2006), (Constantinides & Ulm, 2007), (Bobko & Ulm, 2008), (Ulm et al., 2007), (Lee, Vimonsatit, & Chindaprasirt, 2016), (Borodich, Keer, & Korach, 2003), (Durst, Göken, & Vehoff, 2004), (Durst, Backes, Franke, & Göken, 2006), (Mondal, Shah, & Marks, 2007) have studied the nanoindentation method to verify the method with properties of microstructure using multiscale mechanical modelling. Constantinides, Chandran, Ulm, & Van Vliet (2006) has also verified the nanoindentation analysis of composite microstructure and mechanics using “continuum indentation analysis”. To use his proposed methodology, the indentation depth needs to be chosen carefully. Representative volume Element (RVE) is one of the most significant elements of the continuum indentation analysis to provide information about heterogeneous materials. The condition of RVE of continuum approach for homogeneous materials is that the characteristic of the material at a length scale of L_i must confirm to the length scale separability condition as (Constantinides et al., 2006):

$$d_i \ll L_i \ll (h_i, a_i, D_i) \quad (4.1.1)$$

when d_i , h_i , a_i and D_i are the characteristic length scale of the local heterogeneities in RVE, the indentation depth, the indentation radius and characteristic microstructural length scale, respectively. Figure 4.1 illustrates the principles of indentation testing in relation to Equation 4.1.1.

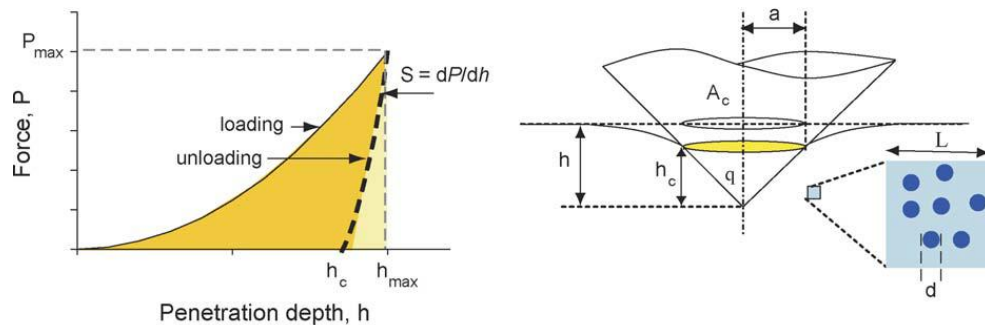


Figure 4.1: Principles of Indentation Testing (Constantinides et al., 2006).

In order to evaluate the mechanical behaviour and to determine the mechanical properties of individual soil grains, nanoindentation tests using Berkovich indenter tip was conducted on individual Pindan red sands from Broom, Kimberley Region of Western Australia. The hardness and Young's modulus were measured from the load – displacement curve and the fracture toughness was obtained based on the analysis of indentation process. An application of nanoindentation technique was successfully made for the microporomechanics of Pindan sand, and a wide variation behaviour in the Pindan sands was observed and presented in this chapter. A number of researchers (Emery et al., 2003), (Kenneally et al., 1996), (Sinclair Knight Merz, 2009) have written about the behaviour of Pindan sands when their moisture contents rise, and there have been several conflicting results. Among them, Emery et al (2003) defined Pindan sands as collapsible soil.

4.2 Evaluating Indentation Properties of Pindan Soil

Numerous cases have been recorded regarding the problems caused by problematic soil such as expansive, dispersive and collapsible soils and it has been a significant challenge to engineers. Geotechnical engineers have found ways to deal with the problematic soils, but have proved ineffective under certain circumstances. Thus, there is a requirement to research and understand the identification and characteristics of Pindan sands and investigating the Pindan particles is significantly important to understand the behaviour of Pindan. However, due to the sizes of individual sand particles, the physical properties of the sand particles are difficult to determine at a macroscale (Daphalapurkar, Wang, Fu, Lu, & Komanduri, 2011).

Mechanical properties, such as fracture toughness, hardness and elastic modulus, relate to individual sand grains, which dictate the overall characteristic of the sand.

However, difficulties arise during testing sand material with conventional test method to subject compression or tensile strength for the measurement of mechanical properties.

Nanoindentation is considered one of the best techniques that can be used to obtain mechanical properties of materials. The test came from the nanotechnology implementation in material science and engineering to evaluate physical properties at a small scale. Indentation testing is performed essentially by touching the material whose mechanical properties are not known, such as hardness and elastic modulus, by using other materials whose properties are known (Fischer-Cripps, 2011). The nanoindentation instrument is recently accepted as a standard test process for the characterisation of physical properties of materials (Daphalapurkar et al., 2011). An advantage of the indentation test is that the material can be characterised based on the indentation load and depth of the material during loading and unloading. Thus, nanoindentation provides a highly effective and successful technique for measuring local material responses in term of elastic modulus and hardness.

In this study, nanoindentation tests were conducted using Berkovich indenter tip on individual Pindan red soil from Broom, Kimberley Region of Western Australia to obtain the load – displacement curve for determining elastic modulus and hardness. Furthermore, the fracture toughness was obtained based on the analysis of the indentation data. The information on the Pindan sands used in the nanoindentation tests is presented in Table 4.1. Specific gravity, Plasticity index, Classification and Collapsibility were determined according to AS 1289.3.51 (2006), ASTM D4318 (2010), ASTM D2487 (2011a) and ASTM D2435/2435M (2011b), respectively.

Table 4.1: Properties of Pindan soil grain used in Nanoindentation

Broome-Pindan Sample						
	Sample collected Location	Soil Condition	Specific Gravity (G _s)	Plasticity Index (PI)	Classification	Collapsibility
Property	Cape Leviqve (C.L)	Raw Material (Sand)	2.61	Non-Plastic	Silty Sand (SM)	Slightly collapsible

4.3 Experimental Result and Discussion

A sample of sand was cast with epoxy matrix then was grinded and polished to reduce the surface roughness (Bobko & Ulm, 2008). The mechanical properties such as hardness (H) and elastic modulus (E) of the sand grain based on contact mechanics of nanoindentation as can be found in some literatures (Cheng & Cheng, 2004; Constantinides & Ulm, 2007; Fischer-Cripps, 2011; Lee et al., 2016; Warren C Oliver & Pharr, 2004):

$$H = \frac{P_{max}}{A_c} \quad (4.3.1a)$$

$$E_r = \frac{\sqrt{\pi}}{2} \frac{S}{A_c} \quad (4.3.1b)$$

Where A_c is the projected contact area corresponding the contact depth (h_c), P_{max} is the maximum indentation load, and $S = dP/dh$ is the slope of the upper portion of the unloading curve as shown in Figure 4.2. The reduced modulus E_r can be expressed as elastic modulus of sample (E) as:

$$\frac{1}{E_r} = \frac{1 - \nu_s}{E} + \frac{1 - \nu'^2}{E'} \quad (4.3.2)$$

where ν' , ν_s and E' are Poisson's ratio of indenter tip and sample, and the elastic modulus of indenter tip, respectively.

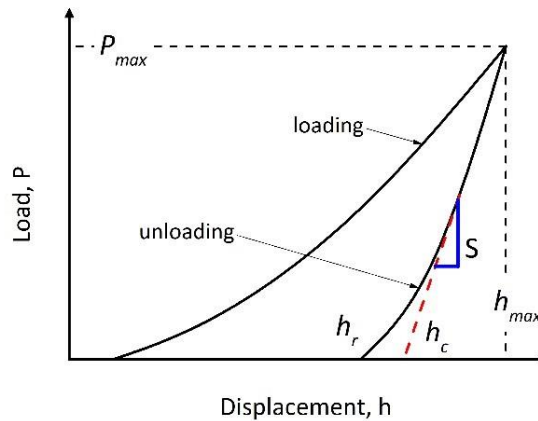


Figure 4.2: Typical load – displacement curve for indentation.

For the measurement of hardness and elastic modulus of sand grain, nanoindentation test was carried out with XP system and Poisson's ratio of 0.25 was assumed. Thus, Equation (4.3.1) to (4.3.2) was applied to determine the hardness and elastic modulus of the samples. According to deconvolution technique from literature (Lee et al., 2016), hardness and elastic modulus complete as presented in Figure 4.3. From the deconvolution results, the elastic modulus and hardness values for Pindan sand were observed as 68.1 ± 12.7 GPa and 10.6 ± 0.9 GPa, respectively. The elastic modulus of Pindan sand, however, is lower than the elastic modulus of quartz, which has an elastic modulus of around 124 GPa with indentation test (Warren Carl Oliver & Pharr, 1992). It can be encouraged by a different material constituent in Pindan sand.

Similarly, the stiffness and hardness-packing density scaling were employed on Pindan sand (Lee et al., 2016). The results of sand particle properties were obtained that stiffness and cohesion were 92.7 GPa, 4.1 GPa, respectively. The packing density

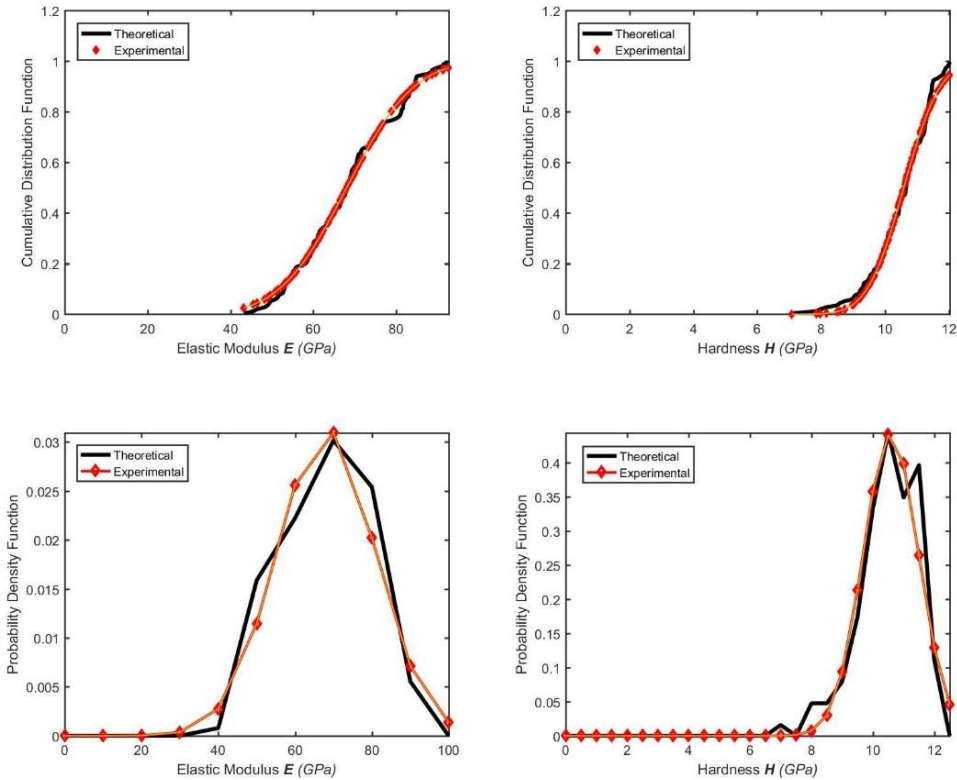


Figure 4.3: Statistical Indentation Analysis; Top - cumulative distribution functions (CDF), Bottom – probability density function of elastic modulus (left) and hardness (right).

of the sample was determined as 0.863 ± 0.032 as shown in Figure 4.4. From the results of the packing density distribution, it is possible to evaluate the total porosity of the material using the relationship between the packing density and the total porosity summarised by Ulm et al. (Ulm et al., 2007) as:

$$\xi = \sum (1 - \eta) \tag{4.3.3}$$

where ξ and η are total porosity and packing density of material. Application of Equation (4.3.3) to Pindan sand yields $\xi = 0.137$. This way of determining the porosity using statistical technique provides a new non-invasive approach which, otherwise, would be difficult to estimate the porosity of ground materials using a classical method (Ulm et al., 2007).

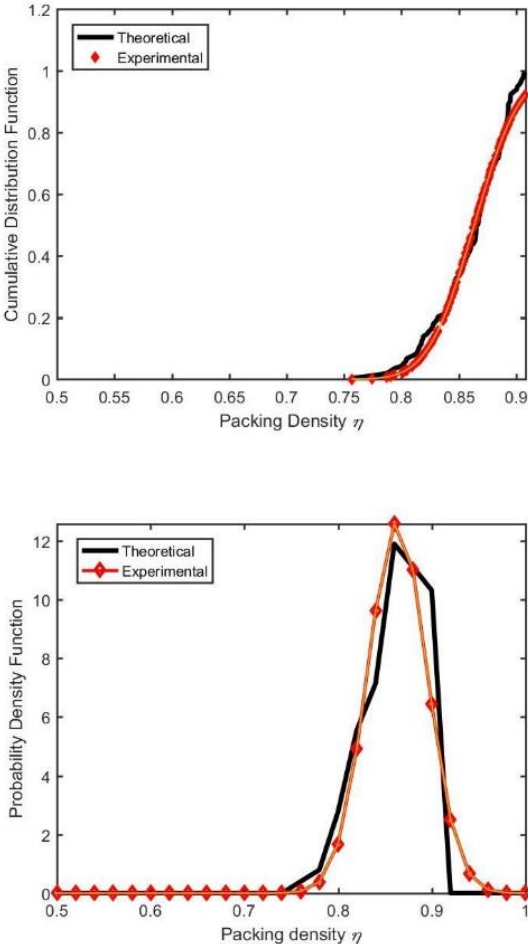


Figure 4.4: Statistical Indentation Analysis; Top - cumulative distribution functions (CDF), Bottom – probability density function of packing density.

Cracks propagate at the indenter corners while a brittle material is loaded by a sharp indenter tip. In this case, fracture toughness could be obtained the measurement of radial and later cracks indentation points (Chen & Bull, 2007). According to Lawn et al. (Lawn, Evans, & Marshall, 1980), the indentation fracture toughness is formulated as:

$$K_c = \varepsilon \left(\frac{E}{H} \right)^n \frac{P}{c^{3/2}} \quad (4.3.4)$$

where ε is an empirical calibration constant and c is the radial crack length. Numerous researchers (Anstis, Chantikul, Lawn, & Marshall, 1981; Dukino & Swain, 1992; Field, Swain, & Dukino, 2003; Laugier, 1987) determined n and ε in Equation (4.3.3) using indentation tests. It can be calculated from indentation with Berkovich indenter that:

$$K_c = 1.073x_v \left(\frac{a}{L} \right)^{1/2} \left(\frac{E}{H} \right)^{2/3} \frac{P}{c^{3/2}} \quad (4.3.5)$$

where x_v is 0.015, and L and a are calculated by radial cracking length as presented in Figure 4.5.

Figure 4.6 presented an inverted image (3D) and a typical residual impression was achieved using the Nano Vision on Pindan sand. It could be found that the crack is formed when indented with Berkovich tip on the sample. The ratio of E/H form the indentation test is needed for determining fracture toughness. The E/H ratio of Pindan sand was achieved an average value of all ratios as 6.5. The radial and later cracks length were determined from the surface scan in Equation (4.3.5). Thus, the

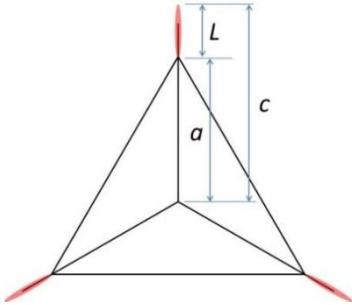


Figure 4.5: Geometrical relationship between the extended radial cracks and the indentation impression with Berkovich tip

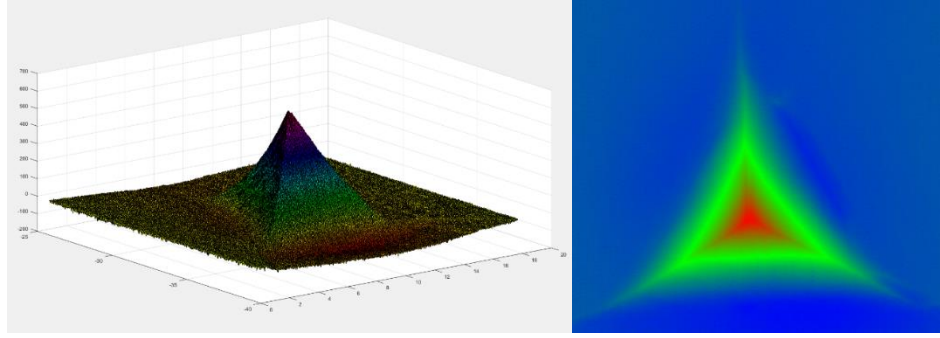


Figure 4.6: Inverted 3D image (left) and residual impression (right)

obtained median value of the fracture toughness of Pindan sand was $3.7 \pm 0.5 \text{ MPa m}^{1/2}$.

Similarly, the indentation load-displacement curve can be taken into account when considering the energy delivered during loading and unloading (Warren Carl Oliver & Pharr, 1992). The area under the load ($P_{loading}$) and unloading ($P_{unloading}$) versus the indentation displacement (h) curves represents the plastic energy (W_p) and elastic energy (W_e). The total energy (W_t) is the sum of W_p and W_e , or the total area under the load-displacement curve. By fitting the loading and unloading curve with power load function (Warren C Oliver & Pharr, 2004), W_t and W_e can be obtained as:

$$W_t = \int_0^{h_{max}} P_{loading} dh \quad (4.3.6a)$$

$$W_e = \int_{h_r}^{h_{max}} P_{unloading} dh \quad (4.3.6b)$$

The relationship between W_p/W_t and h_r/h_{max} can be expressed as (Chen & Bull, 2007; Cheng & Cheng, 2004):

$$\frac{W_p}{W_t} = 1 - \left[\frac{1 - 3\left(\frac{h_r}{h_{max}}\right)^2 + 2\left(\frac{h_r}{h_{max}}\right)^3}{1 - \left(\frac{h_r}{h_{max}}\right)^2} \right] \quad (4.3.7)$$

The total indentation work W_t can be determined from:

$$W_t = W_p + U_{fracture} + W_e + W_{other} \quad (4.3.8)$$

where W_{other} is another energy transferred such as thermal drift or heat energy dissipation, and $U_{fracture}$ is the fracture dissipated energy. However, in this study, W_{other} from the thermal drift is disregarded in the calculation of W_t . The fracture toughness (K_c) and critical energy (G_c) can be expressed as (Taha, Soliman, Sheyka, Reinhardt, & Al-Haik, 2010):

$$G_c = \frac{\partial W_{fracture}}{\partial A} = \frac{U_{fracture}}{A_c} \quad (4.3.9a)$$

$$K_c = (G_c E)^{1/2} \quad (4.3.9b)$$

From Equations (4.3.6) to (4.3.9), the fracture toughness of Pindan sand was determined based on energy transferred. This approach assumes that the crack growth is stable under indentation loading. The results of energy transferred fracture toughness of Pindan sand was obtained as $3.1 \pm 0.8 \text{ MPa m}^{1/2}$. The approach of using energy transferred fracture toughness was able to extract the fracture toughness of indentation test results.

The deformation of subgrade or subbase is critical to mechanical behaviour of pavement. The fracture energy that is significantly important for the post-peak behaviour can be simply obtained from the nanoindentation. If the material is linear elastic, then the deformation can be predicted using the fracture energy graph as shown in Figure 4.7.

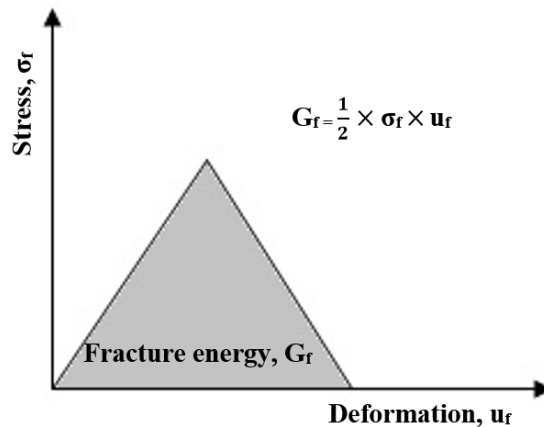


Figure 4.7: Fracture energy graph of linear material (Bazant & Pfeiffer, 1987)

4.4 Summary

The results are based on nanoindentation experiments on Pindan sand. Based on the results of this investigation, the following conclusion can be made:

- 1) An application of nanoindentation technique is successfully applied to the microporomechanics of Pindan sand. Statistical analysis based on deconvolution technique is performed to obtain the physical properties of Pindan.
- 2) Hardness, elastic modulus, and packing density of Pindan sand are determined as 10.6 ± 0.9 GPa, 68.1 ± 12.7 GPa and 0.863 ± 0.032 , respectively. Based on microporomechanics, stiffness and cohesion are obtained as 92.7 GPa and 4.1 GPa, respectively.
- 3) The results of the fracture toughness of Pindan sand based on the energy transferred and the measurement of radial and later cracks indentation points are obtained as 3.1 ± 0.8 MPa m^{1/2} and 3.7 ± 0.5 MPa m^{1/2}, respectively. The difference between the two results is because other energy (W_{other}) was ignored in the calculation of the total indentation work (W_t).

Chapter 5

5 Stabilisation of Broom-Pindan

5.1 Introduction

Strength is one of the critical components of a material and one of the essential elements in road design to resist the stresses imposed and prevent deformation (Sharp & Andrews, 2009). Sometimes it is necessary to strengthen the ability of the road material to build roads. Depending on soil characteristics or construction site conditions, soil stabilisation methods can be selected. There are generally two stabilisations that are commonly used for soil stabilisation. Mechanical stabilisation enhances soil strength by applying loads to the soil, and chemical stabilization improves soil strength by using chemical stabilisers such as cement, lime, fly ash and polymers. The process of strengthening road materials with additives is called stabilisation. According to recent studies, polymers for soil stabilisation provide a high water resistance and good physical properties. Polymers play an important role in coating and bonding aggregates, therefore the polymer's ability is directly applied to enhance strength and physical bonding (Welling, 2012).

Pindan has limited information on the fundamental interaction with polymers and on the stabilisation mechanism and properties for road pavement. Soils from Broom, commonly known as Pindan, are tested with Polymers as the stabilising agent. Three polymer commercial products from Australia are used in the study. There are several important processes for sample testing; selection of suitable polymers, appropriate amount of polymer and water, the mixing and curing process, and appropriate methods for testing of stabilised materials.

In this chapter, the properties of Pindan soil were examined to determine its microstructure, chemical and mechanical properties, and Pindan soils stabilised with polymer stabilisers were evaluated to determine the performance of polymer-based products, and the chemical and microstructural reactions between Pindan and Polymer. The bonding mechanisms and the effects of polymer on Pindan soils were investigated using the production of Broome-Pindan soils stabilised with polymers.

The laboratory experiment consisted of producing a number of Pindan soils-polymer mixture batches with varying polymer contents and curing times. The investigation of chemical and microstructural properties of Pindan soils was examined using XRD and SEM, respectively, and the waterproof effect of the polymers on the stabilised Pindan soil was investigated by carrying out capillary rise tests. To obtain the compressive and bearing strength of Pindan soils and polymer modified Pindan soils with respect to polymer contents and curing times through unconfined compression strength tests (UCS), and California bearing tests (CBR).

5.2 Material Preparation

The material used for this investigation primarily consisted of Pindan soil collected in Broome, Western Australia and three polymer products manufactured in Australia. The information of the polymers are provided in Table 5.1. Polymer A consists of hydrated lime and cationic polymer. Polymer B and C are a polyacrylamide polymer and a styrene-acrylate copolymer. Preparation of the sample materials involves mixing between Pindan soil, three polymers and water. Images of the polymers through a scanning electron microscope are shown in Figure 5.1. The polymers are smaller than the Pindan soil particles as shown in the images. Figures 5.1(A) and (B) show the shape and size of polymer A and C, respectively. Since polymer B is composed of four different components, it has various sizes as shown in Figures 5.1(C) and (D).

Polymer A and B have been used in the field since they are manufactured to use for soil stabilisations. Usually, polymer A is mixed with soil and water, and compacted. Then, the material is re-mixed, which gives a better mix of the additive and water and the soil. There are typically two ways to use polymer B; premixing polymer B into a solution in a water cart and spraying that onto areas requiring treatment or spreading it in a dry powder form and adding raw water whilst mixing. Polymer C does not have a protocol for soil stabilisation as it is used for a raw material binder and has not been used as a soil stabiliser.

In this experiment, firstly, the soil was simply mixed with polymer A, and then correct portion of water was added to the mixture to achieve its maximum dry density. It was mixed till it looked uniform and cured for 2 hours in a sealed condition to allow for even moisture distribution and to minimise fluctuations in moisture content. After

Table 5.1: Polymer Information

	Polymer A	Polymer B	Polymer C
Recommended Use	Soil stabiliser	Soil stabiliser	raw material binder
manufacturers' recommended dosage	1.5%	0.002%	N/P
Polymer Active Range	1.0% - 3.0%	0.001% - 0.003%	0.5% - 1.0%
Polymer Type	Cationic Polymer (with Hydrated Lime)	Anionic Polyacrylamides	Styrene - Acrylate Copolymer
Form	Powder	Powder	Powder
solubility in water	Insoluble	Miscible	dispersible

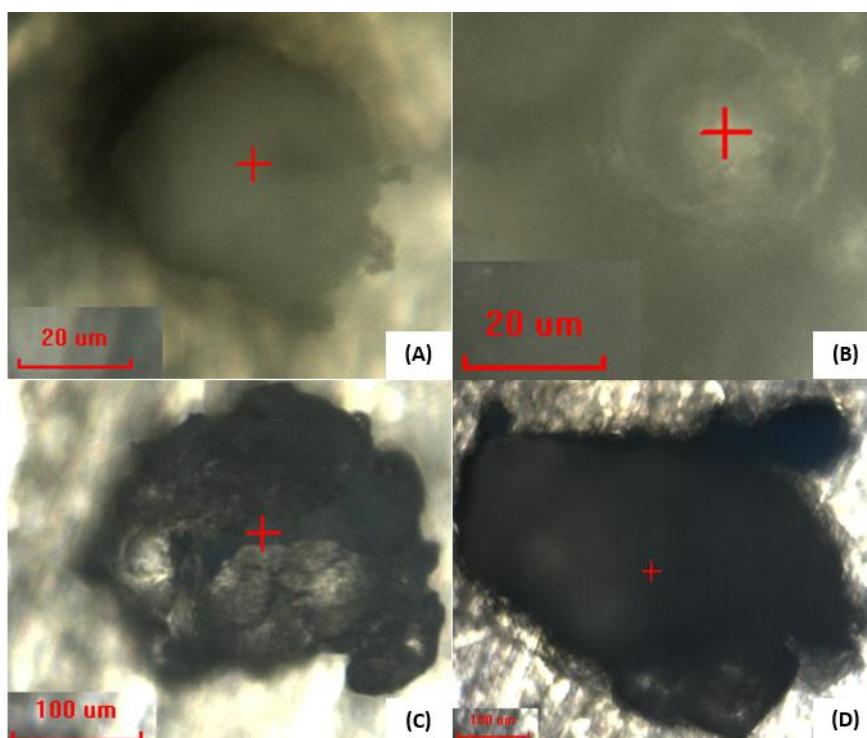


Figure 5.1: Microscope Images of Polymers. (A) Polymer A, (B) Polymer C, (C) and (D) Polymer B.

curing, compaction was performed. The Pindan soil was treated by adding polymer A by weights of 1%, 2%, and 3% of the soil. For polymer B and C, solutions of a mixture of polymer and water were created in required polymer concentrations and then the soil was mixed with the solutions. The mixture was mixed till it looks uniform and cured for 2 hours in a sealed condition to avoid water evaporation. After curing, the samples were compacted using the modified compactive effort of 2703 kJ/m³ described in Australian Standard AS 1289.5.2.1 (2017a).

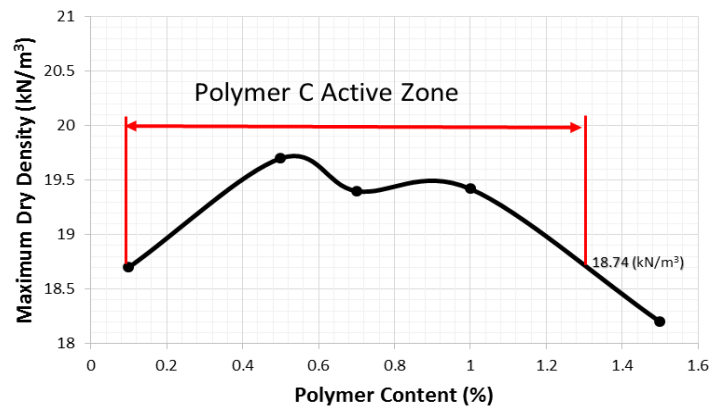
Polymer B and C were well mixed with water prior to adding to the soil and correct portion of the solutions were added to the soil to achieve its maximum dry density. For the polymer B and C, adding the correct portion is one of the importance steps in the procedure. Three different proportions of polymer B and C were added to the soil. The polymer B was added using ratio by weights of 0.001%, 0.002% and 0.003% of the soil. The activity range of the polymer A and B have been provided from the manufacturers. Since the polymer C has not been used for soil stabilisation, the activity range of the polymer C was obtained based on the maximum dry density through the compaction test as shown in Figure 5.2(a). The activity range zone of the polymer C was selected in comparison with the maximum dry density of Pindan soil of 18.74 kN/m³. Figure 5.2(b) provides the degree of activation for the polymer C, which can show the range of the activation zone. The polymer C was mixed with water to create the required polymer concentrations and added to the soil using ratio by weights of 0.5%, 0.7% and 1% of the soil. All specimens were tested under both saturated and unsaturated conditions. Since polymer B is a polyacrylamide polymer, it forms a soft gel when hydrated. Also, polymer A contains hydrated lime, which when water is added, it turns into gel formation due to the pozzolanic reaction. Polymer C may have components in an amorphous form. More information on the chemical and microstructural properties of the polymers are given in Section 5.7.

Three mixtures were used to test for investigating the stabilisation of the Pindan soil and the polymers. Mixture A, B and C are a mixture of the Pindan sand with the Polymer A, B and C, respectively. The proposed specimens for the testing are listed as follows:

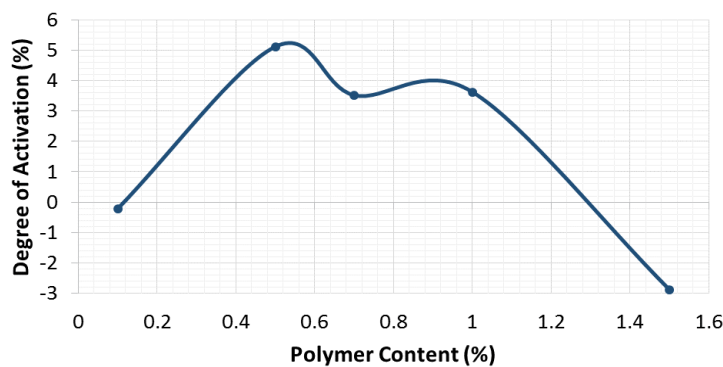
- Untreated Sample: Pindan Soil
- Mixture A: Pindan soil + Polymer A (1, 2 and 3%)

- Mixture B: Pindan soil + Polymer B (0.001, 0.002 and 0.003%)
- Mixture C: Pindan soil + Polymer C (0.5, 0.7 and 1%)

The specimens were prepared by well mixing the Pindan soil with the desired percentage of the polymers in the mixtures for the treated sample. The samples were compacted for the relative compaction values of 93% and 98% of maximum dry density at its optimum moisture content using the modified proctor compaction method for CBR and UCS tests, respectively. Experiments of compaction, strengths, XRD and SEM were conducted to investigate the properties of Pindan soil, and the results were compared to find out the interaction of between the physical properties and the microstructural properties.



(a)



(b)

Figure 5.2: Polymer C Active Range Zone. (a) Maximum dry density versus Polymer content, (b) Degree of Activation for Polymer C.

5.3 Modified Compaction Test

Earthwork is important when designing the pavement structures, because the behaviour of the unsealed road depends on the behaviour of the deposits of soil. Compaction is applied to improve the engineering properties of road materials and to withstand repeated loads from vehicles. Soil compaction is the process of increasing the soil density by reducing the space between soil particles by applying force. Reduction of pore space is accompanied by increase in soil density, and in laboratory conditions, an increase in soil density is generally seen as an increase in soil strength due to adding more soil. Adding water during the compaction process allows soil particles to slip more easily, which cause more reducing pore spaces and increasing density and soil strength. According to Rahman et al. (2011), the relative compaction of more than 95% of the standard proctor compaction test in the road construction is usable for heavy vehicle and 90 to 95% for all other vehicles. In this chapter, compaction tests provide the optimum moisture content (OMC) and maximum dry unit weight (MDD) of the Pindan soil with and without polymer stabilisers added. Dry unit weights are obtained at various moisture contents, and the OMC and MDD properties are obtained by plotting the compaction curves. The OMC obtained from the compaction curves was used in the unconfined compressive strength test and the California bearing ratio test.

The soil was mixed with polymer A, and then the correct portion of water was added. For polymers B and C, solutions of the mixture of the polymer and water were created and added to the soil. The mixture was mixed until the colour of the mixture looks uniform and cured for 2 hours in a sealed condition. A cylindrical metal mould of an internal diameter of 105mm and effective height of 115.5mm, and a rammer were prepared in accordance with AS 1289.5.2.1 (2017). After curing, the samples were compacted in five layers at 25 blows per layer using the modified compactive effort (2703 kJ/m³) as described in Australian Standard AS 1289.5.2.1 (2017a). The modified proctor test was used to determine the dry density in various moisture contents for the Pindan soil and the mixtures. Figure 5.3 illustrates the compaction curves within the same scale to compare the untreated and treated samples. The results of the modified proctor compaction test for the Pindan soil and the mixtures A, B and C are presented in Figures 5.4(a), (b), (c) and (d), respectively. Table 5.2 provides the

optimum moisture contents and maximum dry density values obtained from the moisture-density relationship curve of the compacted samples.

As can be seen in Figure 5.3, the effect of adding the polymers on the moisture-density relationship for the Pindan soil can be assessed through the compaction test results. Comparing the optimum moisture content (OMC) and maximum dry density (MDD) between the untreated sample and all mixtures, all polymers reduced OMC and increased MDD values. The mixture can reduce the required water content to achieve the maximum dry density, which is desirable for the construction of the Kimberley region. However, the dry unit weight was getting rapidly reduced after each OMC and the dry density decreased to or below the dry unit weight of the untreated sample. The changes in OMC and MDD of mixture C were significantly large when compared to other samples. Mixture C minimized the OMC and indicated the maximum MDD. However, as shown in the graph in Figure 5.3, the MDD of the mixture C after the OMC point dropped sharply and recorded the lowest value in the MDD. When using polymers for soil stabilisation, it may not be desirable to use more water than necessary, especially when polymer C is used, MDD and strength might be greatly affected by the amount of water. The increase in density is probably because the polymers filled the pore space and reduced the porosity of the treated samples. This is explained further with SEM images in Section 5.7.

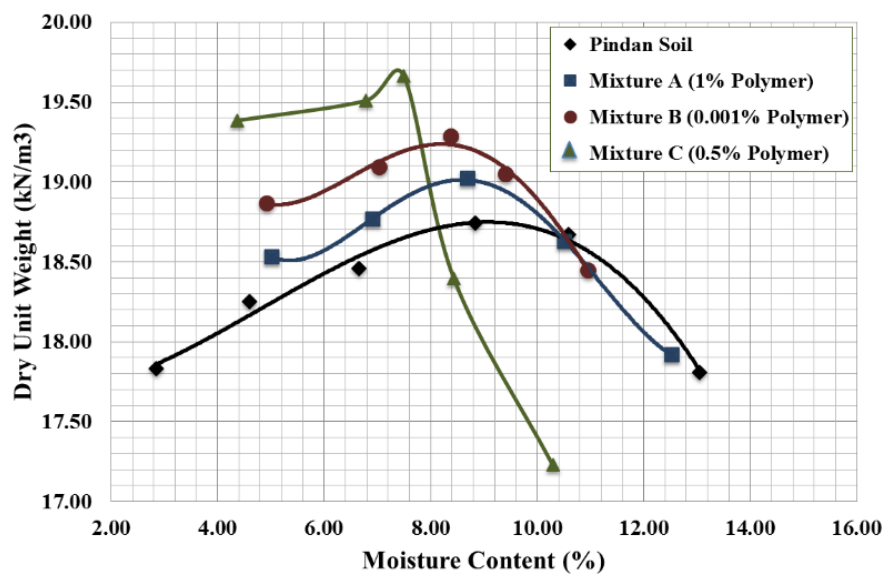
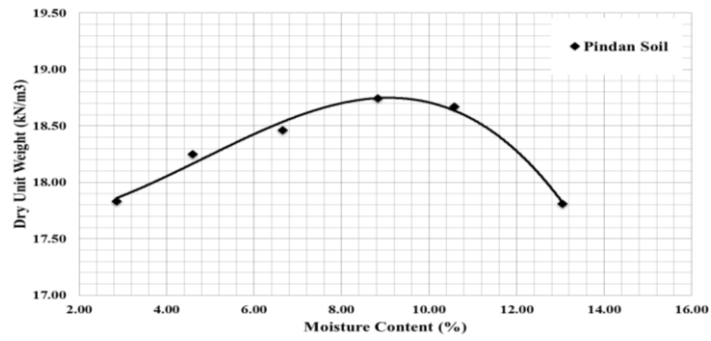


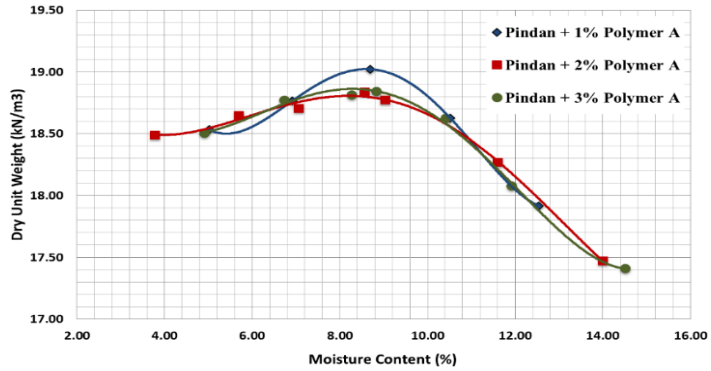
Figure 5.3: Comparison of the untreated sample and the treated samples

Each compaction curve is shown in Figure 5.4. Figure 5.4(a) shows the compaction results for the Pindan soil, while Figures 5.4(b), (c) and (d) show the results for the polymers. As shown in Figure 4(a), the Pindan soil recorded a maximum dry unit weight at a moisture content of 9.4%. When the moisture content is below 9.4%, the compaction is interrupted because of the high friction between the soil particles and the moisture content interferes with the compaction due to the high pore water pressure after 9.4%. The results in Figures 5.4(b), (c) and (d) show that the samples with the lowest amount of polymer achieved the highest dry density. Since the amounts of the polymers are all within the activation zone as shown in Figure 5.2, the lowest amounts of the polymers might be already close to the optimum amount for the Pindan soil and the amount of polymers is no longer filling the void space between the sand. In addition, in the case of mixture A, there was almost no change with the amount of polymer. This means that there was little change in the reaction of the polymer. And, looking at the curves shown in Figures 5.4(b), (c) and (d), some of the polymers did not seem to react properly due to the lack of water in the water contents below the OMC. At OMC, it seems that the polymer and the proper amount of water react well, therefore the density increased. After the OMC, the reaction of water and polymer occurs, but the polymer might leak out with the water during or after the compaction process. Another reason is that after the polymers fill the void spaces between the soil particles, these materials, which have smaller densities than the density of the soil, could replace the small particles of the sand or clay to reduce the density rapidly. This might happen in this order because the size of the polymer is smaller than the particle size of the Pindan sand. In Figure 5.4(d), mixture C achieved the maximum MDD compared to other mixtures but sharply decreased after OMC. It is probably because the polymer C filled the voids well and achieved the maximum dry density but after OMC, most of the polymer might leak out with the water during or after the compaction process due to a small size.

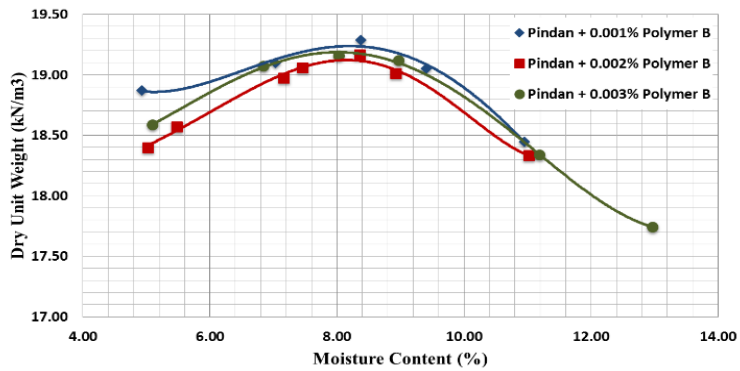
From the results, it clearly shows that there was an increase in MDD for the treated samples compared to the untreated samples up to the optimum moisture content. This may be because the polymers filled the pore space and reduced the porosity of the treated samples until it reached the optimum moisture content. However, there was a decrease in MDD for the treated samples after the OMC, which was equal or more reduced than the untreated samples decreased. In addition, comparing the results of



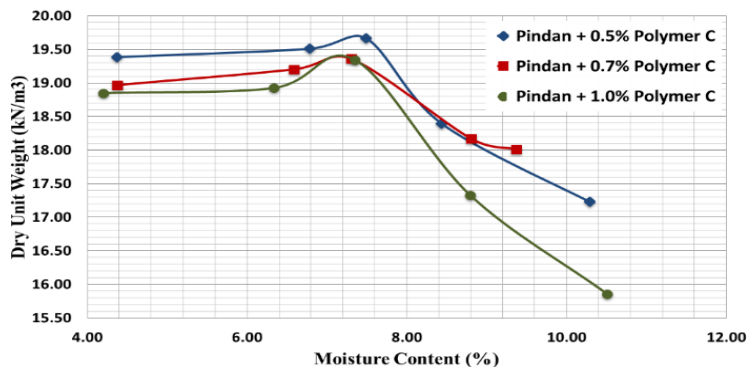
(a)



(b)



(c)



(d)

Figure 5.4: Compaction Test using the Modified Proctor Compaction Method. (a) Pindan soil, (b) Mixture A, (c) Mixture B, and (d) Mixture C.

Table 5.2: Optimum Moisture Contents (OMC) and Maximum Dry Density (MDD) of Broome-Pindan Soil and Mixtures

Modified Proctor Compaction Test		
Sample	OMC (%)	MDD (kN/m ³)
Untreated Pindan Soil	9.4	18.74
Mixture A (1% Polymer)	8.6	19.05
Mixture A (2% Polymer)	8.2	18.80
Mixture A (3% Polymer)	8.2	18.90
Mixture B (0.001% Polymer)	8.3	19.21
Mixture B (0.002% Polymer)	8.2	19.15
Mixture B (0.003% Polymer)	8.0	19.19
Mixture C (0.5% Polymer)	7.4	19.70
Mixture C (0.7% Polymer)	7.2	19.40
Mixture C (1.0% Polymer)	7.2	19.42

the OMC and MDD for the Pindan soil under the different compaction effort; the standard compaction effort in Chapter 3 and the modified compaction as shown in Figure 5.4(a), there was a decrease in OMC and an increase in MDD when the compaction effort was increased.

5.4 Capillary Rise

Capillary rise refers to the action of groundwater being sucked upward through pore spaces in the soil by the action of two forces, cohesive and adhesion forces. It is a phenomenon that occurs between the cohesive force, which is the force that water and water want to bond with each other, and the adhesive force, which is the force that water attaches to another substance. That is, the forces that pull each other in the contact area between the water particles and the soil particles, and the water, refer to

the forces through hydrogen bonding to each other. This is a phenomenon in which water moves up through the soil particles due to adhesion, cohesion and surface tension. The capillary action of the water is high when the adhesion is greater than the cohesion force. For example, water in a thin tube has stronger adhesion due to the bonds that form between water and the tube wall than water in a larger tube. When the capillary action occurs in the soil, it depends largely on the pore size, because the water rises up through the spaces between the soil particles against gravity. And, because the capillary rise is higher with smaller soil pores, sand with smaller particles has higher capillary rise than sand with larger particles (Moore, 1939).

Capillary rise of the compacted Pindan materials was performed for testing the stabilised Pindan soils to assess the waterproofing effect of the polymers in accordance with testing guideline specified in Australian standard AS1141.53 (1996a). This test can simply evaluate the performance of the polymers with the Pindan soil to determine whether the polymers can improve the performance of the Broome-Pindan soil in wet conditions. This chapter details the performance of the untreated and treated samples and confirms that the polymer-stabilised Broome-Pindan soil can be used as a pavement material. The Pindan soil was treated with polymer A, B and C at the rate of 2%, 0.002% and 0.7% by weight, respectively. The samples were compacted to 98% of the OMC using the modified proctor compaction method and cured for 16 days in a humidity cabinet. The temperature of the cabinet remained in the range of 21°C to 25°C at 90% humidity. The test was carried out according to the test procedure detailed in AS1141.53 (1996a). The samples A, B and C are the compacted mixtures A, B and C, respectively.

Figure 5.5 presented the capillary rise (CR) as a percentage of the specimen height using the Equation (5.4.1) as provided in AS 1141.53 (1996a):

$$CR = \frac{h}{H} \times 100 \quad (5.4.1)$$

where CR is a capillary rise in the sample, h is a height of the capillary rise and H is an initial height of the sample. The compacted samples were placed in 10 mm deep of water at a room temperature for 72 hours.

Water risen approximately 20 mm for the untreated sample and sample C within 1 minute. For the sample B, water risen approximately 30 mm within 1 minute. In the

case of sample A, there was no change within 1 minute. Two minutes after the start, the untreated sample and sample B started to slump from the surface and the water risen up to 30 mm and 50 mm, respectively. And, the water risen up to 5 mm and 35 mm for samples A and C, respectively. The water risen up to 20 mm and dropped again to 0 mm for polymer A. The untreated sample and polymer C sample were risen the water similarly and fully saturated after around 2.5 hours from the start. And, polymer B sample was fully saturated within 2 hours from the start. The surface of the untreated sample and sample B started to slump when the samples were placed in 10mm of water and the untreated sample was completely collapsed after around 1.5 hours after the fully saturated point, and sample B initially seemed to have an effect on the surface, but after that it was no longer affected by water. The all treated samples remained unchanged and seemed to maintain some strength as well as shape. Sample A almost did not change at all and maintain the sample in a dry condition. The capillary rise did not occur very much, and it went down to the original water position again for sample A. Polymer A provided more resistance to water ingress than other polymers. Polymer A decreased the capillary rise rate and reduced the moisture sensitivity significantly. The sample B and C were full saturated at about the similar time as the untreated sample, but there appeared to be no change after that and it seemed that they are stable unlike the untreated sample. Swelling (S) does not appear on the treated samples after immersion, and the untreated sample could not be measured as the sample shape was collapsed after saturated. It has been found that the polymer could provide sufficient water resistance to the soil during long-term exposure to water.

From the results, it clearly shows the capillary rise rate of the mixtures B and C was higher than the untreated sample. There is the Lucas-Washburn equation for the rise of the capillary (H) with time (t) as (Dimitrov, Milchev, & Binder, 2007):

$$H(t) = \left(\frac{\gamma_{LV} R \cos\theta}{2\eta} \right)^{1/2} \sqrt{t} \quad (5.4.2)$$

where γ_{LV} is the surface tension of the liquid, R is the pore radius, η is the shear viscosity of the liquid. In this study, water was used as a liquid in all capillary rise test, so the pore radius governs the rate of the capillary rise. Based on the equation, polymers B and C filled the void spaces and thereby reduced the void size of the

treated samples. Therefore, since the size of the voids became thinner and the rate of the capillary rise was increased. The reason for this is the same as the results for the modified compaction curves.

The capillary rise did not occur for the sample of the mixture A. Lacey (2004) explained that polymer A reacts with water and sands to create a hydrophobic soil matrix between the soil particles, limiting water penetration. It may be because the hydrated lime, $\text{Ca}(\text{OH})_2$ was reacted with water as:



And, pozzolanic reaction occurs between the free calcium (Ca^{2+}) and dissolved silica and alumina from the clay. When the reaction happens slowly in a high pH of around 12.4 over time, it turns into gel formation in amorphous form and thereby the voids filled up by the cementitious material. Sample A was not saturated with water as the void space between the soil particles is filled by the cementitious material. When the $\text{Ca}(\text{OH})_2$ is added to soils, the clay particles are flocculated by ion exchange of calcium on the surface of the soil particles. The long-term effect of the adding lime is achieved and determined by the amount of pozzolans, lime and water and its time is determined by the rate of chemical breakdown and hydration of silicate and aluminate. When the reaction happens over a long period with a sufficient amount of pozzolans, the soil particles bond together by the formation of a cementitious material (Lim, Jeon, Lee, Lee, & Kim, 2002).

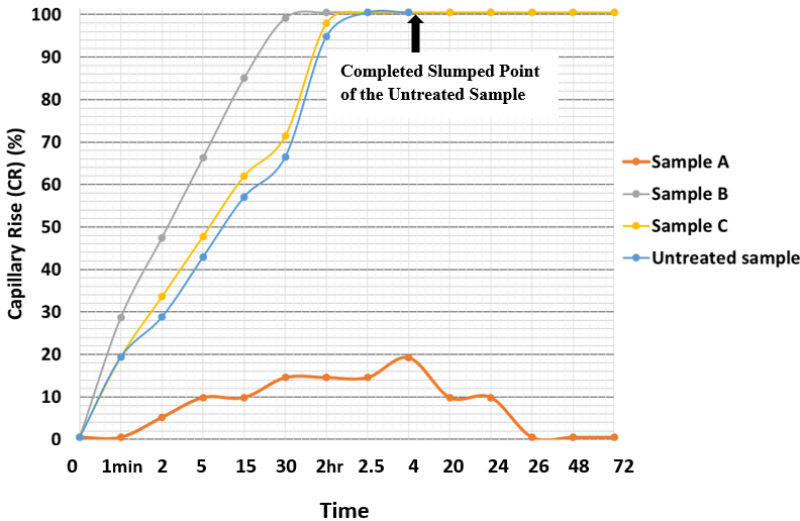


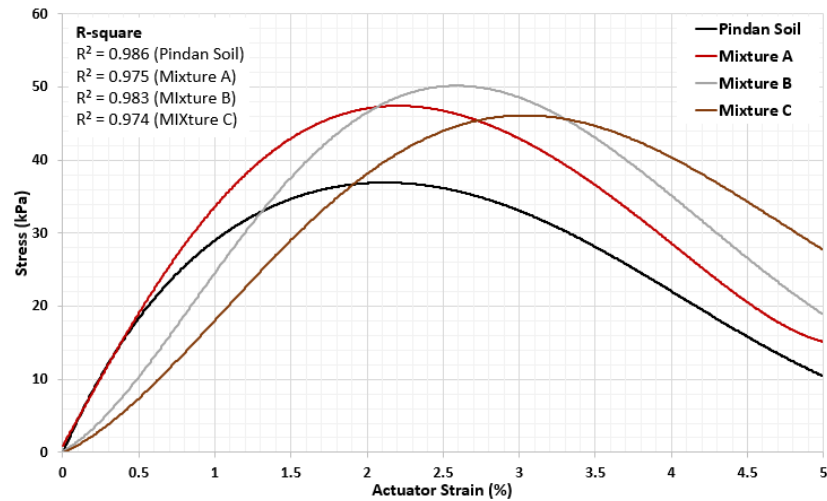
Figure 5.5: Capillary Rise of Compacted Samples

5.5 Unconfined Compressive Strength Test

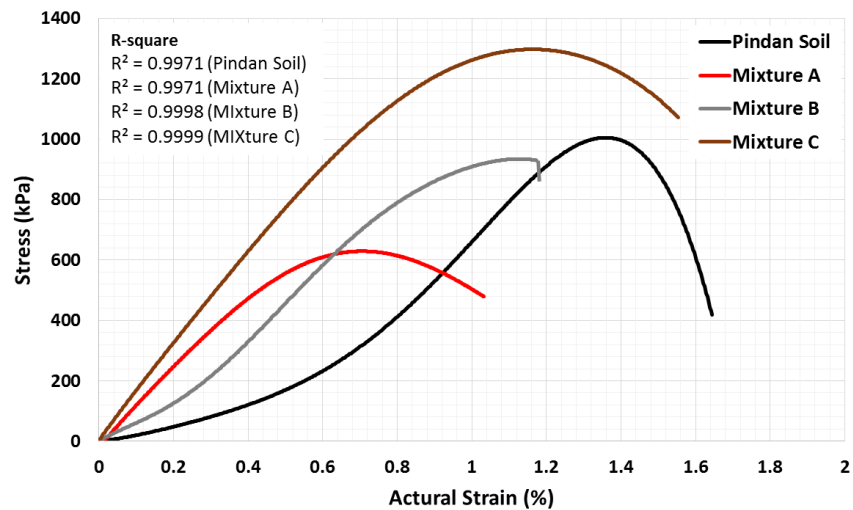
Unconfined Compressive Strength (UCS) test was conducted according to the Australian Standard AS 5101.4 (2008). A cylindrical metal mould and a rammer were prepared in accordance with AS 1289.5.2.1 (2017a). The specimens were compacted in five layers at 25 blows per layer using modified compactive effort of 2703 kJ/m³ as detailed in AS 1289.5.2.1 (2017a). UCS testing was performed on untreated and treated samples at two different curing times of 1 hour and 16 days. One hour curing is conducted to assess when the road opens to the public immediately after road construction or repair. 16day curing is to assess the change in strength over time after road stabilisation. The effect of using three different polymers on compressive strength of the untreated and treated samples under unconfined conditions was assessed using the UCS testing. The test was conducted at loading rate of 1 mm per minute as described in AS 5101.4 (2008).

Typical graphs of UCS for 1 hour cured samples are presented graphically in Figure 5.6(a). The samples were cured for 1 hour prior to testing. The average of UCS data is presented in Table 5.3 for each samples. All UCS data is included in detail in Appendix A. The samples were selected using the standard deviation with 90% confidence level. In Table 5.3, an increase in strain and compressive stress was recorded for all samples treated with the polymers as compared to the untreated samples. Polymers A and C showed the greatest increase in strain and polymer B showed the greatest increase in compressive stress. For 16 day curing samples, the samples were compacted to 98% of the MDD using the modified proctor compaction method and cured for 16 days in a humidity cabinet after extrusion. The temperature of the cabinet remained in the range of 21°C to 25°C at 90% humidity for 16days. Stress versus strain data for the samples are graphically provided in Figure 5.6(b). The average of the maximum UCS values of the 16day cured samples for the untreated and treated samples are presented in Table 5.4. The results were also selected using the standard deviation with the 90% confidence interval.

In 1 hour curing condition, the average UCS value of untreated soil samples was 34.7 kPa and all treated samples showed better UCS values ranging from 37.7 to 49.1 kPa as shown in Table 5.3. In particular, polymer B increased the strength the most. In 16 day curing condition, the UCS value of 1021 kPa for the samples with no stabiliser



(a)



(b)

Figure 5.6: Typical Unconfined Compressive Strength Curves of the compacted samples. (a) 1 hour cured samples, (b) 16 day cured samples.

was measured and the highest UCS value of 1948 kPa was obtained from samples treated with polymer C as shown in Table 5.4.

In Figure 5.7, which compares the results of the 1 hour cured samples, the polymers affected the stress and strain as compared to the untreated sample. The polymers increased the compressive stress and the percentage of the strain at peak loads compared to the untreated sample. However, in Figure 5.8, which compares the results of the 16 day cured samples, the effects of the polymers on the stress and the percentage of the strain were different from the results for the 1 hour cured samples. The results of the 16 day cured samples show that polymer C increased the

Table 5.3: Averages of UCS Results for the 1 hour cured samples

UCS – 1 hour Curing Samples		
Sample	Actuator strain at peak load (%)	Peak compressive strength (kPa)
Pindan Sand	2.25	34.67
Mixture A (1%)	2.28	37.67
Mixture A (2%)	2.78	38.5
Mixture A (3%)	3.15	39.17
Mixture B (0.001%)	2.53	48.5
Mixture B (0.002%)	2.43	48.8
Mixture B (0.003%)	2.48	49.1
Mixture C (0.5%)	2.55	38.5
Mixture C (0.7%)	2.93	43.8
Mixture C (1.0%)	3.20	44.4

Table 5.4: Averages of UCS Results for the 16 day cured samples

UCS – 16 day Curing Samples		
Sample	Actuator strain at peak load (%)	Peak compressive strength (kPa)
Pindan Sand	1.26	1021
Mixture A (1%)	0.83	603
Mixture A (2%)	0.83	762
Mixture A (3%)	0.88	628
Mixture B (0.001%)	0.89	895
Mixture B (0.002%)	1.28	949
Mixture B (0.003%)	1.02	979
Mixture C (0.5%)	1.10	1313
Mixture C (0.7%)	1.37	1648
Mixture C (1.0%)	1.34	1948

compressive strength as compared to the untreated sample, but polymers A and B caused a decrease in strength and strain. Regarding strength, the strength increased as the amount of polymer increased regardless of curing age except for the 16 day cured

sample of mixture A. In the case of the strain, the strain was also increased when the amount of polymers was increased similar to the strength except for polymer B. In particular, polymer C seems to have the most effect on the strain increase. However, the strain at peak loads seems to have less relation with the amount of polymers over time.

Polymer A influenced the colour of the sample and showed micro-cracks on the surface of the sample during curing as shown in Figure 5.9. Thus, the results of both stress and strain were reduced. This may be just due to shrinkage cracking or due to carbonation of the hydrated lime, or could be the corrosion due to iron-hydroxide (i.e. $\text{Fe}(\text{OH})_2$). Polymer B had no significantly effect on the stress of the 16 day cured samples while had significantly effect on the stress of the 1 hour cured samples, and polymer C significantly increased strength as compared to the 16 day cured untreated samples and other polymer mixtures. Polymer B caused a blow at the point of failure, which seems to occur when the bonding was broken at one time. Polymer B changed the properties of the soil from ductile behaviour to brittle behaviour as shown in Figure 5.6(b). When polymers A and C were observed on the curves of the 16 day cured samples, the curves appeared to fall slightly more slowly in strength after the ultimate tensile strengths, while the untreated sample sharply decreased. It seems to be due to the polymer holding between the soil particles.

From the results, when compared to the performance of soil with no stabilisers in one hour curing condition, it appears that all treated samples provide higher strength and strain. This may be because the polymer reacts with the soil and water to increase the strength, or the polymer may increase the density by filling voids between the soil particles and thereby increase the strength. In 16day curing condition, polymer A seemed to cause a decrease in strength as micro-cracks occurred in the curing process, while polymer C increased strength and strain. Polymer B did not significantly affect strength, but changed the failure behaviour of the soil from ductile to brittle. In the case of strength, the amount of polymers was increased, and it was increased regardless of curing days. In the case of polymer A, the cause of micro-crack in the curing process needs to be more studied and prevented to increase strength. The effects of polymer B on the microstructure and the bonding structures should be investigated to understand the change in failure behaviour. The change in microstructure depending on the polymers is covered in Section 5.7.

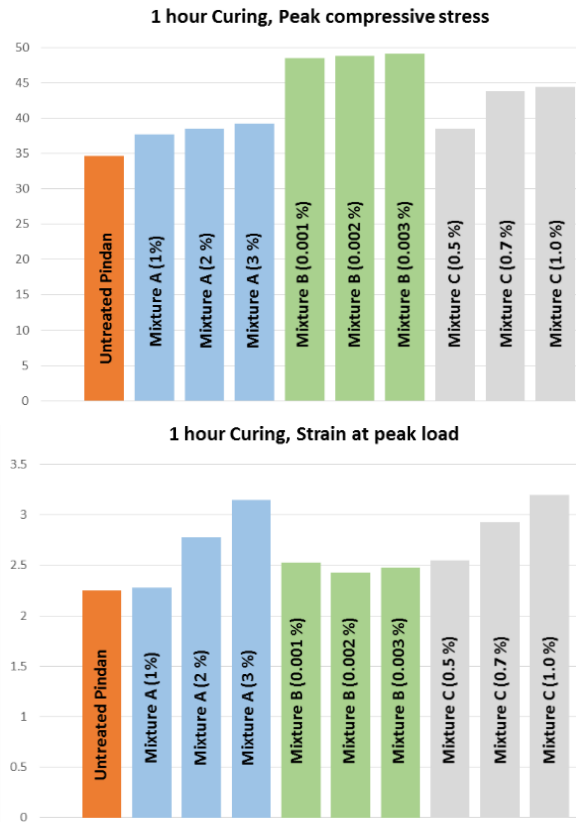


Figure 5.7: UCS Results for 1 Hour curing

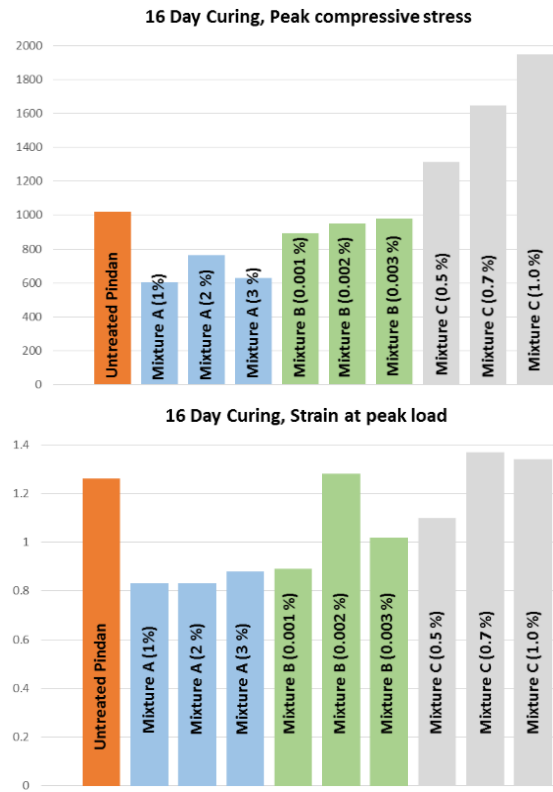


Figure 5.8: UCS Results for 16 Day curing

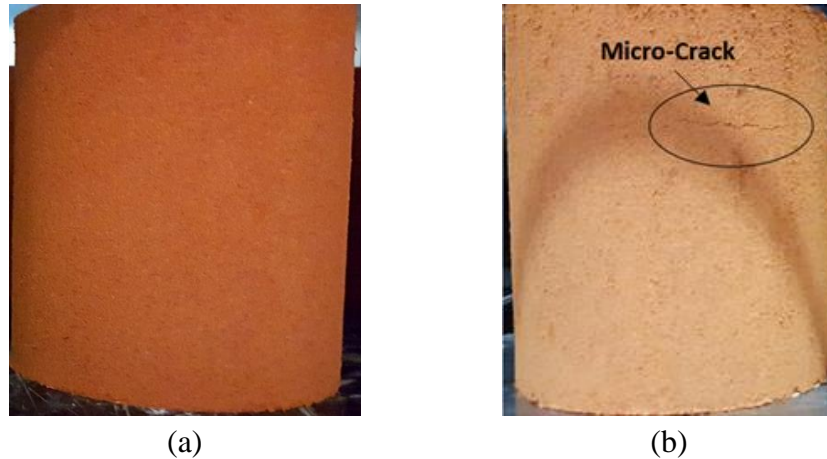


Figure 5.9: UCS Samples. (a) Untreated Pindan Sample, (b) Mixture A

5.6 California Bearing Ratio (CBR)

CBR was performed in accordance with Australian Standard AS 1289.6.1.1 (2014). The samples were compacted in five layers as described in AS 1289.6.1.1 (2014) using modified compactive effort (2703 kJ/m³) as detailed in AS 1289.5.2.1 (2017a). This test was performed immediately after compaction for unsoaked samples. Samples were cured after compaction for 4 days in water to obtain bearing ratios for soaked samples with or without polymer stabilisers. All CBR data is included in detail in Appendix B. The results of CBR test for unsoaked and soaked conditions are presented in Table 5.5. In the CBR test, when mixing the polymer C with Pindan sand, the moisture content should not exceed the optimum moisture content. When the amount of water greater than the optimum moisture content was added, the density of the compacted sample dropped remarkably. In relation to this, the CBR values of the samples also dropped significantly up to a CBR of 4 regardless of the amount of the polymer.

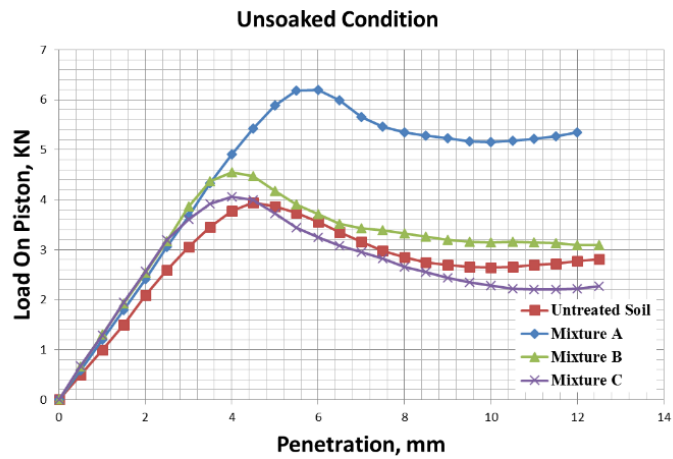
The average CBR value of the untreated soil samples was measured to be around 19. Most of the treated samples in both unsoaked and soaked conditions provided similar or greater CBR values than the untreated samples. The unsoaked and soaked samples did not show much different results. In the CBR test, mixture A showed the highest CBR values of 30.13 and 26.18, respectively, in unsoaked and soaked conditions. And, polymer C showed the lowest CBR values in both unsoaked and soaked conditions. The 1% content of the polymer A did not affect the CBR value, which may increase over time as shown in the UCS results. The reaction of the polymer might not be

started and the reaction would gradually take place over time. This also applies to all polymers. The polymers might need more time to react to increase the CBR value.

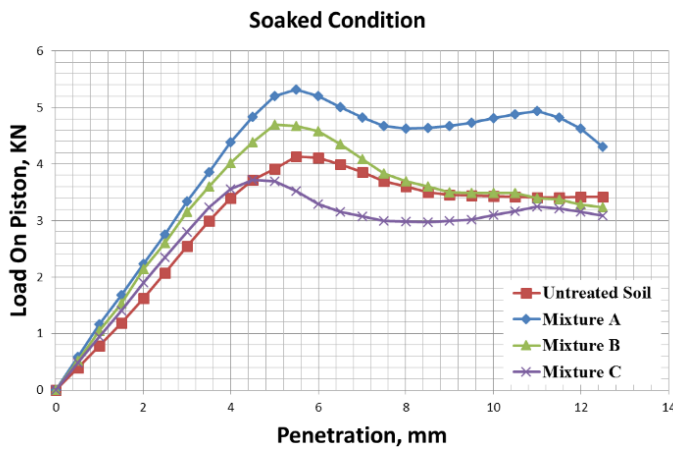
The typical UCS graphs for samples with and without polymer stabilisers in unsoaked and soaked conditions are presented in Figures 5.10(a) and (b), respectively. For CBR values, the maximum values calculated for penetrations at 2.5 mm and 5.0 mm are recorded as a CBR. In the case of mixture C, CBR was lower than the untreated sample after penetration of 4 mm as shown in Figures 5.10(a) and (b). Therefore, the CBR value of mixture C was recorded lower than the untreated sample at 5 mm penetration. Polymer A showed higher CBR value as the amount of polymer increased, whereas the CBR value decreased as polymer amount of polymer C increased. For polymer B, it had the highest CBR values when the polymer ratio was 0.002% in both unsoaked and soaked conditions. Pindan soil is known to be affected by water in the field as a collapsible soil. Unlike the field, Pindan soil had no difference in strength between the unsoaked and soaked samples in laboratory conditions. This is probably due to the sample is a disturbed sample which is different to the conditions of the soil in-situ.

Table 5.5: Averages of the CBR values for saturated and unsaturated samples

Sample	CBR (%)	
	Unsoaked Condition	Soaked Condition
	Sample	Sample
Pindan Sand	19.05	19.08
Mixture A (1%)	18.64	18.91
Mixture A (2%)	22.87	20.20
Mixture A (3%)	30.13	26.18
Mixture B (0.001%)	24.39	18.35
Mixture B (0.002%)	25.03	25.25
Mixture B (0.003%)	23.31	24.24
Mixture C (0.5%)	23.88	19.53
Mixture C (0.7%)	20.11	18.35
Mixture C (1.0%)	11.11	9.68



(a)



(b)

Figure 5.10: Typical UCS. (a) Unsoaked Condition, (b) Soaked Condition.

The CBR test is generally used to evaluate the subgrade strength of roads and its value can be used to determine the thickness of pavement layers. In general, the unsealed pavements are used for low trafficked rural roads. The unsealed pavement design should use the lowest CBR values, mostly from soaked samples. According to Austroads Unsealed Pavements Design (2009), unsealed roads using Pindan soil should be stabilised and must have a minimum compacted surfacing thickness of 100mm. It is not recommended to use polymer C as a road stabiliser since it reduced CBR value to a CBR of 4. For subgrade layers, the minimum thickness for unsealed road construction is 150mm based on the CBR results. The total pavement thickness required for the stabilised Pindan soil is at least 250mm. Road failures are often caused by structural weaknesses, and particularly unsealed roads are vulnerable to water as water easily flow into road structures. Polymer A reduces water ingress into

the subgrade and minimises moisture in the base-course. Therefore, a stabilised base-course maintains its strength and prevents deformation of subgrade structures, which increases the lifetime of unsealed pavements. Polymer B also has economic benefits in road design by stabilising the soil and increasing its strengths. However, in the case of polymer A, it is necessary to investigate the cause of the micro-cracks generated during the curing process of the UCS test. It should conduct a long-term study on the influence of the CBR. If micro-cracks were affected by carbonation, they might also affect the CBR values over time.

5.7 Chemical and Physical Bonding Mechanism

It is well known that material properties such as strength and shrinkage are affected and related to the microstructures. However, the microstructure of Pindan soil is not well investigated and information on the relationship between the microstructure and strength of the Pindan soil have not been determined. In this chapter, the chemical and microstructural properties of the Broom-Pindan soil with the three polymers have been determined and the bonding mechanism between the Broome-Pindan soil and the polymers has been introduced. Furthermore, the interaction of the bonding mechanism with strength has been investigated.

X-ray diffraction (XRD) and Scanning Electron Microscope (SEM) were used in the SM-Pindan sand and mixtures to investigate the chemical and microstructures. The mixture is a mixture of SM-Pindan sand and the respective three polymers. The results of the XRD analysis provide the chemical composition of the Pindan sand and mixtures, and the results of the quantitative X-ray diffraction (QXRD) analysis provide the quantitative numbers of chemical compositions for the Pindan sand. SEM images of the microstructure of Pindan sand and the polymer bridges between sand particles are shown in this chapter. And also, SEM pictures are accomplished with each energy dispersive X-ray spectroscopy (EDS). EDS analysis is a quantitative X-ray microanalysis used with SEM to determine the chemical composition of particles and their relative proportions. There are three polymers for mixing with SM-Pindan sand. Polymer A is a cationic polymer, B is a polyacrylamides polymer and C is a Styrene-Acrylate copolymer as displayed in Table 5.1. Polymer C was not able to perform the Quantitative-XRD because the slurry once dried, it dried as a thin film of plastic as shown in Figure 5.11 but not in powder form.



Figure 5.11: Polymer C for QXRD became a thin film of plastic after dried

5.7.1 Chemical and Microstructural Properties

The Quantitative-XRD (QXRD) analysis for Pindan sand showed the following results as shown in Table 5.6. The quantity is calculated only for materials with a crystal structure and not for amorphous materials. Iron (Fe) was not detected in the XRD test because the amount of iron in the Pindan sand was too small. In the EDS experiment, Fe was detected in Pindan sand and also in the bonding structure between the soil particles in the mixtures. Further information on Iron in Pindan sand is described below along with the EDS results. The amount of Haematite (FeO) in Pindan sand might be less than 1%. Even though the amount of Haematite is below 1%, it has a great influence on the colour of Pindan sand. According to the results of the Quantitative-XRD, Pindan sand consists mostly of quartz and kaolinite.

Figures 5.12(A) and (B) provide SEM images of Pindan sand grains collected from Gantheaume Point Rd (G.P) and Cape Leveque (C.L) in Broome, respectively. The shape of the pindan particles are sub-rounded sand grains. Figures 5.12(C) and (D) show the crystal form of Pindan sand, and Figures 5.12(E) and (F) more clearly show the crystal form of the Pindan sand of G.P and C.L, respectively. The images of Figures 5.12(E) and (F) provide that the crystal form is a loose structures. Both Sands from G.P and C.L have a similar microstructure.

Table 5.6: Quantitative XRD Analysis for Pindan Sand

Crystalline Mineral	%
Quartz SiO ₂	95 – 96
Kaolinite Al ₄ Si ₄ O ₁₀ (OH) ₈	4 - 5

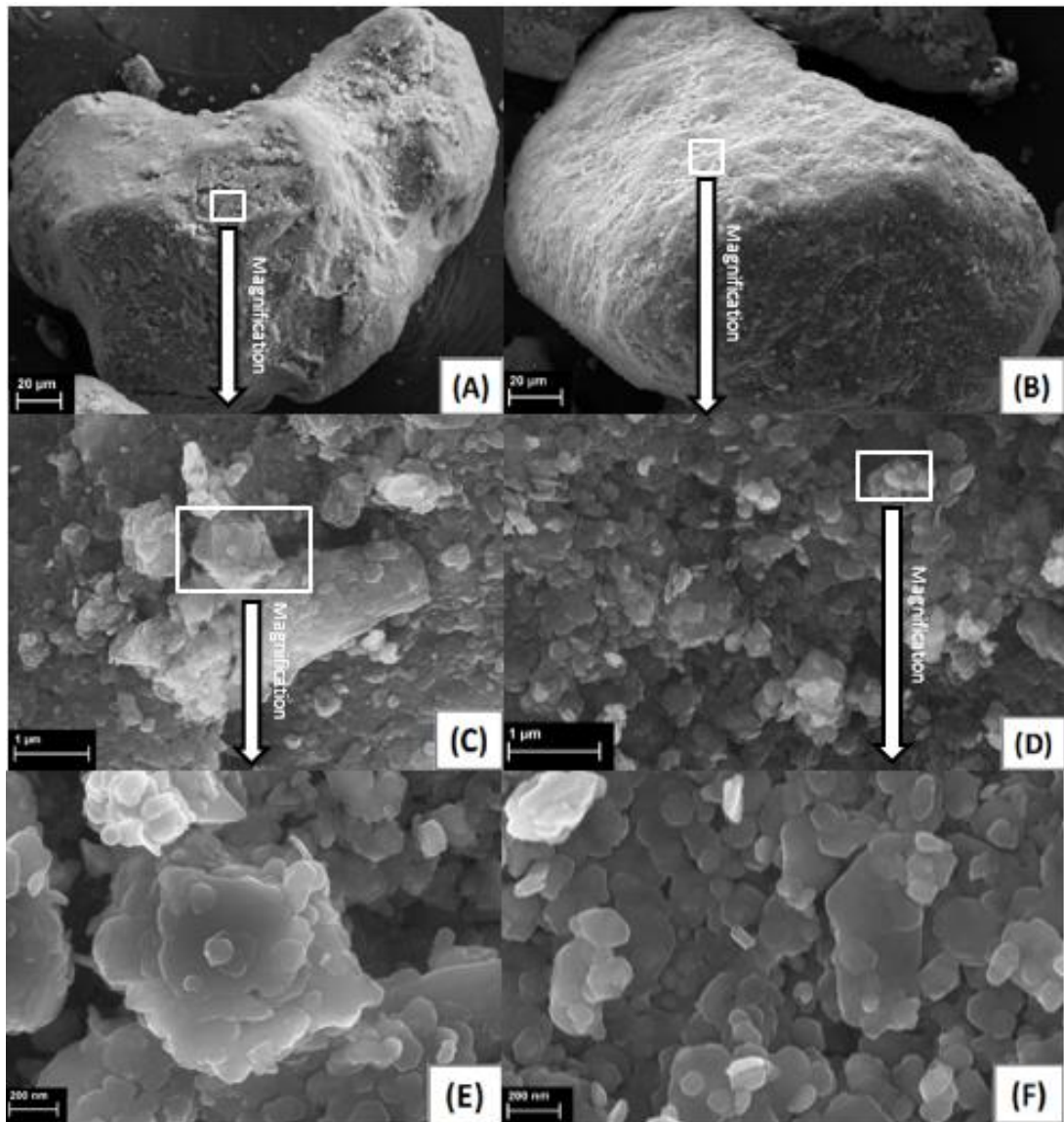


Figure 5.12: G.P and C.L Sand Grain. (A) G.P Sub-rounded Grain, (B) C.L Sub-rounded Grain, (C) G.P Microstructure, (D) C.L Microstructure, (E) Magnification of (C) showing the clear form, (F) Magnification of (D) showing the clear form.

SEM pictures are accomplished with each energy dispersive X-ray spectroscopy (EDS) analysis. The EDS spectra of the selected areas within the SEM samples of Mixtures A, B and C is provided with the SEM images. EDS test was used for element analysis of specimens. Carbon in the EDS spectra is mostly due to the carbon coating for sample preparation. The SEM images of the mixtures of pindan sands and the three Polymers are also provided to determine the microstructures, and the microstructures are compared to the mechanical properties. The SEM and EDS were tested on 16 day cured mixtures.

Figure 5.13 shows the bonding bridge between the sand particles of the mixture A. Figure 5.13(A) illustrates that the polymer A might affect the bonding structures between the particles, and Figure 5.13(B) shows that the Polymer A might also affect the crystal forms and make them denser compared to the untreated pindan sands as shown in Figures 5.12(C) and (D). Polymer A might make the sand structure more coherent as the image of Figure 5.13(B) looks denser and less porosity between the crystal forms compared to the untreated pindan sand. The SEM images showed the microstructure of the Pindan sand and that the polymers might be forming the bridges between the sand particles. Figure 5.14 provides the chemical property of Pindan sand and mixture A through XRD analysis. And, a SEM image combined with EDS locates and mineral identifications is provided together in Figure 5.15. In the Mixture A, $\text{Ca}(\text{OH})_2$ and Calcium are detected in the XRD analysis and EDS spectra of Figures 5.14 and 5.15, respectively. Figures 5.15(A) and (B) show the EDS spectra on the bonding structure and the EDS spectra on the sand, respectively. The EDS spectra on the bonding structure clearly shows that calcium is detected and most of chemical component are silica and aluminium. The EDS spectra on the sand also indicates the detected calcium, silica and aluminium, but aluminium and calcium are relatively small proportions compared to silica. It is noted that the sand surface was coated by the polymer and the polymer affected the bonding structures according to the EDS spectra results. And, Iron (Fe) was detected in both the bonding structure and sand surface. Iron comes from Pindan sand, which shows that Pindan sand has iron and also affects bonding structure.

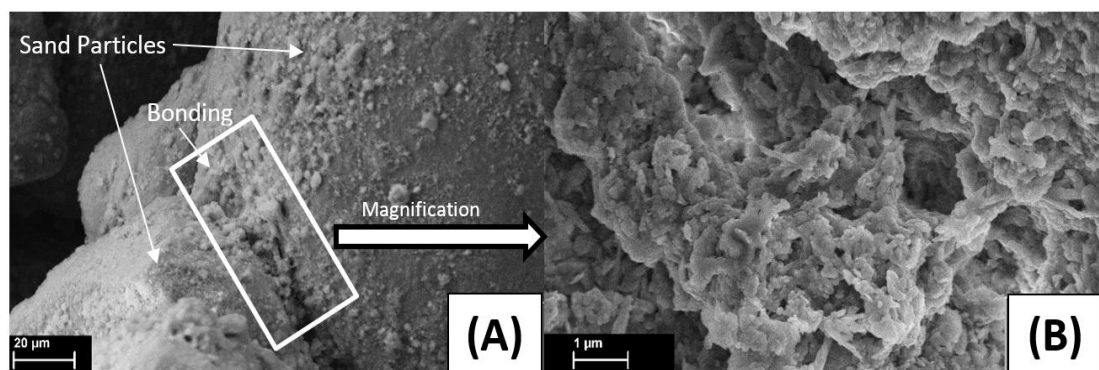


Figure 5.13: SEM Images of Mixture A after 16day curing. (A) Bonding of Mixture A, (B) Magnification of (A) showing the bonding structure.

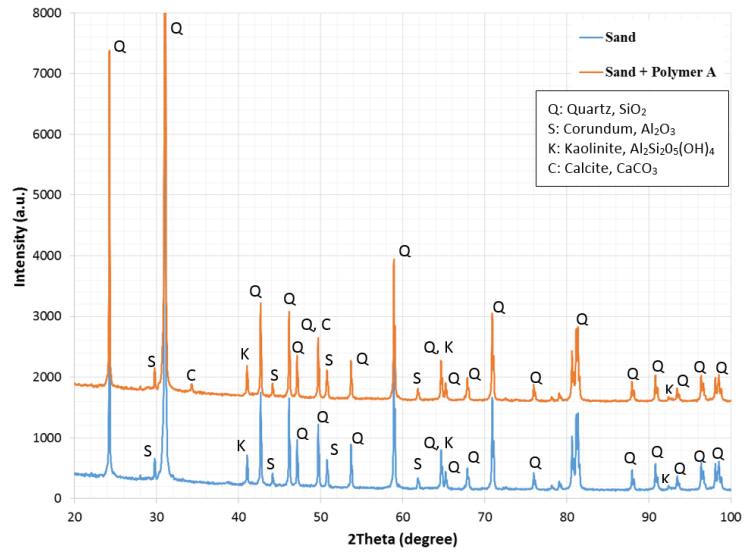


Figure 5.14: XRD phase analysis of Pindan sand and Mixture A

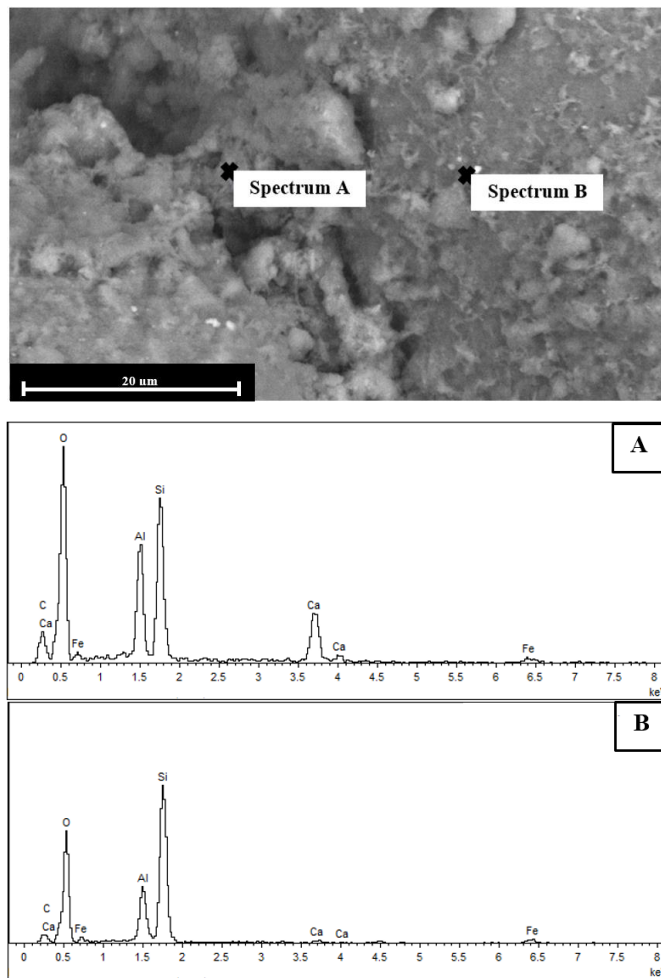


Figure 5.15: EDS Spectra of the mixture A. (A) EDS on bonding, (B) EDS on Sand Particle.

Figure 5.16 demonstrates that polymers B and C might affect the bonding between the particles. Figure 5.16(A) and (B) presented the bonding between the sand particles of the mixture B and C, respectively. The SEM images of Figures 5.16(C) and (D) more clearly show the bonding between the particles for the mixtures of the Pindan sand with the polymer B and Polymer C, respectively. Comparing Figures 5.16(E) and (F) with Figures 5.12(E) and (F), the polymers might affect not only the bonding between the particles but also provide the cohesive or the bonding between the crystals, but the change of crystal form has not been observed. The polymers might not influence the crystal structure. Figure 5.16(F) clearly shows the needle structures of the polymer between the crystal forms.

Polymer B might provide cohesive between the crystal forms but might not affect the bonding structure between the crystal forms, on the contrary, polymer C could provide the bonding between the crystals but might not influence the cohesive of the crystal forms while the Polymer A might provide the bonding and improve the cohesive between the crystal forms according to the XRD and SEM analysis. However, the crystal forms has not been changed in all polymer mixtures. From the SEM test, it is noted that the polymers could provide the bonding between the particles and the crystals, and could increase the density by bonding crystal forms and make them more cohesive due to reducing the porosity compared to the untreated sands.

Figures 5.17(A) and (B) are the SEM image of the mixture B and EDS spectra on the bonding structure and the sand particle, respectively. Figures 5.18(A) and (B) show EDS spectra of the mixture C on the bonding structure and the sand particle, respectively. In the EDS spectra of Figure 5.18(A), aluminium is detected at a similar proportion to silica, whereas aluminium in the EDS spectra in Figure 5.18(B) is not detected due to a small proportion. In EDS test, Fe was also detected on the bonding structures due to the clay bonding between the sand particles. From the EDS results, it is proven that Iron affects the bonding structures between the sand particles. Also, when comparing the EDS spectra of the bonding structure to the sand, the proportion of aluminium was much higher in the bonding structures then in the EDS of Pindan sand. Aluminium also affects the bonding structures between the soil particles. Pindan sands are cemented by iron oxides (Fe_2O_3) and aluminium oxides ($\text{Al}(\text{OH})_3$).

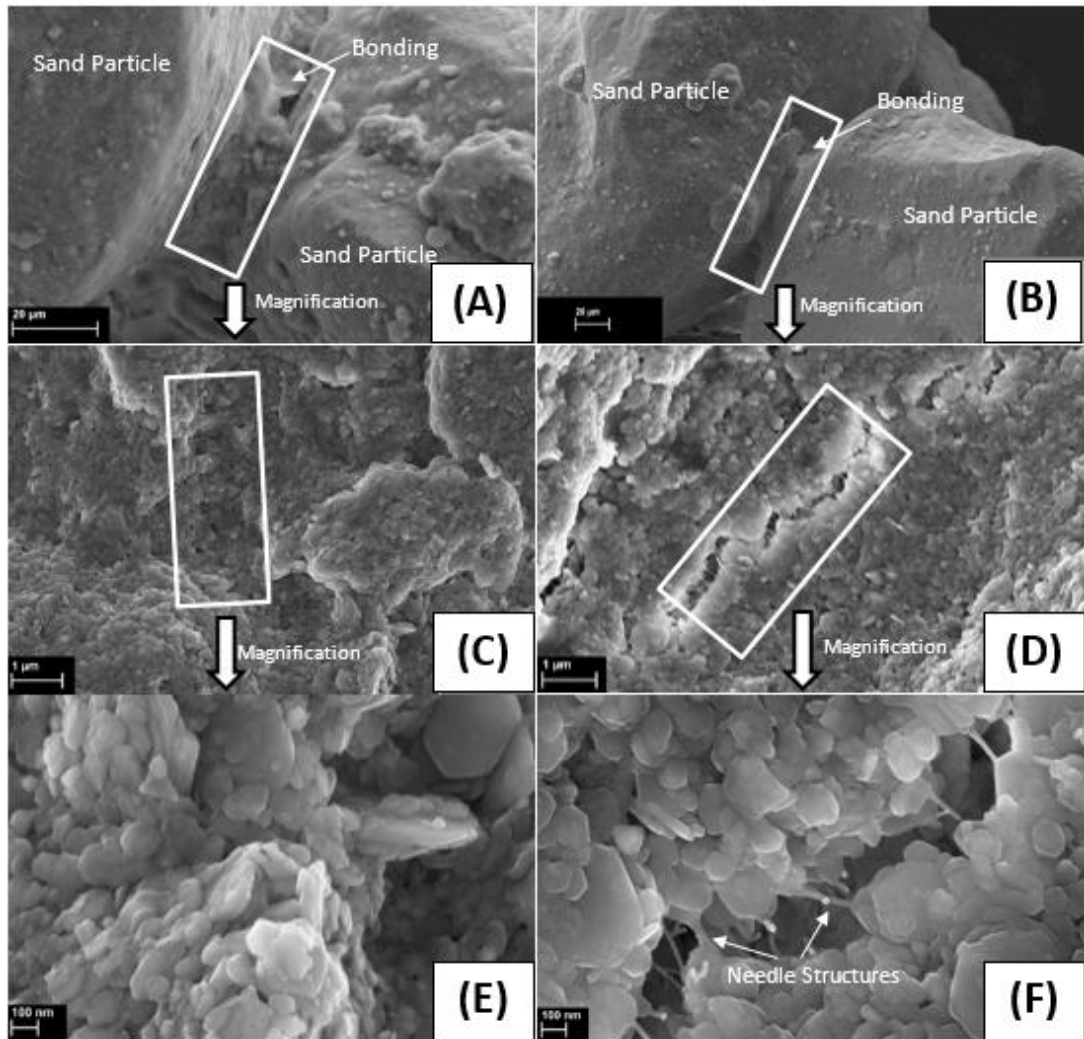


Figure 5.16: SEM Images of Mixture B and C after 16day curing. (A) Bonding of Mixture B, (B) Bonding of Mixture C, (C) Magnification of (A) showing the bonding structure, (D) Magnification of (B) showing the bonding structure, (E) Magnification of (C) showing microstructures, (F) Magnification of (C) showing microstructures.

According to the EDS analysis as shown in Figures 5.17 and 5.18, no significant difference was found in the chemical composition tested between the bonding structure and the sand. Also, the XRD analysis shown in Figure 19 did not detect any change in chemical composition between Pindan sand and the mixtures. The reason for this is that the XRD test showed no change because the amount of polymer contained was too low compared to the sands with relatively high intensity. Another reason for no difference is that some components of the polymers are composed of components similar to the Pindan sand. In the case of polymers A and B, Al_2O_3 and SiO_2 were contained in the polymer component, and particularly the polymer B was mainly composed of the two components. Polymer C seems to have amorphous

components as shown in Figure 5.20 that presents the XRD phase analysis of the polymers.

Form the results, SEM images showed that the bonding structure differs depending on the polymers, and it was found that polymers affect the bridges between particles. Iron and aluminium have also been shown to influence on the bridges through the EDS analysis. The amount of polymer in the sample was too small to find any particular change in the XRD test.

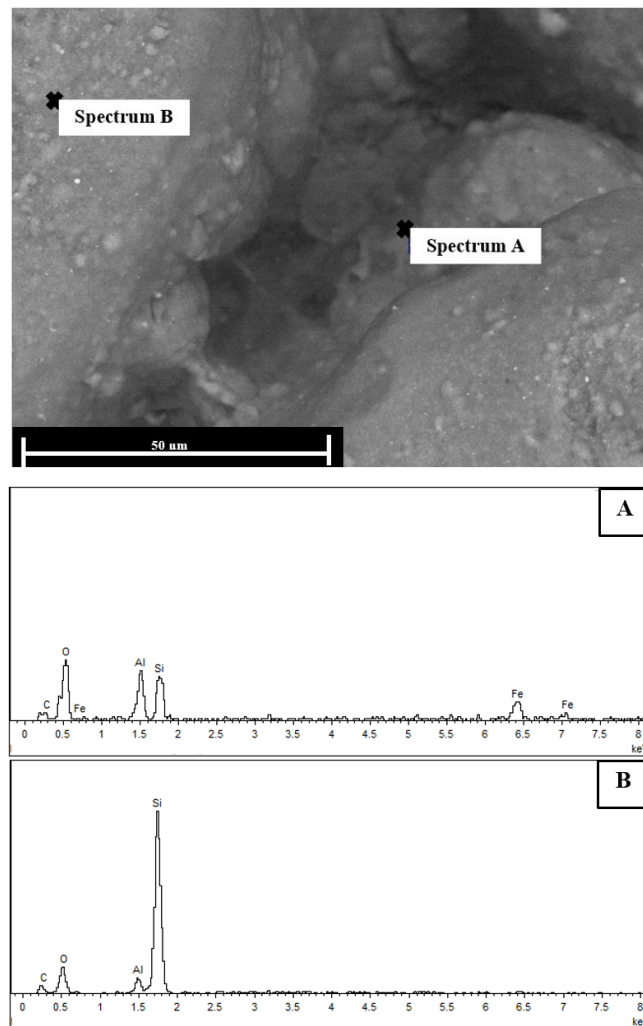


Figure 5.17: EDS Spectra of the mixture B. (A) EDS on bonding, (B) EDS on Sand Particle.

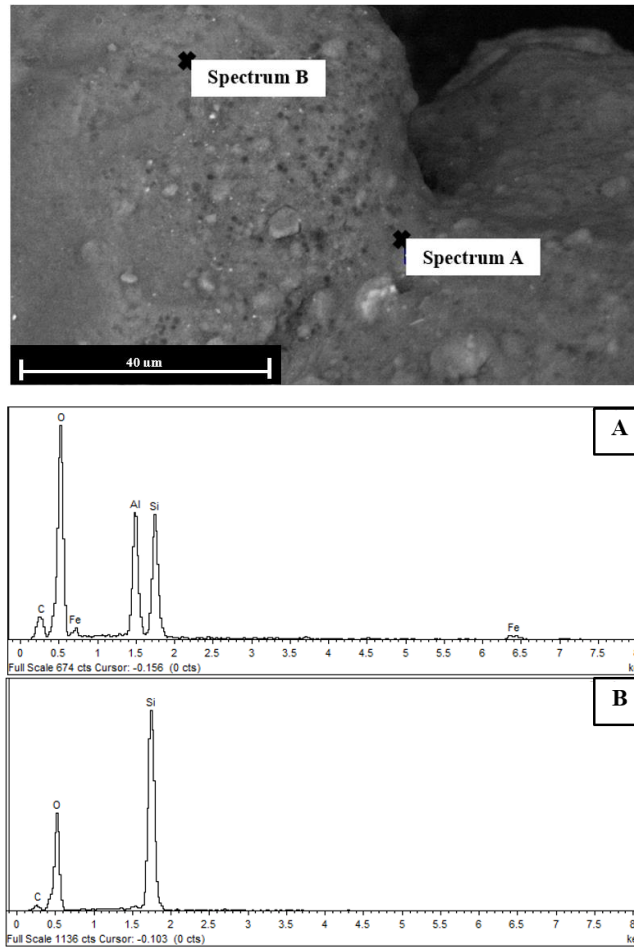


Figure 5.18: EDS Spectra of the mixture C. (A) EDS on bonding, (B) EDS on Sand Particle.

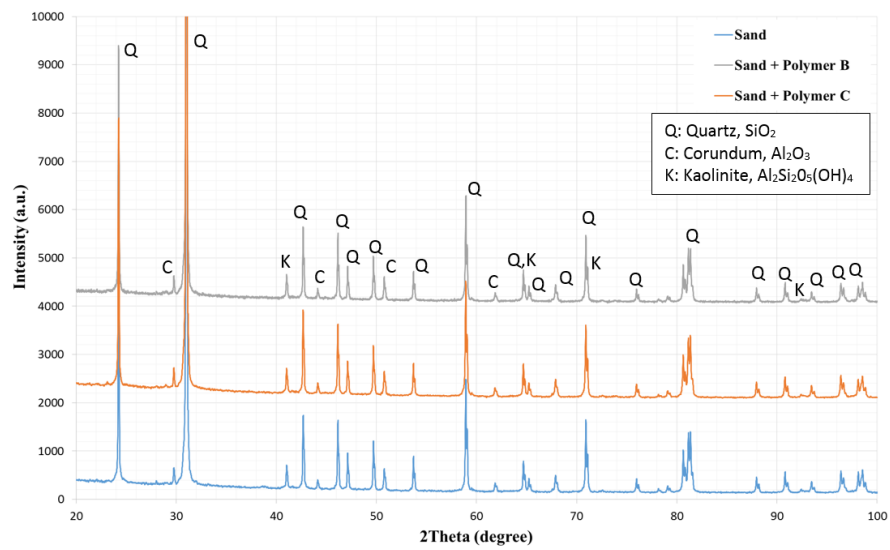


Figure 5.19: XRD phase analysis of Pindan sand, Mixture B and C.

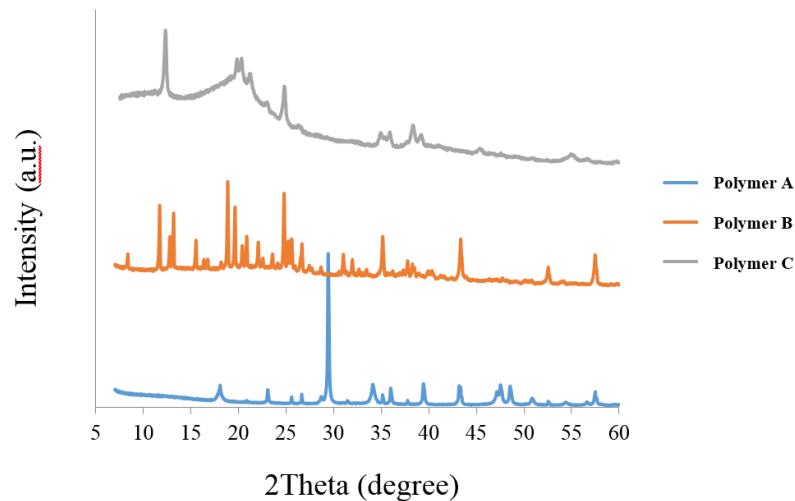


Figure 5.20: XRD Phase analysis of Polymers

Note: Polymer components are confidential and therefore does not display components.

5.7.2 Interaction of Microstructural Properties and Mechanical properties

In the compaction test, the polymers reduced the optimum moisture content and increased the maximum dry density. This can be demonstrated by SEM test, which shows that the polymer has reduced the porosity as can be seen from the SEM images of the mixtures. The reduction of the void ratio is also related to the strength, and the UCS results show that the compressive stress of the mixtures increases. This shows that as the SEM images of the mixtures show, the polymer the compressive stress by reducing the void ratio of the samples. This is also the reason for the increase in capillary rise ratio. Polymer A caused a decrease in strength by micro-cracks during the curing process. In addition, in Figure 5.16(E), crystals are well formed together and have high cohesion. The bonding breaks at the failure point at one time due to high cohesion, resulting in brittle failure in the UCS test.

In relation to CBR and microstructure changes, the CBR values of mixture B are similar regardless of the change in the amount of the polymer. This is because the polymer dose not link crystals but rather coalesces the crystals with each other as shown in Figure 5.16(E). This was also appears in the UCS results, as the change in the amount of polymer did not change the UCS results significantly. In the UCS test for the mixture B, the compressive stress and strain were not significantly different with respect to the amount of the polymer. In mixture A, CBR increases as the amount

of polymer increases. This is because the polymer is smaller than Pindan sand as shown in Figure 5.1, which increase the amount of void filling during compaction. Also, as the amount of polymer increase, the sand surface can be covered more, and calcium can affect the bonding bridges more. The same result is displayed in the UCS test as well. In the UCS test for the mixture A, the compressive stress and strain increased in proportion to the amount of the polymer. Polymer C also showed the same increase in compressive strength and strain as the amount of polymer was increased. This is because the polymer can provide more needle bonding as shown in Figure 5.16(F), as the amount of polymer increases. However, at 0.5% of polymer C, CBR value was much higher than that of untreated sample, but the amount of polymer increased and CBR decreased. The reason for this is shown in Figure 5.21, where the force against the piston increased as it did for UCS results, but the stain also increased as the amount of polymer increased. As shown in Figure 5.21, the results of CBR showed that the highest value was recorded at 0.25 mm of penetration for samples with 0.5% polymer C, while the highest value was recorded at 5 mm for samples with 0.7% polymer C. This also resulted in a lower CBR value due to a decrease in the slope of the curves. In addition, as the amount of moisture content increased, the result showed a sharp drop in the CBR result, indication that the polymer easily dissolves in water and therefore the bonding is easily broken by water. For the same reason, the CBR of the soaked sample is lower than that of the unsoaked sample because the polymer may also escape during the water drainage.

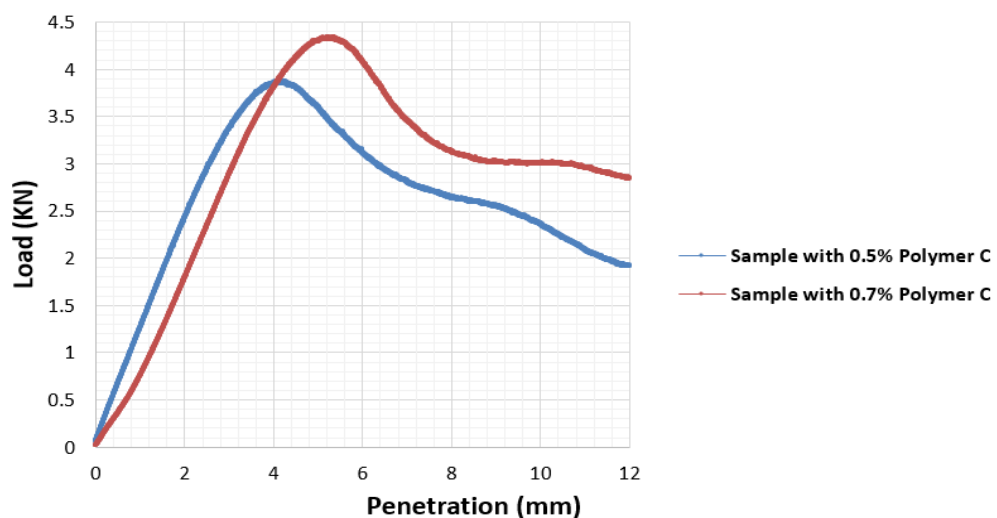


Figure 5.21: CBR Test for the Mixtures with 0.5% and 0.7% of Polymer C

5.8 Chapter Summary

The SEM images clearly showed the microstructure change of the mixtures compared to the microstructures of the Pindan sand. It is proven that polymers affect the bonding bridges between the soil particles. Based on the XRD analysis and SEM images, it is contemplated that polymer A provides a bond and cohesion between the crystal forms, polymer B improves cohesive and polymer C provides a bond between the crystal forms. It is also noted that the polymers could reduce porosity and increase density by bonding the crystal forms together as compared to the untreated Pindan sands. Change in microstructure could affect and relative to mechanical properties such as strength and strain. This chapter determined the relationship between the microstructure and mechanical properties and provided more support the XRD and SEM analysis.

According to the SEM analysis, polymers A and B might improve cohesion between the particles and crystal forms, which means the void ratio and porosity is decreased. In general, reducing the porosity and void ratio means that the optimum moisture content (OMC) is reduced and the maximum dry density (MDD) are increased. Both polymers A and B reduced the optimum moisture contents. Polymer C could provide the bonding between the crystals but might not influence the cohesive of the crystal forms according to the SEM analysis. Polymer C reduced the OMC the most. It is probably because that polymer C provided bonding between the sand particles and reduced void ratio, which seems to be due to the fact that the amount of water in the void occupies more than the moisture content in the porosity of the sands. Compressibility and strength are also relative to void ratio. Generally, high void ratio soil has low strength and compressibility and low void ratio soil shows high strength and incompressible. The increase in density and UCS after polymer mixed showed that the polymers affected the bonding between the particles and the crystal forms in the particles as shown in the SEM images. From the EDS analysis, the bridges between Pindan sand particles form from iron and aluminium which would be the chemical compound with formula Fe_2O_3 (i.e. iron oxides) and $\text{Al}(\text{OH})_3$ (i.e., aluminium oxides).

Based on the CBR results, it is recommended that polymer C is not to be used as a road stabiliser because the bonding is weak to water and significantly reduces the

CBR values. Polymer A, on the other hand, is resistant to water and reduces water ingress, thus stabilising the pavement structures to maintain strength, increasing the life of unsealed pavement. Polymer B also stabilises the soil well and increases its strength even when the amount of polymer is changed. The total pavement thickness required for the stabilised Pindan soil is at least 250mm.

This study shows the microstructure and the properties of Pindan soil. In particular, the microstructure changes depend on the type of polymer and the mechanical properties vary accordingly. The mechanical properties and microstructure changes, show a close relationship. Basically, it is evident that the failure behaviour, strain and strength as well as the basic properties are affected and changed by the microstructure change.

Chapter 6

6 Conclusion and Future Research

This research examines properties of Pindan soils and Pindan-mixtures with various polymers with objective of understanding of the fundamental properties performed in the nano- and micro-scale. Indentation properties such as elastic modulus, hardness, packing density, stiffness and cohesion of Pindan soils were obtained using nanoindentation. Classification tests such as plastic index and specific gravity and particle size distribution were carried to obtain the basic properties. Compaction, collapsibility, unconfined compressive strength and California bearing ratio tests were performed to determine the mechanical properties of stabilised Pindan soils. Furthermore, chemical and microstructural properties were examined using X-ray diffraction and scanning electron microscope, and linked with the mechanical properties.

6.1 Conclusion

Based on this study, the following conclusion can be drawn:

- a) Nanoindentation technology can be used to determine mechanical properties of soils. This method provides various information such as elastic modulus, hardness, packing density, stiffness, cohesion and fracture toughness of soils at nano-scales. This technology is useful compared to conventional methods to get various information at once in a quick and easy way.

- b) The Pindan soils have been successfully used as a pavement material in Western Australia, although limited information exists with Pindan properties. Thus, Pindan soil were investigated to contribute to the evaluation of the fundamental properties of Pindan soils. Pindan soils were classified into classification categories based on basic physical characteristics such as index properties and particle size distribution and they were classified as silty sand (SM) and the plasticity index was non-plastic. The collapsible index from the double oedometer test was 1.24% which corresponds to a moderate trouble

soil or slightly collapsible soil. CBR results for the samples compacted to be greater than 95% of standard proctor maximum dry density were ranged between 11 – 14 % and 10 – 12 % in the unsoaked and soaked conditions, respectively.

- c) Polymers are widely used for soil stabilisation in civil engineering thus polymers were used to stabilise Pindan soils. The type of polymer influenced the optimum moisture contents and strengths rather than the amount of polymer. Particularly, the capillary rise rate and bonding structures showed different results depending on the type of polymer. Different bonding structures were observed depending on the type of polymer, which was not only related to strengths and also to failure behaviours. From SEM and EDS analysis, it is found that chemical elements such as Iron and Aluminium affect the bonding structures. According to the SEM analysis, the polymers affected the bonding structures not only between the particles but also between the crystal forms in the particle. The capillary rise test proved that polymer stabilising bonders has a high resistance to water and can play a role of waterproofing. Each of the polymers showed a different bonding mechanism, which also affected the mechanical properties and even material failure modes.

- d) Polymer stabilisation is more efficient method for soil stabilisation due to its low cost and ease of application compared to traditional stabilisation. From the economic point of view, polymer stabilisers are profitable in term of price due to the small proportion of the polymers required (adding polymers by weigh of 0.001 – 3% of the soil).

6.2 Recommendation for future research

To get a better understanding of Pindan soils, more performance on properties such as mechanical and indentation properties are required. Mechanical properties are moist important material characteristics in civil engineering in the present. However, in order to obtain a better understanding and knowledge of the materials, it is important to find out the indigenous properties of the materials through indentation

tests. Although this research has shown mechanical and indentation properties for Pindan soils, it still lacks information on Pindan soils, and should be tested for more Pindan soils. In addition, it was found through this study that the bonding mechanism varies greatly depending on the type of binders. Investigation further the influence of mechanical properties on the bonding mechanism depending on the type of binders are also required. A better understanding of soil stabilisation by finding out the fundamental properties of materials and correlating it with the mechanical properties through more studying the mechanical properties of the bonding mechanism using various stabilisers are required and recommended.

Non-traditional stabilisation has less environment impacts than traditional stabilisers such as cement and lime. According to the manufacturer's safety data sheet, the polymers used in this study do not have any significant environment impacts. And the polymer A has been approved by the Western Australian Department of Health as compaction aid within drinking water catchment areas. However, the polymers still contain some toxic components which could affect the environment. And because only limited information is available, the environmental impacts should be more studied.

An important object of future research is to formulate a mathematical representation of the relationship between polymers and Pindan soils to derive the predicted equations for the mechanical behaviour of pavement. A conserved equation of the strength stiffness for such polymer stabilised soils needs to be created from theoretical formulas and support it with experimental results. In order to do so, more advanced experiments need to be conducted. And, finding and providing the relationship between the results from the nanoindentation tests and the advanced experiments is one of the most important research in the future.

Appendices

Appendix A

This appendix contains the UCS results for 1hour and 16day cured samples. Moisture contents are determined at compaction. The samples that compacted more than 98% modified compaction proctor were accepted.

UCS – 1 hour Curing Samples					
Pindan Sand (OMC: 9.4%)					
	Actuator strain at peak load (%)	Peak compressive stress (kPa)	MDD (kN/m ³)	LDR (%)	Moisture Content (%)
Sample 1	2.25	32.5	18.82	100.4%	9.25
Sample 2	2.15	37.0	18.98	101.3%	9.48
Sample 3	2.35	34.5	19.01	101.5%	9.51
Average	2.25	34.67			
Mixture A (1%) (OMC: 8.6%)					
Sample 1	2.25	41.0	19.19	100.7%	8.53
Sample 2	2.85	35.5	19.17	100.6%	8.70
Sample 3	2.00	36.5	19.12	100.4%	8.76
Average	2.37	37.67			
Mixture A (2%) (OMC: 8.2%)					
Sample 1	2.75	42.0	18.79	100.0%	8.26
Sample 2	2.65	37.5	18.83	100.2%	8.28
Sample 3	2.95	36.0	18.80	100.0%	8.14
Average	2.78	38.5			
Mixture A (3%) (OMC: 8.2%)					
Sample 1	3.45	37.5	19.05	100.8	8.14
Sample 2	3.00	38.5	19.07	100.9	8.18
Sample 3	3.00	41.5	19.08	100.9	8.07
Average	3.15	39.17			
Mixture B (0.001%) (OMC: 8.3%)					
Sample 1	2.60	50.3	19.61	101.9	8.10
Sample 2	2.65	49.0	19.60	101.8	8.25
Sample 3	2.35	46.1	19.59	101.8	8.28
Average	2.53	48.5			
Mixture B (0.002%) (OMC: 8.2%)					

Sample 1	2.25	47.9	19.48	101.7	8.32
Sample 2	2.40	49.2	19.50	101.8	8.12
Sample 3	2.65	49.3	19.50	101.8	8.09
Average	2.43	48.8			
Mixture B (0.003%) (OMC: 8.0%)					
Sample 1	2.60	46.5	19.50	101.6	7.98
Sample 2	2.33	51.4	19.51	101.7	7.91
Sample 3	2.50	49.5	19.50	101.6	8.18
Average	2.48	49.1			
Mixture C (0.5%) (OMC: 7.4%)					
Sample 1	2.55	38.0	19.46	98.8	7.30
Sample 2	2.65	38.3	19.56	99.3	7.35
Sample 3	2.45	39.1	19.70	100.0	7.33
Average	2.55	38.5			
Mixture C (0.7%) (OMC: 7.2%)					
Sample 1	3.15	42.6	19.19	98.9	7.09
Sample 2	2.85	42.8	19.10	98.5	7.14
Sample 3	2.80	46.1	19.26	99.3	7.13
Average	2.93	43.8			
Mixture C (1.0%) (OMC: 7.2%)					
Sample 1	3.50	41.0	19.16	98.7	7.09
Sample 2	3.05	46.1	19.15	98.6	7.28
Sample 3	3.05	46.2	19.27	99.2	7.19
Average	3.20	44.4			

UCS – 16 Day Curing Samples

Pindan Sand (OMC: 9.4%)					
	Actuator strain at peak load (%)	Peak compressive stress (kPa)	MDD (kN/m ³)	LDR (%)	Moisture Content (%)
Sample 1	1.30	1025	18.88	100.7	9.2
Sample 2	1.20	1010	18.87	100.7	9.5
Sample 3	1.30	1030	18.89	100.8	9.4
Average	1.26	1021			
Mixture A (1%) (OMC: 8.6%)					
Sample 1	0.80	595	19.39	101.8	8.8
Sample 2	0.85	600	19.38	101.7	8.7
Sample 3	0.85	615	19.42	101.9	8.8
Average	0.83	603			
Mixture A (2%) (OMC: 8.2%)					

Sample 1	0.85	776	19.31	102.7	8.4
Sample 2	0.85	752	19.27	102.5	8.4
Sample 3	0.80	760	19.26	102.5	8.4
Average	0.83	762			
Mixture A (3%) (OMC: 8.2%)					
Sample 1	0.85	625	18.84	99.7	8.2
Sample 2	0.90	660	18.85	99.7	8.1
Sample 3	0.90	600	18.86	99.8	8.1
Average	0.88	628			
Mixture B (0.001%) (OMC: 8.3%)					
Sample 1	0.90	885	18.87	98.2	8.30
Sample 2	0.98	905	18.91	98.4	8.20
Sample 3	0.78	895	18.91	98.5	8.20
Average	0.89	895			
Mixture B (0.002%) (OMC: 8.2%)					
Sample 1	1.27	950	19.02	99.3	8.05
Sample 2	1.28	959	19.00	99.2	8.06
Sample 3	1.28	937	18.88	98.6	8.09
Average	1.28	949			
Mixture B (0.003%) (OMC: 8.0%)					
Sample 1	1.00	991	19.34	100.8	7.91
Sample 2	0.98	977	19.33	100.8	7.93
Sample 3	1.07	969	19.27	100.4	7.96
Average	1.02	979			
Mixture C (0.5%) (OMC: 7.4%)					
Sample 1	0.98	1325	19.43	98.6	7.2
Sample 2	1.15	1310	19.38	98.4	7.5
Sample 3	1.16	1305	19.35	98.2	7.3
Average	1.10	1313			
Mixture C (0.7%) (OMC: 7.2%)					
Sample 1	1.32	1635	19.41	100.0	7.0
Sample 2	1.36	1650	19.52	100.6	7.1
Sample 3	1.42	1660	19.52	100.6	7.1
Average	1.37	1648			
Mixture C (1.0%) (OMC: 7.2%)					
Sample 1	1.32	1930	19.44	100.1	7.0
Sample 2	1.36	1955	19.66	101.2	7.0
Sample 3	1.35	1960	19.56	100.7	7.1
Average	1.34	1948			

Appendix B

This appendix contains the CBR results for the unsoaked and soaked samples. The samples that compacted more than 93% modified compaction proctor were accepted.

Unsoaked Condition Sample	CBR (%)	Swell (%)	Actual MC (%) at Compaction	OMC (%)	LDR (%)
Pindan Sand					
1	19.54		9.5		95.0
2	18.64	N/A	9.4	9.4	94.5
3	19.24		9.3		94.7
4	18.79		9.4		95.4
Average	19.05				
Mixture A (1%)					
1	18.33		8.5		93.1
2	18.43	N/A	8.4	8.6	93.3
3	19.14		8.3		93.1
Average	18.64				
Mixture A (2%)					
1	23.78		8.0		97.43
2	21.74	N/A	8.0	8.2	97.48
3	23.08		8.4		97.16
Average	22.87				
Mixture A (3%)					
1	30.30		8.2		99.23
2	30.30	N/A	8.3	8.2	99.88
3	29.80		8.1		100.62
Average	30.13				
Mixture B (0.001%)					
1	24.24		8.4		96.55
2	24.32	N/A	8.2	8.3	96.41
3	24.62		8.5		96.46

Average	24.39				
Mixture B					
(0.002%)					
1	24.02		8.4		95.78
2	24.55	N/A	8.4	8.2	95.00
3	26.52		8.4		94.63
Average	25.03				
Mixture B					
(0.003%)					
1	25.76		7.9		93.34
2	23.48	N/A	8.1	8.0	93.01
3	20.68		8.0		93.01
Average	23.31				
Mixture C (0.5%)					
1	22.89		7.3		93.39
2	24.24	N/A	7.3	7.4	93.96
3	24.51		7.2		93.02
Average	23.88				
Mixture C (0.7%)					
1	20.00		7.0		94.90
2	21.64	N/A	7.0	7.2	94.91
3	18.69		7.1		94.64
Average	20.11				
Mixture C (1.0%)					
1	11.62		7.2		93.01
2	10.10	N/A	7.1	7.2	93.02
3	11.62		7.0		93.01
Average	11.11				

Soaked Condition Sample	CBR (%)	Swell (%)	Actual MC (%) at Compaction	OMC (%)	LDR (%)
Pindan Sand					
1	19.75		9.2		95.7
2	17.93	0	9.4	9.4	93.9
3	19.55		9.5		94.4
Average	19.08				
Mixture A (1%)					
1	18.84		8.8		93.94
2	18.23	0	8.7	8.6	93.08
3	19.65		8.8		93.04
Average	18.91				
Mixture A (2%)					
1	19.44		8.4		99.00
2	21.46	0	8.2	8.2	98.15
3	19.70		8.2		99.98
Average	20.20				
Mixture A (3%)					
1	27.02		8.0		95.66
2	26.26	0	8.1	8.2	96.42
3	25.25		8.2		99.00
Average	26.18				
Mixture B (0.001%)					
1	17.68		8.4		93.13
2	18.43	0	8.1	8.3	93.20
3	18.94		8.4		93.04
Average	18.35				
Mixture B (0.002%)					
1	26.77		8.4		96.54
2	25.25	0	8.3	8.2	94.13

3	23.74		8.1		97.16
Average	25.25				
Mixture B					
(0.003%)					
1	26.26		8.0		95.47
2	23.74	0	8.2	8.0	95.68
3	22.73		8.1		95.20
Average	24.24				
Mixture C (0.5%)					
1	20.20		7.24		93.11
2	19.14	0	7.16	7.4	93.01
3	19.24		7.35		93.05
Average	19.53				
Mixture C (0.7%)					
1	18.18		7.08		95.69
2	18.69	0	6.98	7.2	93.93
3	18.18		6.93		93.42
Average	18.35				
Mixture C (1.0%)					
1	9.60		7.1		94.89
2	9.34	0	7.0	7.2	95.19
3	10.10		7.0		94.52
Average	9.68				

Appendix C

This appendix contains the nanoindentation results of Pindan Soil.

Modulus	Hardness	Drift Correction	Displacement	Load
GPa	GPa	nm/s	nm	mN
70.356	10.754	-0.101	2041.342	519.277
68.455	10.679	-0.066	2027.966	502.83
74.014	11.204	-0.034	2023.622	534.295
71.974	10.951	-0.025	2022.826	520.702
66.639	10.643	-0.02	2021.407	490.676
61.035	10.092	-0.036	2024.976	457.379
70.851	10.744	-0.005	2018.146	510.036
54.37	9.845	0.027	2002.968	411.128
53.442	9.793	0.006	2014.74	410.219
49.451	9.21	0.004	2057.793	398.038
67.846	10.795	0.035	2008.834	492.663
69.204	10.85	0.021	2011.151	500.855
69.613	10.952	0.044	2009.538	503.486
66.406	10.696	0.034	2001.175	480.945
51.502	8.733	0.01	2067.178	407.008
76.156	11.248	0.034	2009.934	537.416
68.829	10.692	0.033	2005.304	493.97
63.518	10.454	0.027	2009.565	467.666
60.02	10.282	0.009	2013.548	449.871
61.181	10.204	0.026	2009.055	452.706
80.099	11.358	0.036	2006.652	554.118
81.237	11.288	0.039	2003.481	555.769
81.696	11.332	0.026	2005.145	559.284
81.69	11.397	0.016	2011.574	563.918
80.804	11.376	0.023	2004.589	556.218
81.232	11.499	0.025	2006.36	561.099
78.852	11.244	0.015	2008.478	547.943
81.05	11.474	0.027	2001.158	557.12

76.119	11.284	0.021	2011.128	538.468
76.075	11.285	0.01	2009.3	537.36
75.09	11.135	0.008	2012.484	532.249
70.81	11.097	0.014	2010.211	511.461
69.936	10.901	0.01	2009.107	503.988
37.18	6.908	0.066	2283.932	368.668
39.982	6.532	0.036	2042.145	307.319
45.524	7.923	0.044	2008.768	344.359
58.54	10.076	0.066	1999.815	434.036
64.606	10.48	0.067	1999.719	468.808
59.387	9.779	0.059	2006.116	436.987
54.531	9.441	0.036	2007.006	408.822
63.673	10.424	0.038	2006.587	466.674
66.93	10.693	0.046	2000.61	483.08
65.545	10.323	0.04	2011.091	476.078
68.682	10.672	0.042	2006.324	493.483
67.388	10.644	0.044	2007.247	487.59
61.509	9.946	0.032	2010.409	451.317
59.56	9.324	0.003	2032.708	442.28
68.936	10.485	0.032	2010.124	493.515
69.238	10.709	0.033	2007.937	497.332
61.989	10.281	0.038	2002.901	454.997
66.925	10.331	0.016	2014.396	484.044
65.315	9.939	0.005	2021.138	473.598
60.316	9.93	0.009	2016.925	448.146
57.55	8.577	-0.003	2094.722	445.811
54.97	7.966	-0.019	2033.313	398.691
52.65	9.207	0.004	2018.797	400.811
53.492	9.306	-0.004	2019.517	406.689
48.265	8.164	-0.032	2046.58	374.622
68.627	11.113	0.007	2018.948	505.724
75.011	11.424	0.013	2008.107	534.329
76.751	11.363	0.006	2014.969	544.503

75.155	11.298	0	2012.933	535.427
43.253	7.083	-0.024	2249.583	400.086
45.572	7.85	0.009	2028.091	350.067
53.006	9.065	-0.001	2032.866	406.253
65.011	10.102	-0.003	2015.226	472.13
67.846	10.445	0	2013.416	489.541
65.237	10.541	0.016	2009.722	477.187
75.746	10.916	0.021	2005.482	527.771
73.874	10.938	0.017	2010.284	522.619
82.221	11.462	0.003	2011.595	567.262
81.787	11.154	-0.009	2013.49	560.786
61.575	9.647	-0.021	2036.398	458.414
61.057	10.071	-0.024	2023.851	456.708
70.595	10.675	0.029	2003.867	500.9
70.655	10.665	0.013	2010.624	504.256
64.067	10.257	-0.008	2019.171	471.825
63.615	10.243	-0.027	2019.356	469.552
71.596	10.554	-0.019	2019.024	510.616
76.275	10.912	-0.003	2010.7	532.541
74.619	10.911	-0.005	2011.099	525.767
66.448	10.416	-0.017	2015.466	483.65
68.206	10.504	-0.004	2019.594	494.993
67.739	10.619	-0.026	2021.243	495.399
58.299	9.784	-0.031	2026.123	440.053
73.401	10.997	-0.007	2016.961	524.873
68.328	10.659	-0.033	2023.964	500.035
62.543	10.437	-0.018	2021.636	468.055
55.229	9.847	-0.018	2026.889	425.267
51.629	9.536	-0.034	2023.189	400.806
71.553	11.253	-0.008	2016.723	520.419
53.092	9.489	-0.044	2022.129	407.799
58.737	10.015	-0.02	2020.636	443.001
59.928	10.091	-0.028	2022.324	450.706

55.859	9.863	-0.016	2022.776	427.123
54.791	9.67	-0.032	2025.19	420.154
60.045	10.06	-0.028	2018.847	449.39
59.107	9.901	-0.039	2022.157	444.004
52.842	9.521	-0.044	2027.354	408.85
70.438	10.816	-0.01	2014.997	507.807
55.691	9.621	-0.032	2034.332	427.947
53.229	9.34	-0.047	2029.41	409.563
49.626	8.98	-0.059	2028.38	385.582
59.423	10.017	-0.024	2013.524	443.462
46.354	9.019	-0.054	2040.734	371.898
49.006	8.507	-0.083	2052.096	385.084
50.901	9.251	-0.052	2034.821	398.042
84.631	11.453	-0.016	2012.995	577.425
84.247	11.354	-0.008	2012.569	573.774
84.667	11.305	-0.007	2013.667	575.035
83.42	11.38	-0.006	2009.974	569.625
83.098	11.416	-0.016	2011.793	570.019
84.171	11.483	-0.017	2013.679	576.575
83.154	11.231	-0.019	2015.168	568.539
83.176	11.516	-0.026	2019.261	576.289
82.404	11.35	-0.015	2015.624	568.104
81.778	11.238	0.002	2012.122	561.604
59.429	10.16	-0.033	2027.43	451.272
69.296	10.854	-0.009	2013.719	502.579
84.444	11.838	-0.031	2024.252	590.187
84.865	11.647	-0.019	2020.754	586.364
88.611	11.828	-0.031	2019.025	603.58
89.618	12.007	-0.027	2025.494	614.762
92.694	12.025	-0.005	2014.411	620.298
91.454	11.966	-0.024	2021.167	618.44
88.617	11.898	-0.017	2019.196	605.069
87.305	11.738	-0.026	2023.13	599.08

91.234	11.873	-0.023	2017.18	613.361
84.983	11.474	-0.023	2017.752	581.823

Appendix D

This appendix contains the specimen photos from the experiments.



Figure D.1: The collected locations of Pindan soil. (a) Cape Levique (C.L),
(b) Gantheaum Point Road (G.P).

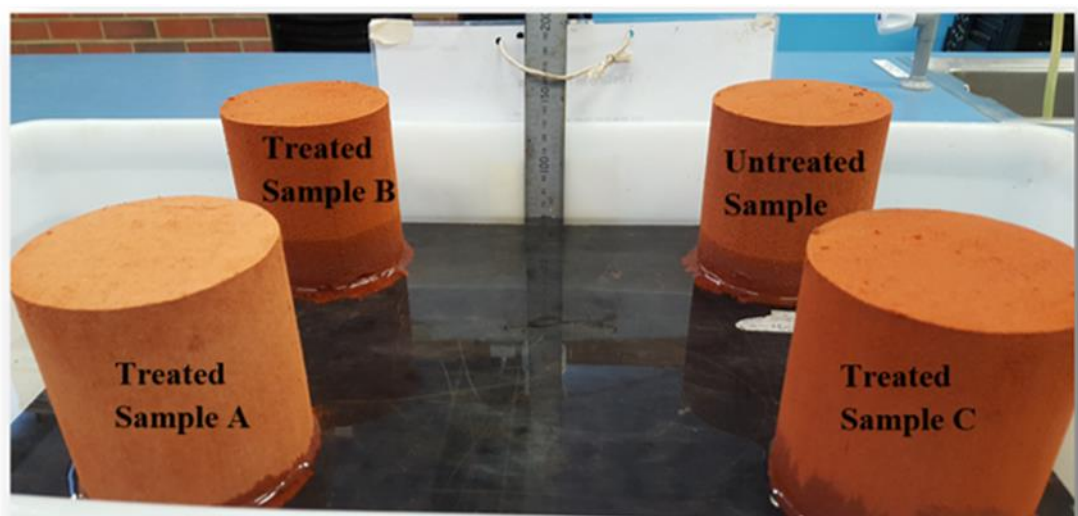


Figure D.2: Capillary Rise of Compacted Samples.



Figure D.3: Capillary Rise of Compacted Samples after 2hours.

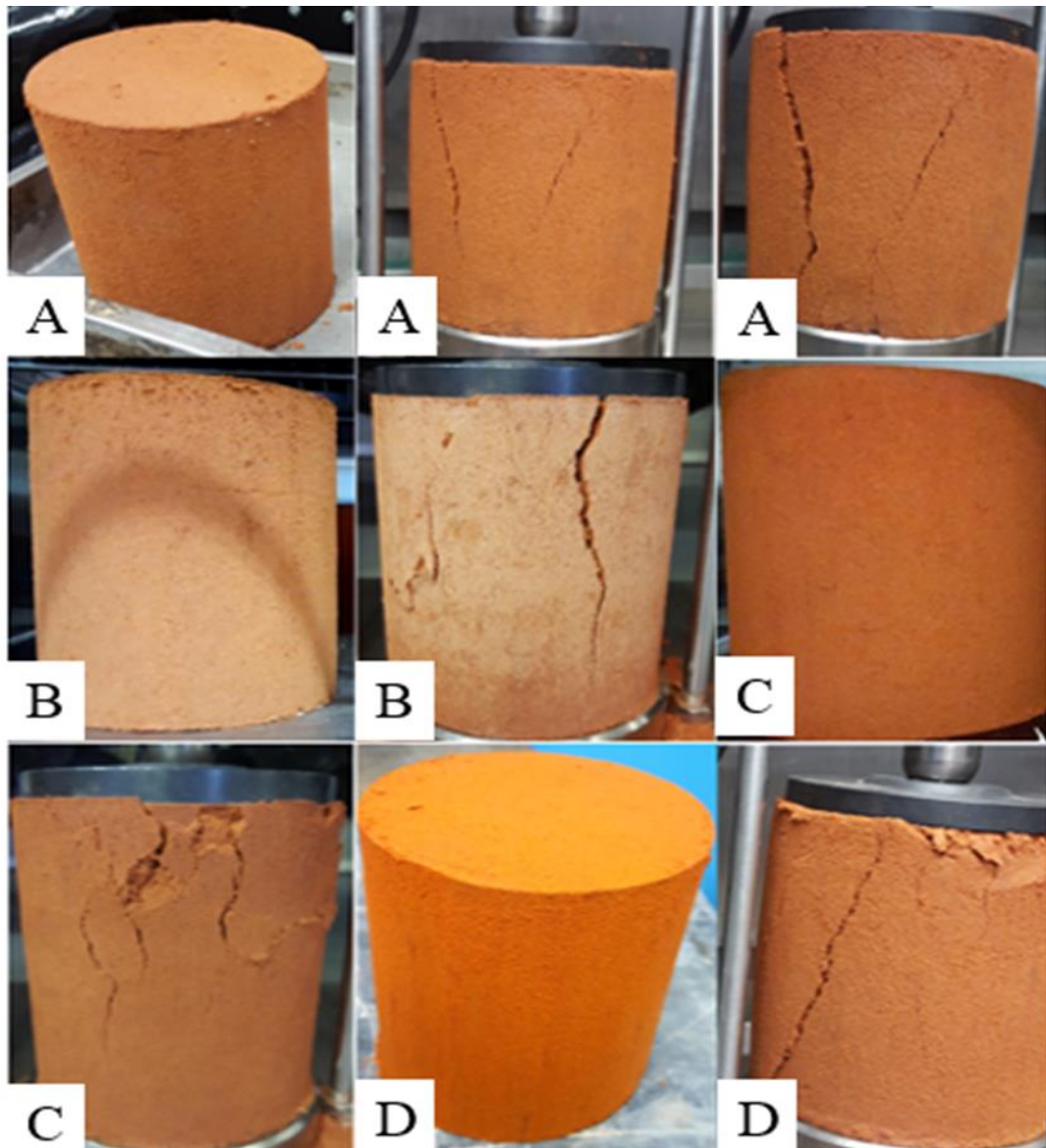


Figure D.4: Unconfined Compressive Strength Test. (a) Untreated Pindan Sample, (b) Polymer A-Pindan Mixture, (c) Polymer B-Pindan Mixture, (d) Polymer C-Pindan Mixture.

References

- Airey, D., Suchowerska, A., & Williams, D. (2012). Limonite—a weathered residual soil heterogeneous at all scales. *Géotechnique Letters*, 2(7-9), 119-122.
- Al-Hadidy, A., & Yi-qiu, T. (2009). Effect of polyethylene on life of flexible pavements. *Construction and Building Materials*, 23(3), 1456-1464.
- Al-Khanbashi, A., & Abdalla, S. W. (2006). Evaluation of three waterborne polymers as stabilizers for sandy soil. *Geotechnical and Geological Engineering*, 24(6), 1603-1625.
- Andrews, B. (2006). Part 4D: Stabilised Materials, Guide to Pavement Technology: Austroads Incorporated.
- Andrews, R., & Duffy, P. (2008). Polymer stabilisation and best value management of unsealed road networks. *Road & Transport Research: A Journal of Australian and New Zealand Research and Practice*, 17(3), 59.
- Anstis, G., Chantikul, P., Lawn, B. R., & Marshall, D. (1981). A critical evaluation of indentation techniques for measuring fracture toughness: I, direct crack measurements. *Journal of the American Ceramic Society*, 64(9), 533-538.
- ARA Inc. (2004). Guide for mechanistic-empirical design of new and rehabilitated pavement structures. *Transportation Research Board of the National Research Council*, 1-91.
- ASTM International. (2010). D4318-10e1: Standard Test Methods for Liquid Limit, Plastic Limit, and Plasticity Index of Soils, ASTM International, West Conshohocken, PA.
- ASTM International. (2011a). ASTM D2487-11: Standard Practice for Classification of Soils for Engineering Purposes (Unified Soil Classification System), ASTM International, West Conshohocken, PA.
- ASTM International. (2011b). D2435/D2435M-11: Standard test method for one-dimensional consolidation properties of soils using incremental loading, ASTM International, West Conshohocken, PA.
- Ateş, A. (2013). The effect of polymer-cement stabilization on the unconfined compressive strength of liquefiable soils. *International Journal of Polymer Science*, 2013.
- Austroads. (2009). *Guide to pavement technology: part 6: unsealed pavements*.
- Azzam, W. R. (2014). Behavior of modified clay microstructure using polymer nanocomposites technique. *Alexandria Engineering Journal*, 53(1), 143-150.
- Azzam, W. R. (2014). Utilization of polymer stabilization for improvement of clay microstructures. *Applied Clay Science*, 93, 94-101.
- Balsam, W., Ji, J., & Chen, J. (2004). Climatic interpretation of the Luochuan and Lingtai loess sections, China, based on changing iron oxide mineralogy and magnetic susceptibility. *Earth and Planetary Science Letters*, 223(3), 335-348.
- Basma, A. A., & Kallas, N. (2004). Modeling soil collapse by artificial neural networks. *Geotechnical & Geological Engineering*, 22(3), 427-438.
- Bazant, Z. P., & Pfeiffer, P. A. (1987). Determination of fracture energy from size effect and brittleness number. *ACI Materials Journal*, 84(6), 463-480.
- Blanton, T., Majumdar, D., & Melpolder, S. (2000). Microstructure of clay-polymer composites. *Advances in X-ray Analysis*, 42, 562-568.
- Bobko, C., & Ulm, F.-J. (2008). The nano-mechanical morphology of shale. *Mechanics of Materials*, 40(4), 318-337.

- Borodich, F. M., Keer, L. M., & Korach, C. S. (2003). Analytical study of fundamental nanoindentation test relations for indenters of non-ideal shapes. *Nanotechnology*, *14*(7), 803.
- Chen, J., & Bull, S. (2007). Indentation fracture and toughness assessment for thin optical coatings on glass. *Journal of Physics D: Applied Physics*, *40*(18), 5401.
- Cheng, Y.-T., & Cheng, C.-M. (2004). Scaling, dimensional analysis, and indentation measurements. *Materials Science and Engineering: R: Reports*, *44*(4-5), 91-149. doi:<http://dx.doi.org/10.1016/j.mser.2004.05.001>
- Clemence, S. P., & Finbarr, A. O. (1981). Design considerations for collapsible soils. *Journal of Geotechnical and Geoenvironmental Engineering*, *107*(ASCE 16106).
- Cocks, G., Keeley, R., Leek, C., WML, P. F., WML, T. B., Cray, A., . . . McInnes, D. (2015). THE USE OF NATURALLY OCCURRING MATERIALS FOR PAVEMENTS IN WESTERN AUSTRALIA.
- Constantinides, G., Chandran, K. R., Ulm, F.-J., & Van Vliet, K. (2006). Grid indentation analysis of composite microstructure and mechanics: Principles and validation. *Materials Science and Engineering: A*, *430*(1-2), 189-202.
- Constantinides, G., & Ulm, F.-J. (2007). The nanogranular nature of C-S-H. *Journal of the Mechanics and Physics of Solids*, *55*(1), 64-90.
- Daphalapurkar, N., Wang, F., Fu, B., Lu, H., & Komanduri, R. (2011). Determination of mechanical properties of sand grains by nanoindentation. *Experimental Mechanics*, *51*(5), 719-728.
- Davenport, F. (2007). *PROBLEM SOILS—A WEST AUSTRALIAN PERSPECTIVE*. Paper presented at the 1st Annual Joint Western Australian Conference, Foundation & Footings Society Australia and Australian Geomechanics Society WA, The Effects of Ground Movements on WA Residences.
- Dimitrov, D., Milchev, A., & Binder, K. (2007). Capillary rise in nanopores: molecular dynamics evidence for the Lucas-Washburn equation. *Physical review letters*, *99*(5), 054501.
- Dukino, R. D., & Swain, M. V. (1992). Comparative measurement of indentation fracture toughness with Berkovich and Vickers indenters. *Journal of the American Ceramic Society*, *75*(12), 3299-3304.
- Durst, K., Backes, B., Franke, O., & Göken, M. (2006). Indentation size effect in metallic materials: Modeling strength from pop-in to macroscopic hardness using geometrically necessary dislocations. *Acta Materialia*, *54*(9), 2547-2555.
- Durst, K., Göken, M., & Vehoff, H. (2004). Finite element study for nanoindentation measurements on two-phase materials. *Journal of materials research*, *19*(1), 85-93.
- El Howayek, A., Huang, P.-T., Bisnett, R., & Santagata, M. C. (2011). Identification and behavior of collapsible soils.
- Elkady, T. Y. (2002). *Static and Dynamic Behaviour of Collapsible Soils*. PhD dissertation. University of Arizona.
- Emery, S., Masterson, S., & Caplehorn, M. (2003). *Sand-Clay pindan material in pavements as a structural layer*. Paper presented at the Proc. 21st Australian Road Research Board Conference.
- Ferry, A. (1998). Unsealed roads are sustainable. *Transactions of the Institution of Professional Engineers New Zealand: General Section*, *25*(1), 54.

- Field, J., Swain, M., & Dukino, R. (2003). Determination of fracture toughness from the extra penetration produced by indentation-induced pop-in. *Journal of materials research*, 18(06), 1412-1419.
- Fischer-Cripps, A. C. (2011). *Nanoindentation*. New York, NY: New York, NY : Springer New York.
- Fu, B., Newham, L. T., & Ramos-Scharron, C. (2010). A review of surface erosion and sediment delivery models for unsealed roads. *Environmental Modelling & Software*, 25(1), 1-14.
- Gaaver, K. E. (2012). Geotechnical properties of Egyptian collapsible soils. *Alexandria Engineering Journal*, 51(3), 205-210.
- Galán-Marín, C., Rivera-Gómez, C., & Petric, J. (2010). Clay-based composite stabilized with natural polymer and fibre. *Construction and Building Materials*, 24(8), 1462-1468.
- Gibbs, H., & Bara, J. (1962). Predicting surface subsidence from basic soil tests *Field Testing of Soils*: ASTM International.
- Gibbs, H. J. (1961). *Properties which divide loose and dense uncemented soils*: United States, Department of the Interior, Bureau of Reclamation.
- Gibbs, H. J., & Holland, W. (1960). *Petrographic and engineering properties of loess*: Technical Information Branch, Denver Federal Center.
- Graham, R. C., & Indorante, S. J. (2017). Concepts of Soil Formation and Soil Survey *The Soils of the USA* (pp. 9-27): Springer.
- Haeri, S. M., Garakani, A. A., Khosravi, A., & Meehan, C. L. (2013). Assessing the hydro-mechanical behavior of collapsible soils using a modified triaxial test device.
- Hamory, G., & Ladner, P. (1976). *Bitumen stabilisation of a limestone (Calcareous Aeolinite)*. Paper presented at the Australian Road Research Board Conference Proc.
- Heelas, R. (2001). *Tropical Environments: Costrasting Regimes and Challenges*: Nelson Thornes Limited.
- Holtz, W. G. (1961). *Settlement of Soil Foundations Due to Saturation*.
- Homauoni, Z. J., & Yasrobi, S. S. (2011). Stabilization of dune sand with poly (methyl methacrylate) and polyvinyl acetate using dry and wet processing. *Geotechnical and Geological Engineering*, 29(4), 571-579.
- Huat, B. B., Gue, S. S., & Ali, F. H. (2007). *Tropical residual soils engineering*: CRC Press.
- Iyengar, S. R., Masad, E., Rodriguez, A. K., Bazzi, H. S., Little, D., & Hanley, H. J. (2012). Pavement subgrade stabilization using polymers: characterization and performance. *Journal of Materials in Civil Engineering*, 25(4), 472-483.
- Jackson, P., Northmore, K., Entwisle, D., Gunn, D., Milodowski, A., Boardman, D., . . . Dixon, N. (2006). Electrical resistivity monitoring of a collapsing meta-stable soil. *Quarterly Journal of Engineering Geology and Hydrogeology*, 39(2), 151-172.
- Jawad, I. T., Taha, M. R., Majeed, Z. H., & Khan, T. A. (2014). Soil stabilization using lime: Advantages, disadvantages and proposing a potential alternative. *Research Journal of Applied Sciences, Engineering and Technology*, 8(4), 510-520.
- Jennings, J., & Knight, K. (1957). *The additional settlement of foundations due to a collapse of structure of sandy subsoils on wetting*. Paper presented at the Proceedings.

- Jennings, J. N. (1975). Desert dunes and estuarine fill in the Fitzroy estuary (north-western Australia). *Catena*, 2, 215-262.
- Jenny, H. (1994). *Factors of soil formation: a system of quantitative pedology*: Courier Corporation.
- Kalantari, B. (2013). Foundations on collapsible soils: a review. *Proceedings of the Institution of Civil Engineers-Forensic Engineering*, 166(2), 57-63.
- Kemp, A. (2004). Sediment control on unsealed roads: a handbook of practical guidelines for improving stormwater quality. *TECHNICAL REPORT*.
- Kenneally, K. F., Edinger, D. C., & Willing, T. (1996). Broome and beyond: plants and people of the Dampier Peninsula, Kimberley, Western Australia. *Como, Western Australia: Department of Conservation and Land Management vi, 256p.-col. illus.. ISBN 073096972X En Plant records. Geog, 7*.
- Khemissa, M., & Mahamedi, A. (2014). Cement and lime mixture stabilization of an expansive overconsolidated clay. *Applied Clay Science*, 95, 104-110.
- Kilvington, D., & Hamory, G. (1986). *The performance of natural gravels as basecourse in a sealed pavement*. Paper presented at the Australian Road Research Board (ARRB) Conference, 13th, 1986, Adelaide, Australia.
- Kumar, A., & Gupta, R. K. (2003). *Fundamentals of polymer engineering, revised and expanded*: CRC Press.
- Lacey, G. (2004). *Do dry powdered polymers work*. Paper presented at the Proceedings from stabilisation of road pavements seminar, NZ Highway Institute of Technology, Auckland, NZ.
- Laugier, M. (1987). Palmqvist indentation toughness in WC-Co composites. *Journal of materials science letters*, 6(8), 897-900.
- Lawn, B. R., Evans, A., & Marshall, D. (1980). Elastic/plastic indentation damage in ceramics: the median/radial crack system. *Journal of the American Ceramic Society*, 63(9-10), 574-581.
- Lawton, E. C., Fragaszy, R. J., & Hetherington, M. D. (1992). Review of wetting-induced collapse in compacted soil. *Journal of geotechnical engineering*, 118(9), 1376-1394.
- Lee, H., Vimonsatit, V., & Chindaprasirt, P. (2016). Mechanical and micromechanical properties of alkali activated fly-ash cement based on nano-indentation. *Construction and Building Materials*, 107, 95-102.
- Lim, S., Jeon, W., Lee, J., Lee, K., & Kim, N. (2002). Engineering properties of water/wastewater-treatment sludge modified by hydrated lime, fly ash and loess. *Water research*, 36(17), 4177-4184.
- Little, D. N., & Nair, S. (2009). *Recommended practice for stabilization of subgrade soils and base materials*: National Cooperative Highway Research Program, Transportation Research Board of the National Academies.
- Liu, J., Shi, B., Jiang, H., Huang, H., Wang, G., & Kamai, T. (2011). Research on the stabilization treatment of clay slope topsoil by organic polymer soil stabilizer. *Engineering Geology*, 117(1), 114-120.
- Lowe, P. (2003). *Pindan Woodlands*. Broome, W.A: Environs Kimberley.
- Lu, X., Soenen, H., Heyrman, S., & Redelius, P. (2013). *Durability of Polymer Modified Binders in Asphalt Pavements*. Paper presented at the XXVIII International Baltic Road Conference.
- Lutenegger, A. J., & Saber, R. T. (1988). Determination of collapse potential of soils.
- Lynde, M., & Brooks, E. (2005). *Evaluation of latex polymers to resist stripping in asphalt pavements in Oregon*. Retrieved from

- Main Roads, W. A. (2003). A guide to the selection and use of naturally occurring materials as base and subbase in roads in Western Australia: Report.
- Miura, N., Sakai, A., Taesiri, Y., Yamanouchi, T., & Yasuhara, K. (1990). Polymer grid reinforced pavement on soft clay grounds. *Geotextiles and Geomembranes*, 9(1), 99-123.
- Mohamed, A.-M., & El Gamal, M. (2012). Treatment of collapsible soils using sulfur cement. *International Journal of Geotechnical Engineering*, 6(1), 65-77.
- Mondal, P., Shah, S. P., & Marks, L. (2007). A reliable technique to determine the local mechanical properties at the nanoscale for cementitious materials. *Cement and Concrete Research*, 37(10), 1440-1444.
- Moore, R. (1939). Water conduction from shallow water tables. *California Agriculture*, 12(6), 383-426.
- Moustafa, A., Bazaraa, A., & Nour El Din, A. (1981). Soil stabilization by polymeric materials. *Die Angewandte Makromolekulare Chemie*, 97(1), 1-12.
- Naeini, S., & Mahdavi, A. (2009). *Effect of polymer on shear strength of silty sand*. MS Thesis. Civil Engineering Department, Imam Khomeini International University, Qazvin, Iran.
- Naeini, S. A., & Ghorbanalizadeh, M. (2010). Silty Sand Soils Stabilized with Epoxy Resin Polymer. *Journal of Applied Sciences*, 10(22), 2839-2846.
- Naeini, S. A., Naderinia, B., & Izadi, E. (2012). Unconfined compressive strength of clayey soils stabilized with waterborne polymer. *KSCCE Journal of Civil Engineering*, 16(6), 943-949.
- Newman, K., Gill, C., & McCaffrey, T. (2007). Field Testings of Silty Sand Stabilized Using Combinations of Hydraulic Cement, Fibres and Polymer Emulsions. *Transportation Research Board, Washington*.
- Newman, K., & Tingle, J. S. (2004). *Emulsion polymers for soil stabilization*. Paper presented at the Presented for the 2004 FAA Worldwide Airport Technology Transfer Conference.
- Ohama, Y. (1998). Polymer-based admixtures. *Cement and concrete composites*, 20(2-3), 189-212.
- Oliver, W. C., & Pharr, G. M. (1992). An improved technique for determining hardness and elastic modulus using load and displacement sensing indentation experiments. *Journal of materials research*, 7(06), 1564-1583.
- Oliver, W. C., & Pharr, G. M. (2004). Measurement of hardness and elastic modulus by instrumented indentation: Advances in understanding and refinements to methodology. *Journal of materials research*, 19(01), 3-20.
- Papadakis, J. (1975). Climates of the world and their potentialities. *Climates of the world and their potentialities*.
- Pells, P., Robertson, A., Jennings, J., & Knight, K. (1975). *A guide to construction on or with materials exhibiting additional settlement due to "Collapse" of grain structure*. Retrieved from
- Petry, T. M., & Little, D. N. (2002). Review of stabilization of clays and expansive soils in pavements and lightly loaded structures—history, practice, and future. *Journal of Materials in Civil Engineering*, 14(6), 447-460.
- Popescu, M. E. (1986). A comparison between the behaviour of swelling and of collapsing soils. *Engineering Geology*, 23(2), 145-163.
- Rafalko, S., Brandon, T., Filz, G., & Mitchell, J. (2007). Fiber Reinforcement for Rapid Stabilization of Soft Clay Soils. *Transportation Research Record: Journal of the Transportation Research Board*, 2026, 21-29. doi:10.3141/2026-03

- Rahman, M. G. F., Talukder, M., & Rahman, A. (2011). Assessment of Soil Compaction—A Project Study. *MIST Journal: GALAXY (DHAKA)*, 3.
- Ramsamooj, D. (2001). An innovative technique for using polymer composites in airport pavement rehabilitation. *Composites Part B: Engineering*, 32(1), 57-66.
- Rogers, C. (1995). Types and distribution of collapsible soils *Genesis and properties of collapsible soils* (pp. 1-17): Springer.
- Rossel, R. V., Minasny, B., Roudier, P., & McBratney, A. (2006). Colour space models for soil science. *Geoderma*, 133(3), 320-337.
- Santoni, R., Tingle, J., & Nieves, M. (2005). Accelerated strength improvement of silty sand with nontraditional additives. *Transportation Research Record: Journal of the Transportation Research Board*(1936), 34-42.
- Saride, S., Puppala, A. J., & Chikyala, S. R. (2013). Swell-shrink and strength behaviors of lime and cement stabilized expansive organic clays. *Applied Clay Science*, 85, 39-45.
- Schoknecht, N. R., & Pathan, S. (2013). Soil groups of Western Australia: A simple guide to the main soils of Western Australia.
- Sharp, K., & Andrews, B. (2009). Stabilising Unsealed Roads Efficiently. *Road & Transport Research: A Journal of Australian and New Zealand Research and Practice*, 18(3), 69.
- Shirsavkar, S., & Koranne, S. (2010). Innovation in road construction using natural polymer. *Electronic Journal of Geo-Technical Engineering*, 15, 1614-1624.
- Sinclair Knight Merz. (2009). *Broome north development Engineering report*. Retrieved from
- Singh, H., & Huat, B. B. (2004). Origin, formation and occurrence of tropical residual soils *Tropical Residual Soils Engineering* (pp. 1-19): Taylor & Francis.
- Smith, J., & Sullivan, L. (2014). Construction and maintenance of embankments using highly erodible soils in the Pilbara, north-western Australia. *International Journal of GEOMATE*, 6(2), 897-902.
- Smolinski, H. J., Galloway, P., & Laycock, J. (2016). Pindan soils in the La Grange area, West Kimberley: land capability assessment for irrigated agriculture.
- Standards Australia. (1996a). Absorption, swell and capillary rise of compacted materials (AS 1141.53:1996). Retrieved from Standards Online.
- Standards Australia. (1996b). Residential slabs and footings (AS 2870:1996). Retrieved from Standards Online.
- Standards Australia. (2006). Soil classification tests - Determination of the soil particle density of a soil - Standard method (AS 1289.3.5.1:2006). Retrieved from Standards Online.
- Standards Australia. (2008). Unconfined compressive strength of compacted materials (AS 5101.4:2008). Retrieved from Standards Online.
- Standards Australia. (2009). Soil classification tests - Determination of the particle size distribution of a soil - Standard method of analysis by sieving (AS 1289.3.6.1:2009). Retrieved from Standards Online.
- Standards Australia. (2011). Residential slabs and footings (AS 2870:2011). Retrieved from Standards Online.
- Standards Australia. (2014). Soil strength and consolidation tests - Determination of the California Bearing Ratio of a soil - Standard laboratory method for a remoulded (AS 1289.6.1.1:2014). Retrieved from Standards Online. .

- Standards Australia. (2017a). Soil compaction and density tests - Determination of the dry density/moisture content relation of a soil using modified compactive (AS 1289.5.2.1:2017). Retrieved from Standards Online.
- Standards Australia. (2017b). Soil compaction and density tests - Determination of the dry density/moisture content relation of a soil using standard compactive (AS 1289.5.1.1:2017). Retrieved from Standards Online. .
- Taha, M. R., Soliman, E., Sheyka, M., Reinhardt, A., & Al-Haik, M. (2010). Fracture toughness of hydrated cement paste using nanoindentation.
- Tayfur, S., Ozen, H., & Aksoy, A. (2007). Investigation of rutting performance of asphalt mixtures containing polymer modifiers. *Construction and Building Materials*, 21(2), 328-337.
- Tingle, J., Newman, J., Larson, S., Weiss, C., & Rushing, J. (2007). Stabilization mechanisms of nontraditional additives. *Transportation Research Record: Journal of the Transportation Research Board*(1989), 59-67.
- Ulm, F. J., Vandamme, M., Bobko, C., Alberto Ortega, J., Tai, K., & Ortiz, C. (2007). Statistical indentation techniques for hydrated nanocomposites: concrete, bone, and shale. *Journal of the American Ceramic Society*, 90(9), 2677-2692.
- Vázquez, M., Justo, J., & Durand, P. (2013). A simplified model for collapse using suction controlled tests.
- Welling, G. E. (2012). *Engineering performance of polymer amended soils*. California Polytechnic State University San Luis Obispo.
- Western Australia. Department of Regional Development and the North West. (1984). *Stabilisation and compaction of Pindan brick soils for brick manufacture : a report prepared for the government of Western Australia*. Perth, W.A: Dept. of Regional Development and the North West.
- Woodward, H. P. (1891). ... *Report on the Goldfields of the Kimberley District*: R. Pether, government printer.
- Yazdandoust, F., & Yasrobi, S. S. (2010). Effect of cyclic wetting and drying on swelling behavior of polymer-stabilized expansive clays. *Applied Clay Science*, 50(4), 461-468.
- Yildirim, Y. (2007). Polymer modified asphalt binders. *Construction and Building Materials*, 21(1), 66-72.
- Zandieh, A. R., & Yasrobi, S. S. (2010). Study of factors affecting the compressive strength of sandy soil stabilized with polymer. *Geotechnical and Geological Engineering*, 28(2), 139-145.